



TÉCNICO
LISBOA



Effect of the ironing process on parts produced by Fused Filament Fabrication

José Pedro Dinis Lopes

Thesis to obtain the Master of Science degree in

Mechanical Engineering

Supervisors: Prof. Marco Alexandre de Oliveira Leite

Eng. Manuel de Figueiredo Cravo Relvas Sardinha

Examination Committee

Chairperson: Prof. Luís Filipe Galvão dos Reis

Supervisor: Prof. Marco Alexandre de Oliveira Leite

Member of the Committee: Prof. Ricardo António Lamberto Duarte Cláudio

September 2021

Acknowledgments

The author of this document acknowledges the importance it was to have the counsel and time of Professor Marco Leite, Professor Antonio Relógio Ribeiro and Professor Manuel Sardinha, whose careful supervision and guidance have proved valuable at every stage of this thesis. Without their unwavering input, the development of this work would have become way more difficult to be accomplished.

The author also expresses his indebtedness to the collaboration of Instituto Superior Técnico, University of Lisbon, namely in what concerns the valuable access to the Laboratory for Product Development (Lab2Prod) and its AM machines, as well as the measuring equipment and individual expertise provided by *Laboratório de Tecnologias Oficinais*.

The author would like to give a word of appreciation for the work developed by Nuno Frutuoso and the *BigFDM* project team on the software that enabled this thesis to start and for the support provided and to João Ajuda and the members of Lab2Prod for all the patience and help provided whenever needed.

This work was supported by FCT, through IDMEC, under LAETA, project UIDB/50022/2020. The author also gratefully acknowledge the funding of the Big FDM project, FCT reference PTDC/EME–EME/32103/2017.

This work represents the accomplishment of a 5-year journey made easier thanks to the tireless support and understanding of his most important friends: Sofia Alves, Francisco Rodrigues, Inês Rebelo, Madalena Pereira, Miguel Esteves, Márcia Garcia, Carolina Pereira, Miguel Pinto, Gonçalo Felício and Adriana Daehnhart for their tireless support. Last but not the least, the author is deeply grateful to his family who always stood by him during the years it took him to complete the present thesis and to successfully conclude this important stage in his life.

Resumo

O Fabrico de Filamento Fundido (FFF) é um processo de fabrico cujo objetivo é construir objetos tridimensionais através da deposição seletiva de material derretido camada por camada seguindo um percurso pré-determinado. Esta tecnologia está a crescer a um passo muito acelerado, já estando a ser usada para as mais variadas aplicações nos dias de hoje

À medida que o Fabrico Aditivo se torna mais importante, os problemas que dele advêm assumem proporções maiores. O Empeno é uma distorção visível quando a superfície da peça impressa não corresponde às dimensões desenhadas e é um dos problemas mais comuns em impressões com ABS.

Ironing, ou em português 'passar a ferro', um tratamento térmico presente nas impressoras 3D mais recentes, foi proposto como potencial solução para este problema, porém não é claro até que ponto é que esta nova tecnologia pode de facto ajudar.

Com esse objetivo em mente, em primeiro lugar esta tese pretende determinar a influência dos parâmetros do fabrico aditivo no empeno de ABS.

Em segundo lugar, um estudo acerca do impacto de implementar o 'ironing' em peças empenadas propõe averiguar a viabilidade desta solução.

Os resultados foram promissores quanto à implementação desta solução no futuro. O 'ironing' revelou ter a capacidade de diminuir o empeno em certas circunstâncias tendo esta tese contribuído assim para o avanço no conhecimento e tecnologia desta área.

Palavras-chave: Fabrico Aditivo, FFF, ABS, Empeno, Parâmetros de impressão

Abstract

Fused Filament Fabrication (FFF) is an additive manufacturing process intended to build three-dimensional objects through selective deposition of melted material layer-by-layer along a pre-determined path. This technology is growing at an accelerated rate, being already widespread and used in many applications nowadays.

As FFF becomes more important, its problems assume a bigger relevance. Warping is a distortion where the surfaces of the printed part do not follow the intended shape of the design and is one of the most common problems when printing in ABS.

Ironing, a heat treatment process present in the most recent FFF machines, has been proposed as a potential solution for this problem, however it is not clear at what degree is it actually a solution.

In order to meet this need, firstly this thesis aims to determine the influence of FFF printing parameters on the warping process of ABS.

Secondly, a study on the impact of applying the ironing process on warped specimens aims to assess the viability of this solution.

The results obtained were very promising in what regards the implementation of this solution in the future. Ironing revealed having the capacity of reducing warping in certain circumstances therefore contributing to the progress in knowledge of this field.

Keywords: FFF, ABS, Warping, Printing parameters, Ironing

Contents

Acknowledgments	iii
Resumo	iv
Abstract	v
List of figures	ix
List of tables	xii
Nomenclature	xiii
Glossary	xiv
1. INTRODUCTION	1
1.1 Motivation	1
1.2 Objectives	1
1.3 Document outline	2
2. STATE OF THE ART	3
2.1 Additive Manufacturing	3
2.2 Fused Filament Fabrication	3
2.2.1 Main stages	4
2.2.2 Materials	6
2.2.3 Warping	7
2.2.4 Curling	9
2.3 Heat treatments	17
2.3.1 Annealing	17
2.3.2 Plasma	18
2.3.3 Ironing	19
3. METHODOLOGY	21
3.1 Modeling	21
3.1.1 CAD software and specimen's shape	22
3.1.2 3D printer	22
3.2 Pre-processing	22
3.2.1 Slicing software	22
3.2.2 Slicer parameters	23
3.3 Mid-processing	26
3.3.1 Ironing on the first layers	27
3.3.2 Ironing spaced equally	27
3.3.3 Ironing consecutively on the first layers	27

3.4 Manufacturing.....	28
3.4.1 Bed coating application	28
3.4.2 Parts per print.....	28
3.4.3 Printing 'zero's.....	28
3.4.4 Number of prints per series	29
3.4.5 Material.....	29
3.4.6 Various other conditions.....	29
3.5 Measuring.....	29
3.5.1 Measuring points (mp).....	30
3.5.2 Equipment	30
3.5.3 Procedure	31
3.5.4 Uncertainty	32
3.6 Results.....	33
3.6.1 Formulas.....	33
3.6.2 Units	33
3.6.3 Tables.....	34
3.6.4 Graphics	34
4. EXPERIMENTAL PROCEDURE	35
4.1 Preliminary studies	35
4.1.1 Testing warping	35
4.1.2 Testing the ironing process	40
4.2 Main tests	48
4.2.1 Fix parameters.....	48
4.2.2 List of tests	51
5. RESULTS.....	55
5.1 Non-ironed tests	55
(A1) None ironed layers	55
(A2) None ironed layers	56
5.2 Ironing on the first layers	57
(B1) Ironed on the 1 st layer	57
(B2) Ironed on the 2 nd layer	58
(B3) Ironed on the 3 rd layer.....	59
5.3 Ironing spaced equally	60
(C1) Interval of 4 layers	60
(C2) Interval of 4 layers	61
(C3) Interval of 4 layers	61
(D1) Interval of 2 layers	62
(E1) Interval of 6 layers	63

5.4 Ironing concentrated.....	64
(F1) 6 concentrated layers	64
(G1) 3 concentrated layers	65
5.5 Ironing on a different sized specimen	66
(H1) Print 1 'zero' and then print a series of 4 specimens applying ironing only on the first layer	67
6. RESULTS ANALYSIS	69
6.1 Warping on non-ironed tests	69
6.2 Warping when only applying ironing on the first layers	69
6.3 Warping when applying ironing spaced evenly across the specimen.....	71
6.4 Warping when applying concentrated ironing	73
6.5 Warping when applying ironing on a different shaped specimen.....	74
6.6 Warping on different sides.....	75
6.7 Printing times.....	76
6.8 Performance.....	77
7. CONCLUSION	79
7.1 Original contributions.....	80
7.2 Future work.....	80
Bibliography.....	81
Apendix I	86

List of figures

Figure 1 – FFF fundamental process [14].	3
Figure 2 – FFF main stages (1) Modeling, (2) Pre-processing (3) production.	4
Figure 3 – ABS molecular formula.	7
Figure 4 – Types of warping, adapted from [45].	8
Figure 5 – Example of (1) Pincushion (2) Curling (3) Trapezoid (4) Blocked shrinkage, adapted from [45].	8
Figure 6 – Local curling examples on ABS, [35], [28] and [49] accordingly.	9
Figure 7 – Illustration of curling deformation, adapted from [49].	9
Figure 8 – Stress distribution on the bottom and top layers, adapted from [15].	10
Figure 9 – Warping measuring methods, adapted from [35],[50],[45],[3],[49],[28] accordingly.	10
Figure 10 – Calculate warping scheme [35].	11
Figure 11 – Printed parts with different filament materials [28].	11
Figure 12 – Influence of Chamber Temperature on warping [4].	12
Figure 13 – Influence of bed temperature on warping, adapted from [35].	12
Figure 14 – Warping deformation with thermos adhesive [49].	13
Figure 15 – Influence of stacking layers section on warping [4].	13
Figure 16 – Evolution of the temperature distribution (1) s=5mm/s (2) s=40mm/s [4].	14
Figure 17 – Influence of different infill on dimension accuracy [43].	14
Figure 18 – Example of different depositing paths along the (1) short boarder (2) long boarder [17].	15
Figure 19 – Most used depositing paths: (1) ZigZag (2) Concentric/Spiral (3) ZigZag with contours [4].	15
Figure 20 – Influence of number of layers on warping, adapted from [4].	16
Figure 21 – PBMA latex film (a) before and (b) after annealing at 90 °C for 30 min [60].	17
Figure 22 – AFM images of PA-6 films (3µm × 3µm): (a) untreated, (b) 60s treated [69].	18
Figure 23 – Illustration of the ironing process.	19
Figure 24 – Effect of ironing on the 1 st , 2 nd and 3 rd layers on warping [3].	19
Figure 25 – Unintended draining problem, adapted from [3].	20
Figure 26 – 6 methodology steps.	21
Figure 27 – Cuboid 30x10x5 mm illustration.	22
Figure 28 – Ultimaker S5 from LAB2ProD.	22
Figure 29 – Ultimaker Cura 4.6.	23
Figure 30 – Cura ironing parameters.	24
Figure 31 – Iron all top surfaces VS iron only highest layer, adapted from [75].	24
Figure 32 – Illustration of Ironing patterns (1) Concentric (2) ZigZag.	24
Figure 33 – Illustration of ZigZag and concentric patterns swapping direction.	25
Figure 34 – Illustration of a high and low line distancing accordingly.	25
Figure 35 – Illustration of (1) Negative inset, (2) Zero inset, (3) Positive inset.	25
Figure 36 – Mid-processing program layout.	26
Figure 37 – Illustration of ironing applied (1) Equally spaced and using (2) Binary list	26
Figure 38 – Illustration of the comparator’s measurement on a warped specimen.	30
Figure 39 – Illustration of the measuring points.	30
Figure 40 – Measurement equipment.	31
Figure 41 – Initial measuring steps.	31
Figure 42 – Comparator’s reset to the precision table.	31
Figure 43 – Illustration of measurement sequence.	32
Figure 44 – Illustration a normal warped specimen (not at scale).	32
Figure 45 – Illustration of under-measuring error.	32
Figure 46 – Illustration of measured dimensions.	33
Figure 47 – Exemplification of the radar chart used in chapter 5.	34
Figure 48 – Results of tests changing bed temperature.	36
Figure 49 – Results of tests changing bed coating.	36

Figure 50 – Specimen results using (1) UHU glue (2) Isopropyl alcohol and (3) Glass cleaner.	37
.....	37
Figure 51 – Results from plate adhesion type tests with (1) skirt and (2) brim.	37
Figure 52 – Illustration of the 3 positioning setups.	38
Figure 53 – Illustration of the ZigZag pattern applied on (1) the first and (2) second layers.	39
Figure 54 – Illustration of the ZigZag pattern modified applied on the (1) first and (2) second layers.	39
.....	39
Figure 55 – Results from using (1) ZigZag pattern and (2) symmetrical ZigZag pattern.	40
Figure 56 – Unfinished first layer on an irregular glass.	40
Figure 57 – Draining problem (1) from Sardinha M. paper [3] (2) from this thesis first tests.	41
Figure 58 – Graded results for the influence of printing temperature on ironed layers.	42
Figure 59 – inset of (1) -7 ; (2) -2; (3) 0; (4) 2 with T=250 °C.	43
Figure 60 – inset of (1) -7 ; (2) -2; (3) 0; (4) 2 with T=220 °C.	43
Figure 61 – T shape used to test the influence of printing shape on ironing.	44
Figure 62 – Illustration of ZigZag printing/ironing pattern.	44
Figure 63 – Warping and consecutive corner melting when applying ironing on the first layer for h=0.1mm.	45
.....	45
Figure 64 – Nozzle sticking to the warped zone for h=0.1mm.	45
.....	45
Figure 65 – Warped specimen with h=0.1mm.	45
.....	46
Figure 66 – Stratified warping for h=0.2mm.	46
.....	46
Figure 67 – Results from tests with (1) ZigZag (2) Concentric pattern at T=250°C.	46
.....	46
Figure 68 – Results from tests with (1) ZigZag (2) Concentric pattern at T=220°C.	46
.....	47
Figure 69 – Undesired ironing lines on a FFF print [78].	47
.....	47
Figure 70 – Results for tests with ironing and h=0.2 mm.	47
.....	48
Figure 71 - Results for tests with ironing and h=0.1 mm.	48
.....	48
Figure 72 – Illustration of section view of the specimen without any ironing process applied (zero).	51
.....	51
Figure 73 – Representation of ironing on the (B1) first, (B2) second and (B3) third layers, accordingly.	51
.....	52
Figure 74 – Illustration (not at scale) of the ironing process with 4 layers in between (C specimens).	52
.....	52
Figure 75 – Illustration (not at scale) of the ironing process with 2 layers in between (D specimens).	52
.....	52
Figure 76 – Illustration (not at scale) of the ironing process with 6 layers in between (E specimens).	52
.....	53
Figure 77 – Ironing illustration (not at scale) of ‘F’ specimens.	53
.....	53
Figure 78 – Ironing illustration (not at scale) of ‘G’ specimens.	53
.....	53
Figure 79 – 60x20x5 mm specimen illustration.	53
.....	54
Figure 80 – Ironing illustration (not at scale) of ‘H’ specimens.	54
.....	55
Figure 81 – Graphic results of (1) dz and (2) dw of A1 tests.	55
.....	56
Figure 82 – A1 specimens.	56
.....	56
Figure 83 – Graphic results of (1) dz and (2) dw of A2 tests.	56
.....	57
Figure 84 – A2 specimens.	57
.....	57
Figure 85 – Specimen with ‘bed over-sticking’.	57
.....	58
Figure 86 – Graphic results of (1) dz, (2) w5&6 and (3) dw of B1 tests.	58
.....	58
Figure 87 – Graphic results of (1) dz, (2) w5&6 and (3) dw of B2 tests.	58
.....	59
Figure 88 – Over-sticking effect on B2 specimens.	59
.....	59
Figure 89 – Side view from one B3 specimen.	59
.....	59
Figure 90 – Graphic results of (1) dz, (2) w5&6 and (3) dw of B3 tests.	59
.....	60
Figure 91 – Scraps on C1 specimens: (1) General and (2) Detailed view.	60
.....	60
Figure 92 – Graphic results of (1) dz, (2) w5&6 and (3) dw of C1 tests.	60
.....	61
Figure 93 – Graphic results of (1) dz, (2) w5&6 and (3) dw of C2 tests.	61
.....	62
Figure 94 – Graphic results of (1) dz, (2) w5&6 + σ 5&6 and (3) dw of C3 tests.	62
.....	62
Figure 95 – C3 (1) non-ironed and (2) ironed specimens.	62
.....	62
Figure 96 – Stratified warping on D specimens.	62
.....	63
Figure 97 – Graphic results of (1) dz, (2) w5&6 and (3) dw of D1 tests.	63

Figure 98 – Graphic results of (1) dz, (2) w5&6 and (3) dw of E1 tests.....	64
Figure 99 – Ironing traces on E specimens (E1.3).....	64
Figure 100 – Graphic results of (1) dz, (2) w5&6 and (3) dw of F1 tests.....	65
Figure 101 – Melted layers on F1 specimens.....	65
Figure 102 – Graphic results of (1) dz, (2) w5&6 and (3) dw of G1 tests.....	66
Figure 103 – Bed over-sticking effect on G1 specimens: (1) General and (2) Detailed view.	66
Figure 104 – Bed over-sticking on a H1 specimen.....	67
Figure 105 – Graphic results of (1) dz, (2) w5&6 and (3) dw of H1 tests.....	67
Figure 106- Relative warping comparison of ironed B specimens.....	70
Figure 107 – Warping reduction on B specimens.....	70
Figure 108 – Comparison of the ‘bed over-sticking’ effect on B series.....	71
Figure 109 – ‘Over-sticking’ effect predominance on B series.....	71
Figure 110 – Relative warping average of C, D and E specimens.....	72
Figure 111 – Warping increase on C, D and E specimens.....	72
Figure 112 – Standard deviation from D, C and E specimens.....	73
Figure 113 – Warping reduction on F and G specimens.....	74
Figure 114 – Warping reduction and standard deviation on B and G specimens.....	74
Figure 115 – Lowest non-ironing relative warping results.....	75
Figure 116 – Over-sticking effect on (a) 30x10x5mm (b) 60x20x5mm specimens.....	75
Figure 117 – Difference between mp 5 and 6 on all setups.....	76
Figure 118 – Difference between mp 1 and 2 on all setups.....	76
Figure 119 – Printing time by setup (in minutes).....	76
Figure 120 – Performance score of specimens A-G on scenario (1).....	78
Figure 121 – Performance score of specimens A-G on scenario (2).....	78
Figure 122 – Performance score of specimens A-G on scenario (3).....	78

List of tables

Table 1 – Slicing software main commands information.....	5
Table 2 – FFF most used filaments general information [31].....	6
Table 3 – ABS generic properties.	7
Table 4 – Summary of the influence of printing parameters on warping.	16
Table 5 – Advantages and Disadvantages of ironing process.....	20
Table 6 – Ultimaker ABS characteristics.....	29
Table 7 – Measuring errors.	33
Table 8 – Formulas to calculate warping.	33
Table 9 – Unit dimensions.....	33
Table 10 – Illustration of the results.	34
Table 11 – Printing parameters to test the best bed coating.	36
Table 12 – Printing parameters for plate adhesion type tests.....	37
Table 13 – Printing parameters for positioning and bed cleaning tests.	38
Table 14 – Warping average and standard deviation for case (1), (2) and (3).	38
Table 15 – Printing parameters for deposition path influence tests.	39
Table 16 – Draining, according to the ironing temperature, grading.....	41
Table 17 – Printing parameters to test the influence of inset in ironing.	42
Table 18 – Printing parameters to the test the effect of changing the printing shape on ironing.	44
Table 19 – Printing parameters to test the influence of deposition path.	46
Table 20 – Printing parameters to the test the effect of printing height on ironing.	47
Table 21 – Fix parameters list.	48
Table 22 – Summary of the printing parameters of non-ironing layers.	49
Table 23 – Theoretical warping outcome according to the chosen printing parameters.	50
Table 24 – Summary of ironing parameters.....	51
Table 25 – Warping (dw) results from A1 tests.	55
Table 26 – Warping (dw) results from A2 tests.....	56
Table 27 – Warping (dw) results from B1 tests.....	57
Table 28 – Warping (dw) results from B2 tests.....	58
Table 29 – Warping (dw) results from B3 tests.....	59
Table 30 – Warping (dw) results from C1 tests.....	60
Table 31 – Warping (dw) results from C2 tests.....	61
Table 32 – Warping (dw) results from C3 tests.....	62
Table 33 – Warping (dw) results from D1 tests.....	63
Table 34 – Warping (dw) results from E1 tests.....	63
Table 35 – Warping (dw) results from F1 tests.....	64
Table 36 – Warping (dw) results from G1 tests.....	66
Table 37 – Warping (dw) results from H1 tests.....	67
Table 38 – Comparison of the warping results of the non-ironed tests.....	69
Table 39 – B specimens overall results.	70
Table 40 – C, D and E specimens overall results.	72
Table 41 – F and G overall results.	73
Table 42 – Final score comparison table.	77
Table 43 – Weights of each scenario.....	77

Nomenclature

1D	One-Dimensional
2D	Two-Dimensional
3D	Three-Dimensional
ABS	Acrylonitrile Butadiene Styrene
AM	Additive manufacturing
ASTM	American Society of Testing and Materials
CAD	Computer Aided Design
FFF	Fused filament fabrication
IJM	Inkjet modeling
LAB2ProD	Product Development Laboratory from Instituto Superior Técnico
PETG	Polyethylene Terephthalate Glycol
PLA	Polylactic Acid
RP	Rapid Prototyping
SLM	Selective Laser Melting
SLS	Selective Laser Sintering
UV	Ultra-Violet

Glossary

accel	acceleration
\overline{dw}	Absolute warping average in millimeters
dw	Absolute warping in millimeters
dz	Height measured by the comparator in millimeters
h	Height in millimeters
int.	Interval
mp	Measuring point(s)
mpp	Mid-processing program
Ra	Roughness
T	Temperature, measured in °C
T_{bed}	Bed temperature, measured in °C
w	Relative warping in percentage
zero	Non-ironed specimen
σ	Standard deviation in millimeters

1. INTRODUCTION

This chapter describes the underlying reasons for the creation of the present work and explains the relevance and the aims of its subject.

1.1 Motivation

At first computers were far behind today's devices that can easily be carried anywhere inside each one's pockets. Actually, their acceptance as everyday gadgets did not occur, until it was proved that a number of their tasks might be accomplished here and now. Accordingly, their usage has surpassed the ordinary academic or big business areas. Similarly, 3D printers are following a comparable process, as they are changing from mostly business tools into more reasonable and faster desktop type appliances.

Additive Manufacturing (AM) assumes an indisputably important function in today's world. Cited by Forbes, Wohlers Report 2020 [1] states that expects: "(...) the revenue to climb to \$23.9 billion in 2022, and \$35.6 billion in 2024" [1].

AM has become a useful technique in a wide variety of applications, including: prototyping, tissue engineering, materials for energy, chemistry reaction ware, molecular visualization, microfluidics, and low-density, high-strength materials [2].

With such a notable influence these days as well as a remarkable development ability, AM assumes itself as a stimulating and attractive area for research. The present thesis is rooted in and was determined by the drive of giving some contribution to this area development, as well as to its further enhancement and progress.

Among the many different AM processes, the present work will focus on Fused Filament Fabrication (FFF), not only because this is one of the most used AM technologies, but also because the resources which are available at Instituto Superior Técnico (particularly at the Product Development Lab) proved to be suitable and useful for doing so.

AM comes with some disadvantages (e.g. cost, superficial finish, long duration) and internal cooling stresses is one of them. This phenomenon is very visible when the printed parts dimensions differ a lot from the expected, a theme that will be introduced further on, but that for the moment will be referred as 'warping'.

In order to solve the warping problem, this study examined the performance of applying a heat treatment called 'ironing process' or just 'ironing' [3]. Ironing is a superficial heat treatment available on slicer software which enables the heated nozzle to travel over printed layers with reduced or even no extrusion remelting the surface.

1.2 Objectives

This thesis was aimed to better understand the warping phenomenon and study the influence of ironing on FFF parts. Therefore, the following objectives were to be achieved:

1. Provide an overview on FFF technology
2. Explore the esthetical problems of printing with ABS
3. Understand the impact of FFF parameters on warping
4. Achieve constant and controlled warped specimens

5. Ascertain ironing influence on warping
6. Conclude its usability for the industry

1.3 Document outline

The present document is structured as follows:

Chapter 1, Introduction: this section describes the underlying reasons for the creation of the present work and explains the relevance and the aims of its subject.

Chapter 2, State of the art: provides an overview on AM and FFF, explores the problems associated with FFF and benchmarks the existing treatments.

Chapter 3, Methodology: covers the methodology used during the project.

Chapter 4, Experimental Procedure: explains the fixed parameters and the methodology-guided tests performed.

Chapter 5, Results: presents the results obtained from the printed parts.

Chapter 6, Results analysis: the results are compared.

Chapter 7, Conclusions: discloses conclusions and future work to be done.

2. STATE OF THE ART

This chapter provides an overview on AM and FFF, explores the problems associated with warping in FFF and benchmarks the existing treatments. To do so, an analysis across the existing literature, for instance, papers, thesis, articles, books and websites, was performed.

2.1 Additive Manufacturing

Initially called Rapid prototyping (RP), this technology started when Hideo Kodama, in 1981, published his account of a functional rapid-prototyping system using photopolymers. In 1984, Charles Hull made 3D-printing history by inventing stereolithography which allowed designers to create 3D models using digital data. As the technology improved, other fabrication methodologies were created: Fused filament fabrication (FFF) [4], Selective laser sintering (SLS) [5], Selective laser melting (SLM) [6], Inkjet modeling (IJM) [7], among others. Details about these methods, advantages and disadvantages have been studied ever since [8].

Nowadays, AM is defined by ASTM as the "process of joining materials to make objects from 3D model data, usually layer upon layer, as opposed to subtractive manufacturing methodologies" [8]. The norm that establishes the terms used in Additive Manufacturing is ISO / ASTM 52900 [9].

An intensive study in 2018 analyzed the different sectors [10] giving the biggest potential growing scores to the: industrial [11], medical [12], air and spacecraft [13].

2.2 Fused Filament Fabrication

In fused filament fabrication (FFF) the head system attached to a carriage heats a thermoplastic material (supplied by the feeder) to a semi-molten state and extrudes a filament through the hot-end in a raster configuration. The hot-end moves according to a toolpath limited by the part cross-sectional boundary and material is deposited into the build plate layer by layer [4,14,15], as Figure 1 illustrates.

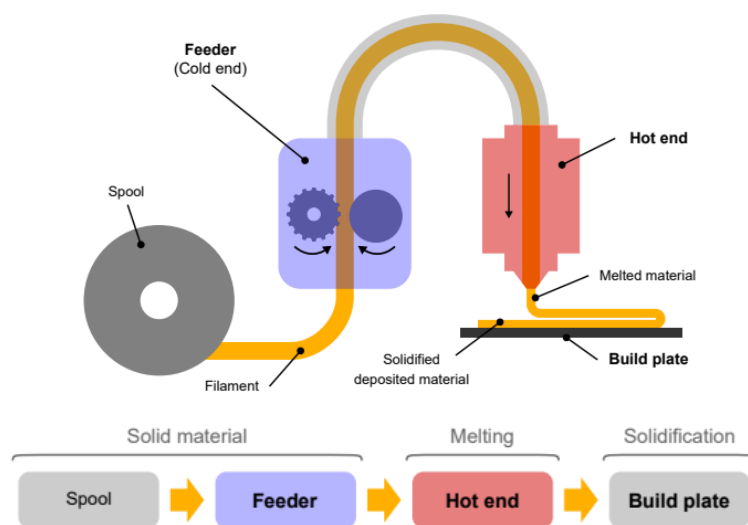


Figure 1 – FFF fundamental process [14].

Heat is dissipated by conduction and forced convection and the reduction in temperature caused by these processes causes the material to quickly solidify onto the surrounding filaments [16].

Bonding between the filaments is caused by local re-melting of previously solidified material [17]. Even so, the re-melting and rapid cooling may aggravate non-uniform thermal gradients, which potentiate residual stresses responsible for the part distortions [15].

FFF is one of the most widely used AM methods since it is able to fabricate very complex three-dimensional shapes with a decent variety of thermoplastic polymer material available, compact, low maintenance cost, good absolute tolerances (less than ± 0.1 mm), easy material adaptation, no need for supervision and requires a low investment when compared to normal producing methods [18,19].

In contrast, the main drawbacks of FFF technology are due to the fact that temperature fluctuations during the printing work could lead to high surface roughness, vertical anisotropy, step-structured surface and warping deformation particularly if compared to other traditional manufacturing technologies [8,19].

2.2.1 Main stages

FFF can be identified by these 3 main required stages [20]: Modeling, Pre-processing and Production, as Figure 2 illustrates.

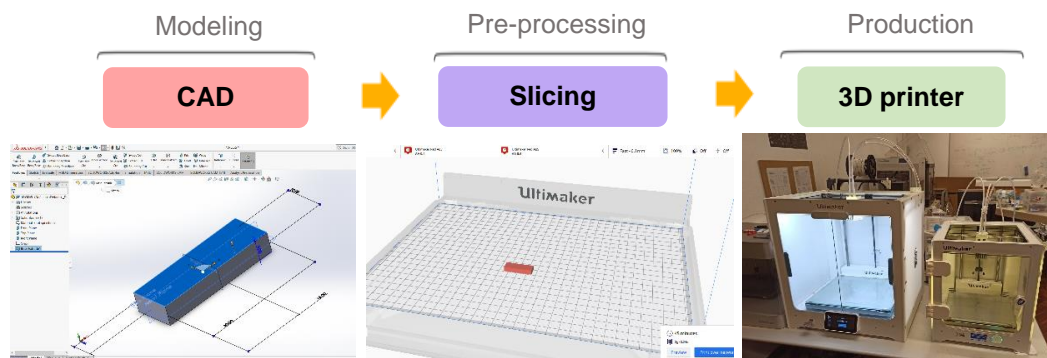


Figure 2 – FFF main stages (1) Modeling, (2) Pre-processing (3) production.

2.2.1.1 Modeling

A digital 3D model is designed with a 3D-CAD software and converted into a standard file format.

CAD is the use of computers (or workstations) to aid in the creation, modification, analysis, or optimization of a design [21]. CAD software is used to increase the productivity of the designer, improve the quality of design, improve communications through documentation, and to create a database for manufacturing [22].

There are a large variety of 3D-CAD software depending on the field of study. For mechanical engineering, the most used are Solidworks, Solidedge and Catia [23,24].

2.2.1.2 Pre-processing

After the CAD model is completed, the printing specifications (e.g. printing speed, nozzle temperature) are set using a slicing software.

The slicing software, also called slicer, is a computer software used in the majority of 3D printing processes for the conversion of a 3D object model (e.g. 3MF file) to specific instructions for the printer [25].

It starts by dividing the object in a stack of flat layers and then describes these layers as linear movements for the extruder to follow. Together with some specific process parameters commands, the movements are finally coded into the g-code file that can afterwards be read by the printer [26].

The user may edit hundreds of commands from which the most usual ones are: the layer height, line width, infill pattern, infill density, printing temperature, bed temperature, build plate adhesion type and printing speed (Table 1).

Table 1 – Slicing software main commands information.

MAIN COMMANDS	UNIT/LIST	OBSERVATIONS	AFFECTS [27]
Layer Height	mm	Higher values produce faster prints in lower resolution Thin layers have smoother surface than thick layers [28]	Number of layers, Printing time
Line Width	mm	Generally, the width of each line should correspond to the width of the nozzle. However, slightly reducing this value could produce better prints [27]	Printing time, Infill deposition path
Infill Pattern	Grid, Lines, Cubic, Octet, Concentric, ZigZag, Gyroid, etc	The <i>Lines</i> and <i>ZigZag</i> patterns swap direction on alternate layers. <i>Gyroid</i> , <i>Cubic</i> and <i>Octet</i> infill change with every layer to provide a more equal distribution of strength over each direction [27]	Infill line distances, Infill overlap, Printing time
Infill Density	%	100% infill density corresponds to a solid material. Different infill densities conjugated with infill patterns may produce parts with identical mechanical properties but with less material than a solid one [29]	Infill line distance, Infill overlap, Printing time
Printing Temperature	°C	Ideal temperatures depend deeply on the material [30]	-
Bed Temperature	°C	Used only for certain materials [31] If this is 0, the bed temperature will not be adjusted [27]	-
Build Plate Adhesion Type	Brim, Raft, Skirt	Brim adds a single layer flat area around the base of your model. Raft adds a thick grid with roof below the model. Skirt is a line printed around the model, but not connected to the model [27]	Printing time
Printing Speed	mm/s	Higher speeds reduce the time of printing but have lower quality [32]	Infill speed, Printing time

2.2.1.3 Production

In this stage the object is formed layer-by-layer by a FFF until the model is finished. A FFF printer is, in most cases, composed by a head system attached to a carriage moving in the horizontal x–y plane, supplied by the feeder, extruding a filament through the nozzle in a raster configuration [4,15]. These machines exhibit a large variety of properties and functionalities: The first difference to consider is the axis configuration. The majority of 3D printers use Cartesian coordinates, but some have cylindrical, delta or even other configurations [33].

For the printers using cartesian coordinates, a very noticeable difference is the moving axis. The majority of low-cost 3D printers use XZ moving head and a moving platform in Y, whereas the majority of high-cost printers prefer XY moving head with the platform moving on the Z axis [14].

Another noticeable difference is the placement of the feeder in relation to the hot end. Some have their feeder and the hot-end assembled together in one single part ('Direct extrusion'), whereas others have their feeder and hot-end physically separated and connected by a guide tube ('bowden extrusion') [14].

Its inputs are the filament, electricity and the g-code produced by the slicer, and its output is the 3D completed part.

Commercially, a variety of traditional feedstock thermoplastic filament materials are supported by FFF based 3D printers, which make them ideal for the consumer market, including acrylonitrile butadiene styrene (ABS) [28].

2.2.2 Materials

Since FFF technology is widely used in the manufacture of prototypes and they are subjected to various resistance tests, it is important that the materials have good mechanical performance. Properties such as yield strength, modulus of elasticity, ductility and hardness are usually considered when choosing the material. There are some less common properties such as transparency (or the opposite, opacity), biocompatibility and UV resistance, which are relevant for certain applications [34].

A wide variety of materials are available nowadays (e.g. ABS), the most used ones nowadays are presented at Table 2.

Table 2 – FFF most used filaments general information [31].

FILAMENT	PROPERTIES	USED FOR	STRENGTH	FLEXIBILITY	DURABILITY	PRINT TEMP. (°C)
PLA	Easy to print, Biodegradable	Consumer products	Medium	Low	Low	180-230
ABS	Durable, impact resistant	Functional parts	Medium	Medium	Medium	210-260
PETG	More flexible than the previous, durable	All	Medium	High	High	220-235
NYLON	Strong, Flexible, Durable	All	High	High	High	220-260
TPE	Extremely flexible, rubber-like	Elastic parts, Wearables	Low	High	Medium	225-235

Some materials can relatively easily meet the conditions for manufacturing whereas others require a challenging adjustment of parameters. ABS (Acrylonitrile Butadiene Styrene) and PLA (Poly Lactic Acid) resin materials for industrial plastics are the most commonly used in manufacturing parts with FFF 3D printers [35–38].

These thermoplastic filament materials are particularly suitable for FFF since they are easily manageable in their pre-fusion state at low temperatures, steadily harden as they cool down at glass transition temperature and revert back to their initial properties [2].

On the one hand, Polylactic acid (PLA) is a thermoplastic aliphatic polyester with molecular formula $(C_3H_4O_2)_n$ derived from renewable resources and manufactured out of plant-based materials, on the other hand, Acrylonitrile Butadiene Styrene (ABS) is also a thermoplastic material displaying a much more complex formula and it is manufactured out of oil-based materials [28].

Both these materials have reinforced versions. PLA+ is an optimized thermoplastic filament material with toughness ten times higher than normal PLA, whereas reinforced ABS (ABS+) has higher toughness, hardness, rigidity, oil resistance and heat resistance than usual ABS [28].

ABS+ is merely a commercial designation that does not offer further indications on the material composition. This filament was created aiming to reduce the sensitivity to shrinkage and warping of ABS, while preserving most of its performance advantages, that is why it is known as “low-warp” ABS [39]. However, such pros come with a higher selling cost than the normal ABS. Companies normally prefer preventing this problem (warping) by using a more cost-effective strategy therefore ABS+ is not as used as ABS [28].

2.2.2.1 ABS

Acrylonitrile butadiene styrene (ABS) is produced from oil-based materials and its molecular formula, visible on Figure 3, is the combination of: Acrylonitrile ('A'), Butadiene ('B') and Styrene ('S') [28].

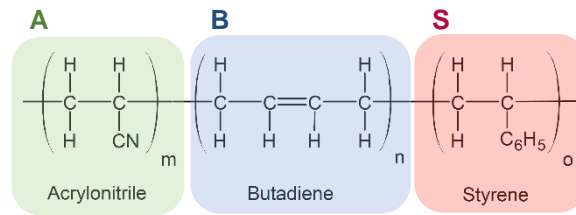


Figure 3 – ABS molecular formula.

A, B and S partial molecule can vary in molar percentage, from 15% to 35%, from 5% to 30% and from 40% to 60% respectively.

ABS is widely used due to its accessibility, high fracture toughness, high impact resistance, low density, wide melting scope, strong thermal–chemical stability and very good finishes [4,40]. Some drawbacks of this material include degrading with sunlight, so it can only be used indoors and at a high heat deflection temperature [12,40].

ABS takes approximately 0.55s to cool down from the melting temperature of 270°C to the glass-transition temperature of 94°C (nozzle with a diameter of 0.254 mm) and for a medium printing speed of 30 mm/s, the time for finishing a layer of a middle-size prototype is much longer than the fiber cooling time [4].

The properties of ABS may vary from brand to brand, Table 3 presents the main properties found in the literature.

Table 3 – ABS generic properties.

SPECIFICATION	UNIT	INTERVAL	SOURCES
Glass-Transition Temperature	°C	85-105	[4,41,42]
Density	g/cm ³	1.0-1.4	[4,28,42]
Distortion Temperature	°C	78	[28]
Tensile Strength	MPa	27-43	[28,42]
Bending Strength	MPa	22	[28]
Flexural Modulus	MPa	66-71	[28,41]
Izod Impact Strength	KJ/m ²	10-19	[28,41]
Young's Modulus (E)	MPa	2230	[4]

The most important printing specifications for ABS are the printing temperature and the bed temperature [38]. The recommended printing temperature is from 215°C to 260°C [28,43] whereas the recommended bed temperature is between 50°C and 110°C [35].

2.2.3 Warping

Warping (δ) is a distortion where the surfaces of the printed part do not follow the intended shape of the design. Warping is caused by residual stresses on the printed material that are generated during the cooling process. If the cooling process is not uniform, some regions of the part will be subjected to stress and possibly deform [3].

For ABS, processes involving rapid temperature gradients (e.g. the phase changes from liquid to solid upon solidification) develop internal stresses, the material decreases its specific volume and

consequently results in shrinkage and warp of the printed component [4,44]. As the inner stresses accumulate throughout the piece they affect the prototype size precision, bringing about prototype deformation and inner-layer delaminating or cracking. Moreover, they destroy the supporting structures between the main body of the prototype and the worktable, and even cause fabrication failure [4].

These warping distortions in the material can be divided into 4 types: Pincushion effect, Trapezoid deformation, Curling and Blocked shrinkage [38,45] as Figure 4 and Figure 5 illustrate.

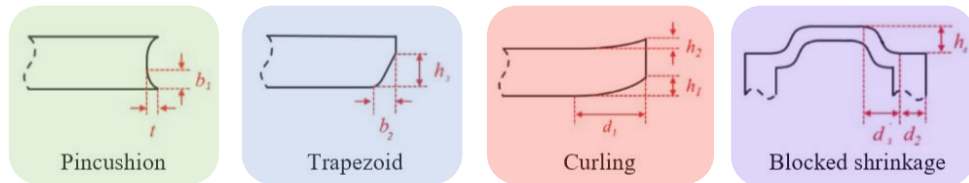


Figure 4 – Types of warping, adapted from [45].

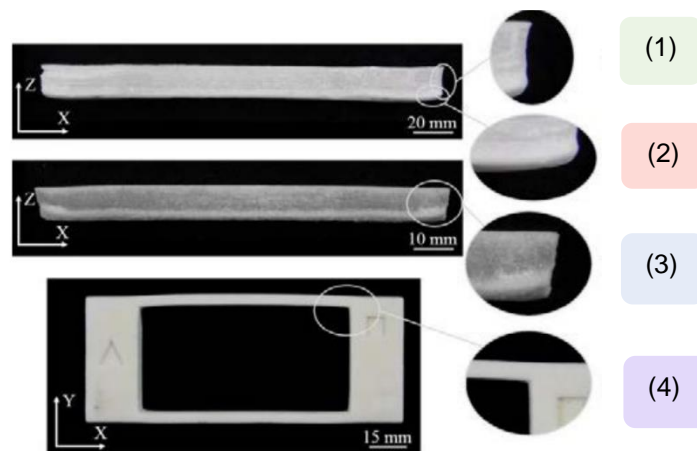


Figure 5 – Example of (1) Pincushion (2) Curling (3) Trapezoid (4) Blocked shrinkage, adapted from [45].

(1) Pincushion

Solidification is completed on the surface faster than in the inner regions leading to a subsidence of side planes in these areas of the component [45].

(2) Curling

Time delayed shrinkage of the separate part layers leads to different elongations and residual stresses in the part, causing an upward bending [46]. The curling effect occurs particularly in the components' edge regions [45].

(3) Trapezoid deformation

Down skin surfaces contract without the interaction with adjacent layers. The delayed shrinkage of further layers on the one hand leads to an additional compression of printed layers below. On the other hand, the shrinkage of subsequently printed layers is inhibited by force transmission, thus distortion is induced [45].

(4) Blocked shrinkage

In case the product has cavities, enclosed under-solidified material causes a resistance against the contraction of the part, which results in a distortion of the part due to its geometry [45].

Not all warping distortions types influence ABS parts equally, being blocked shrinkage and curling the most common and relevant [38,45,47]. Additionally, these conclusions are relatively constant across most of the other filaments [38].

2.2.4 Curling

As explained earlier, curling and blocked shrinkage are the most noticeable types of warping [38] and, consequently, the most studied phenomena [45].

As explained earlier, curling is formed by the different elongations and residual stresses in the part, leading to an upward bending, comparable to a bimetal [48].

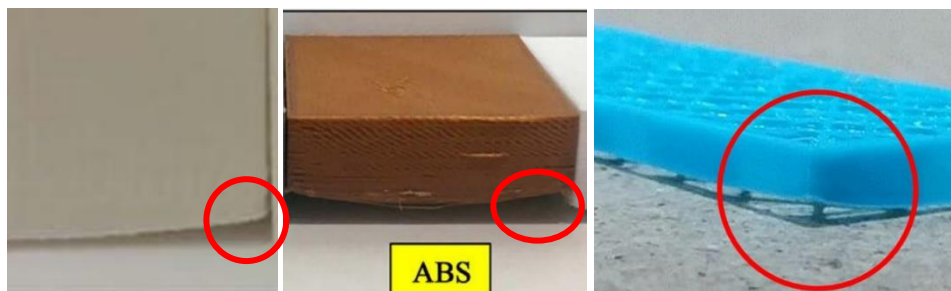


Figure 6 – Local curling examples on ABS, [35], [28] and [49] accordingly.

Curling usually takes place when the first layer does not stick well to the printing platform due to lack of adhesion [38] and it can be seen in Figure 6 that the curling effect particularly occurs in the component's edge regions.

Part distortions are related to the stress accumulation during the deposition [17]. In the interior part of the specimen, stresses can relax by creeping effects due to low strength values of the material at the beginning of the solidification reaction (Figure 7). Contrarily, less relaxation of the internal stresses in the corners tends to occur hence more internal stresses and more curling [45].

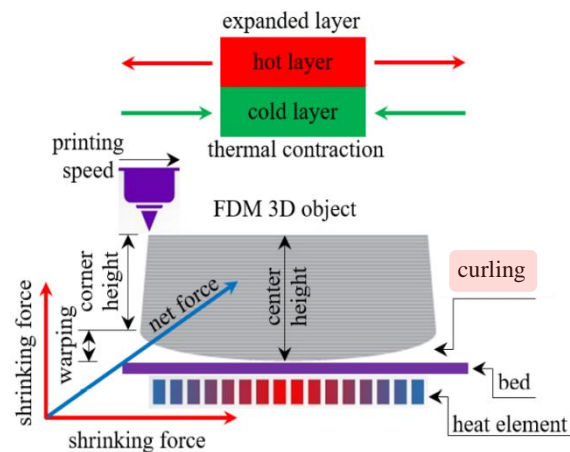


Figure 7 – Illustration of curling deformation, adapted from [49].

A good visual example of the accumulation of stress in the corners and specifically on the bottom of the specimen was conducted by Zhang (2006) [15] and it is visible on Figure 8.

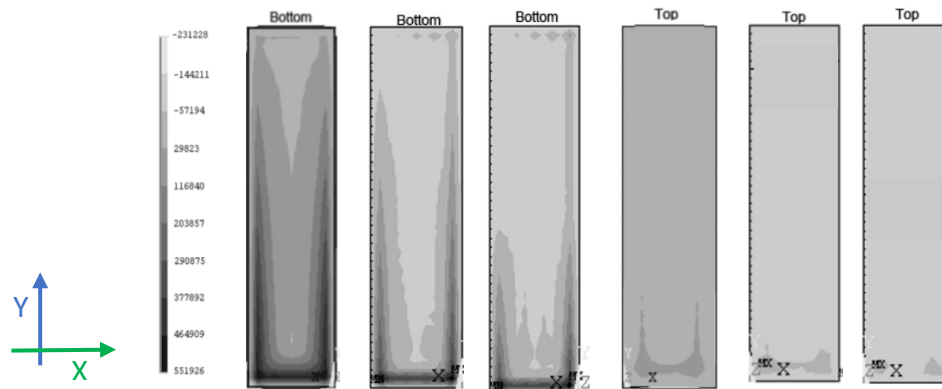


Figure 8 – Stress distribution on the bottom and top layers, adapted from [15].

The first layer is the most affected by thermal stresses and as the part is built, the stress decreases.

Since this is the problem this study intends to address, the term “warping” and “curling” will be used with the same meaning: referring to the deformation on the corners of the specimen.

2.2.4.1 Measuring

Warping can be difficult to measure since it is a 3D deformation, so the literature opted by different approaches (Figure 9):



Figure 9 – Warping measuring methods, adapted from [35],[50],[45],[3],[49],[28] accordingly.

Measuring in 3D and comparing directly with the CAD design as a whole, even in complex designs. Able to measure 3D curvatures and distances, roughness, small details in the XYZ. Examples: 3D optical scanning (e.g. COMET 6 8M from ZEISS Optotechnik) [35] and X-ray scanning (SkyScan 1172 X-ray micro-CT system from Bruker Corp.) [50].

Measuring in 2D, being only able to compare the original distances with the superficial ones. Only applicable to symmetrical specimens. Able to measure 2D curvatures and distances. Examples: industrial laser scanning (e.g. ScanControl 2700 from Micro-Epsilon) [45] and laser scanning from a commercial printer (e.g. HP OfficeJet 4630) [3].

Measuring in 1D, being only able to tell the distance between very specific points on the edges of the specimen. Examples: Digital vernier height gauge [49] and Digital Vernier caliper gauge [28].

2.2.4.2 Calculating warping

Finding a way to compare warping can be challenging. The most frequently used method by the literature ([3,35,38,45,49]) to calculate it uses a 2D method and is represented on Figure 10.

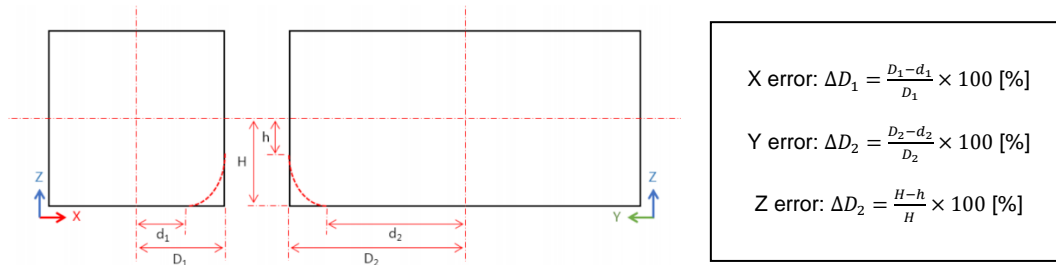


Figure 10 – Calculate warping scheme [35].

Measuring warping this way does not consider the alterations of form other than in the boundaries of the specimen. In case the deformations in the Z direction are too considerable, the values of H and h should be measured from the top of the specimen.

2.2.4.3 Dependence

Having direct correlation of any physical variable and warping can be time-consuming since there are too many variables to consider. Nevertheless, some correlations have been achieved by the literature.

Material

Warping largely depends on the material, among other reasons, it increases with the thermal expansion coefficient and linearly increases with increasing material linear shrinkage rate [4], being less severe in Poly-lactic acid (PLA) than in ABS, for example [3].

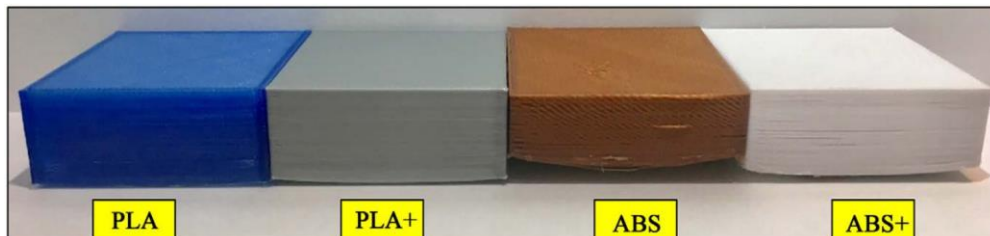


Figure 11 – Printed parts with different filament materials [28].

On Figure 11 it is possible to see the much higher prevalence of the effect on ABS compared with the others.

In fact, literature affirms that PLA presents approximately ten times less warping than ABS [3,28,38].

Even though it is hard to compare different materials since they act differently according to different solicitations, there are already some studies regarding warping on various materials [3,28,47,51].

From the most used FFF materials, warping on materials such as PLA, PETG and TPE is neglectable [28,31,52]. Contrarily, ABS and Nylon seem to be deeply affected by this problem, being it even more aggressive on Nylon than with ABS [50,51].

Heating cycles

According to Y. Zhang and K. Chou [17] heating and rapid cooling cycles of the material results in non-uniform thermal gradients, which causes a stress build-up that leads to distortions. So, if we reduce the printing gradient of temperatures, we can expect less warping.

Chamber temperature

To reduce the shape errors resulting from the heat shrinkage in manufacturing ABS parts with the FFF-based 3D printing, the temperature settings for the inside and outside of the chamber are highly important [35].

T. M. Wang, J. T. Xi, and Y. Jin [4] concluded that warp deformation linearly decreases with increasing chamber temperature, as Figure 12 shows.

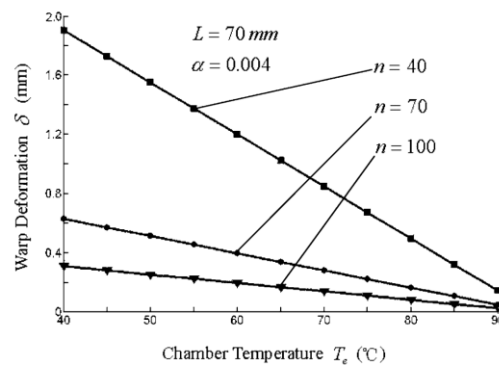


Figure 12 – Influence of Chamber Temperature on warping [4].

These results tend to assume that increasing the chamber temperature would decrease warping, which is true, however, when the chamber temperature is rising, the solidifying time of the deposited material will be prolonged, which may influence the quality of the depositing layer due to the surface not having entirely solidified [4]. A compromise must be achieved here.

Bed temperature

The 3D printing bed temperature is sometimes forgotten, probably because it varies from material to material needing it or not, but it plays a crucial role concerning warping in ABS.

M. A. Nazan [38] addressed this topic, comparing specimens with and without heated bed for ABS, having achieved drastically different results. As it was expected, for the same reasons concerning the chamber temperature, having heated bed decreases warping.

Yet, addressing the same goal in a more detailed way, the influence of the bed temperature on the relative warping for different bed temperatures: 50°C, 70°C, 90°C, and 110°C achieved the results present on Figure 13 [35].

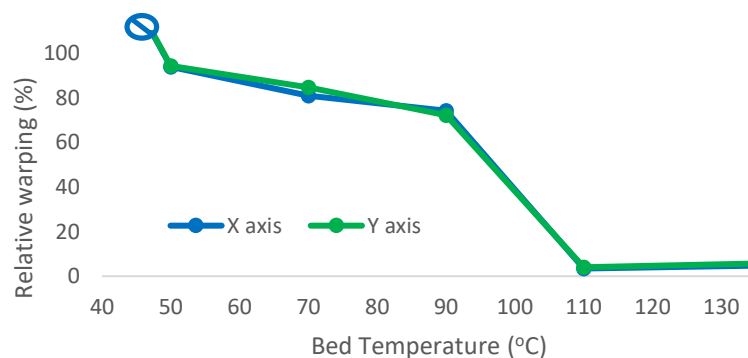


Figure 13 – Influence of bed temperature on warping, adapted from [35].

Note that in this study, the relative warping of the ABS specimen substantially increased when the temperature of the bed was 40°C or lower. As a consequence, inter-layer adhesion hampered, the layers were separated from one another and the printing failed [35].

When the temperature of the bed was 50-90°C the shape errors due to the heat shrinkage remarkably decreased. The bed temperature at 110°C surpasses the ABS's softening point of 104°C (at least the ABS used in this paper), which oversoftens the material resulting in little heat shrinkage [35].

Printing temperature

The nozzle temperature is one of the most important printing parameters [38]. M. S. Alsoufi and A. E. Elsayed [49] studied nozzle temperatures of 180, 190, 200, 210 and 220°C applying a “synthetic thermal adhesive” above the printing glass. The results for ABS are visible on Figure 14.

Nozzle Temperature (°C)	Total Height (mm)	Deflected Height / Warping Deformation (mm)								Mean±SD	overall error (%)
		Corner 1	error (%)	Corner 2	error (%)	Corner 3	error (%)	Corner 4	error (%)		
180	5.00	4.62	7.6	4.25	15	4.51	9.8	4.85	3	4.56±0.25	8.85
190	5.00	4.88	2.4	4.45	11	4.65	7	4.78	4.4	4.69±0.19	6.2
200	5.00	4.81	3.8	4.77	4.6	4.69	6.2	4.70	6	4.74±0.06	5.15
210	5.00	4.88	2.4	4.77	4.6	4.81	3.8	4.51	9.8	4.74±0.16	5.15
220	5.00	4.90	2	4.75	5	4.62	7.6	4.82	3.6	4.77±0.12	4.55

Figure 14 – Warping deformation with thermos adhesive [49].

According with these results, the overall error decreases with the temperature. Additionally, except for the results obtained with T=200 °C, increasing the nozzle temperature also shows more consistent results (with lower standard deviation) too.

Both these conclusions seem to indicate that increasing the printing temperature (for this temperature range and for a constant coating) decreases warping [49,53].

Length of the stacking section

Stacking section length (L) is the path length performed by the nozzle until it changes direction. The relationship between this length and warping was an aspect of study to T. M. Wang, et al. [4] and its findings are visible in Figure 15.

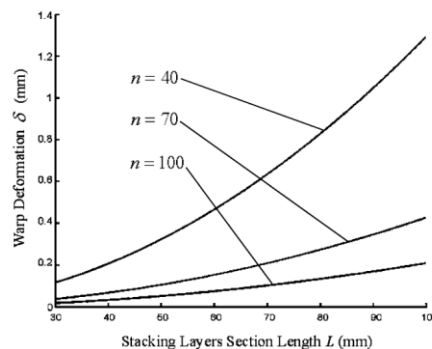


Figure 15 – Influence of stacking layers section on warping [4].

For a fixed number of layers (n), it can be concluded that increasing the stacking length (L), increases the warping deformation (δ) [4,53]. Additionally, the length of the stacking section is strongly correlated with the deposition path so it is a variable to keep in mind when choosing it [17].

Printing Speed

The printing speed is the speed at which the printing nozzle glazes the surface of the specimen. Printing speed is given as one of the most important factors concerning internal residual stresses and consequently warping [17]. This speed is directly correlated with the printing time, that is, higher printing speeds lead to lower printing times and vice-versa.

What might not seem so obvious is the relation between the printing speed and residual stresses: at slower speeds (e.g. $s=5\text{mm/s}$) the heat transferred to the specimen is concentrated at the same region for a longer period of time, creating a better uniformization of residual temperatures across the specimen [4]. Contrarily, if we consider high speeds (e.g. 40mm/s) the heat region becomes longer and less deep which potentiates residual stresses [4]. Figure 16 illustrates the temperature internal distribution for both speeds.

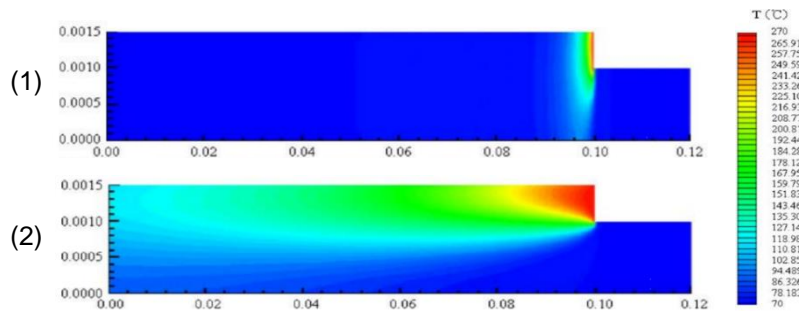


Figure 16 – Evolution of the temperature distribution (1) $s=5\text{mm/s}$ (2) $s=40\text{mm/s}$ [4].

Faster printing speed leads to larger porosity and residual stresses, as well as higher shrinkage after specimen thermal treatments, concluding that as printing speed increases so does warping [4,17].

Layer thickness and Road width

Simulations indicate that the stress accumulations increase with increasing layer thickness [53,54]. Consequently, warping increases also, even though the relation is not linear [17,53].

The road width alone does not affect the residual stress and part distortions in a statistically significant manner [17]. However, the interaction between the road width and the layer thickness seems to be as significant as the layer thickness itself to part distortions but a quantitative correlation is yet to be established [17].

Infill density

Literature seems to have identified accurately the impact of different infill densities on warping, being consensual that the higher the infill density, the higher the dimensions deviation obtained [3,43,50].

For a specific squared part with a hole, it is possible to realize that the higher the infill density, the higher the dimension deviation watched [43].

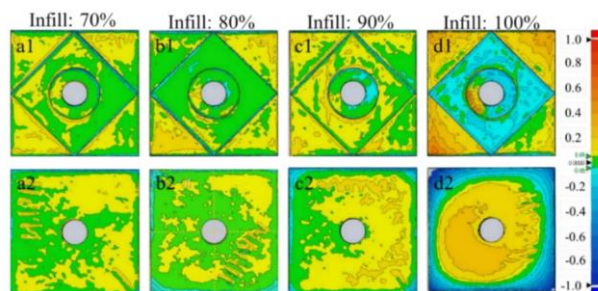


Figure 17 – Influence of different infill on dimension accuracy [43].

Figure 17 allows to identify the most common areas where the dimensional accuracy tends to be lower, which endorses the idea that warping is more accentuated on the corners of the part.

Depositing path

The pattern used to deposit a layer of material has a significant effect on the deflection of the manufactured part [55]. As referred earlier, warp deformation with the depositing path along the short border is much smaller than along the long border, so the depositing path has to be chosen accordingly [17].

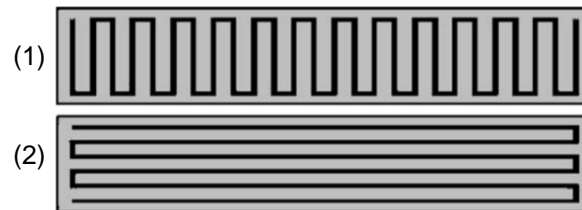


Figure 18 – Example of different depositing paths along the (1) short boarder (2) long boarder [17].

Figure 18 illustrates an example of what the authors means by (1) short boarder and (2) long boarder. Given the complexity of most 3D printed shapes it would be difficult to arrive at the best depositing path scenario applicable to all shapes, so this analysis is only focusing on: beams and plates.

Slicing software (e.g. *Cura*) normally do not advise printing multiple layers using the same depositing path since it could amplify the distortions associated with long deposition paths but for the special case of beams, a raster pattern with lines oriented 90° from the beam's long axes produces the lowest distortions [55].

Alternating the printing direction path between layers has proven to be more effective in reducing warping compared with using same direction paths, for most of the specimens. Illustrated on Figure 19, the most used depositing paths are: ZigZag, Concentric and ZigZag with contours [3,4,55].

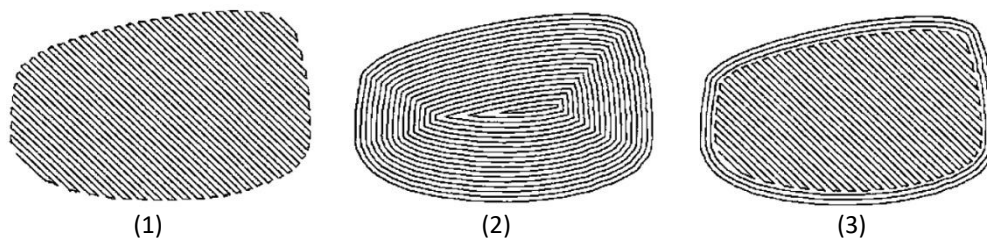


Figure 19 – Most used depositing paths: (1) ZigZag (2) Concentric/Spiral (3) ZigZag with contours [4].

In concentric filling method (2) the boundary of a layer is successively offset until it fills the entire domain. For a plate geometry, the spiral pattern scanned from the outside to the inside produces the lowest and most uniform distortions [55].

ZigZag path (1), the ordinary name given to $\pm 45^\circ$ raster angles, usually suffers from inaccuracies in deposition and bad quality surface [4]. This method is usually compared to parallel deposition paths ($0^\circ/90^\circ$), having less warping for a generic specimen than this last one [3,50].

The combination of the contour and raster methods (3) employs contours to fit the boundaries and raster to fill inside them. It yields good surface quality with a shorter build time. The contours are usually called 'perimeters' and their number often vary depending on the application [4].

There is no evidence indicating significant differences in warping with (3) or without (1) contours using ZigZag path [4].

Number of layers

As previously referred, for a fixed layer section length (L), decreasing the layer height decreases warping and increases the number of layers needed. As Figure 20 shows, increasing the number of layers seems to produce less warping [4,53].

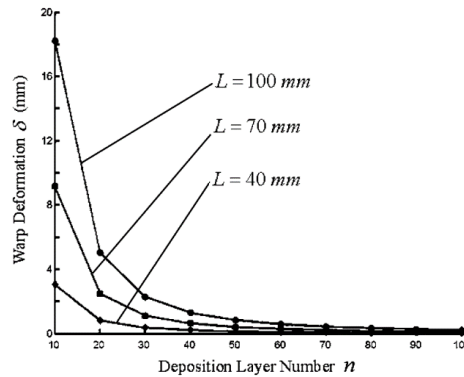


Figure 20 – Influence of number of layers on warping, adapted from [4].

Summary

Warping is an important index to evaluate the quality of a fused filament fabrication (FFF) prototype [4]. Warping depends on the material and its thermal expansion coefficient, being less severe in Polylactic acid (PLA) (less than 3%) than in ABS (up to 34.53%) [3].

The literature research revealed that there is a satisfactory number of studies concerning this subject for ABS. However, the majority of the individual printing parameters has very few papers dedicated to them. Table 4 summarizes the influence of the printing parameters on warping.

Table 4 – Summary of the influence of printing parameters on warping.

	If	Warping	Source
Layer thickness	↑	↑	[17,53,54]
Road width	↑	↑↓	[17]
Time of cooling cycles	↑	↓	[17]
Chamber temperature	↑	↓ ¹	[4]
Printing temperature	↑	↓ ¹	[49,53]
Bed temperature	↑	↓ ¹	[35,38]
Stacking section length	↑	↑	[4,17,53]
Number of layers	↑	↓	[4,53]
Path alongside the border	↑	↑	[17]
Infill density	↑	↑	[3,43,50]
Printing speed	↑	↑	[4,17]
Porosity	↑	↑	[50]
90°/0° or 0°/0° or 90°/90°	-	↑	[3,4,55]

In short, warping increases with the length of the stacking section, layer thickness, porosity, printing speed and infill density. Nevertheless, warping decreases with the time of cooling cycles, the chamber temperature, the bed and the printing temperatures since warping is caused by thermal stresses, a good adhesion between parts and printing table helps to decrease it.

¹ Warping decreases until a certain point.

2.3 Heat treatments

Heat treatments have been used since mankind took control of fire, however the understanding of science and underlying principles of various metals and metal alloy systems have only been significantly developed over the past 75 to 100 years [56].

Heat treatments are likely to be considered for several reasons: mechanical strengths, guarantee precision stable dimensions, esthetics, among others [57] and for numerous materials: pure metals or alloys, polymers, ceramics and glasses. Nevertheless, the reaction is not at all equal [58].

Surfaces of polymer solids are typically different from those of more rigid materials such as metals, glasses, and ceramics due to the mobility and flexibility of the constitutional units, which are organic macromolecules. Polymer molecules have much greater freedom to rearrange themselves at the surface, in order to accommodate a change of chemical potential in the surrounding environment [59].

The surface characteristics of a polymer are particularly settled by the specific organization of atoms at the surface shape and its configuration and not by the configuration of a macromolecule as a whole [59]. This indicates that polymeric surfaces are reasonably mobile and assume different surface shapes in dissimilar environments [60].

Some examples of polymeric heat treatments are: annealing, plasma and ironing.

2.3.1 Annealing

Annealing is a generic term denoting a treatment consisting of heating to and holding at a suitable temperature, followed by cooling at a suitable rate [58].

This treatment changes the microstructure and mechanical properties of the part, being very used on metals [58] and polymers [60]. Typically used to reduce the hardness, it helps to eliminate internal stresses and ensures better mechanical and thermal properties [61].

For polymers with solvents (e.g. PBMA latex), annealing leads to solvent evaporation, packing of particles followed by their gradual coalescence, migration, and redistribution of water-soluble components to yield a homogeneous part. As the annealing temperature is raised, more unwanted molecules (e.g. water) migrate to the air/polymer interface so the cohesion inside the piece is increased [60]. Annealing in this polymeric solutions reduces toughness and decreases plastic zone size due to the increase of the shear yield stress (Figure 21) [62].

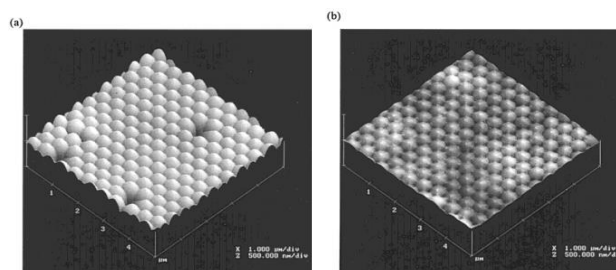


Figure 21 – PBMA latex film (a) before and (b) after annealing at 90 °C for 30 min [60].

This process may involve some downsides, like the occurrence of heterogeneities, such as voids and low crosslinked zones, in the solid film. This situation potentiates the phase-separation

behavior and small insignificant structural changes, which can cause significant differences in the phase behavior [63,64].

2.3.2 Plasma

Plasma constitute a chemically dynamic media, representing a unique and large variety of components, as excited and ionized particles, both atomic and molecular [65]. Plasma constitutes a very reactive environment if in contact with a polymer surface. The physico-chemical reactions lead to the disruption of the physical and chemical bonds and scission products on the polymer surface [66].

Consequently, plasma treatment promotes the removal of the small molecules and fragments, limiting their interfacial dissemination and other specific interactions across the interface, besides generating the formation of a new functionalized surface layer. This characteristic enables its application in low-temperature plasma chemistry and in the treatment of heat-sensitive materials, including polymers and biological tissues [66–68].

For polymers, plasma can be generated by using a dielectric barrier discharge (DBD) or by exposure to UV light and treatments usually occur with exposure times of one minute for DBD and five minutes for UV light [69].

DBD offers the possibility of inducing significant surface chemical modifications thanks to the development of functional groups on the polymer matrix, favorable to further linkage to other molecules. This treatment, for example used in Polyamide 6 (PA-6) (Figure 22) or Nylon 6, rearranges the bulk molecules to the surface, increasing roughness [69].

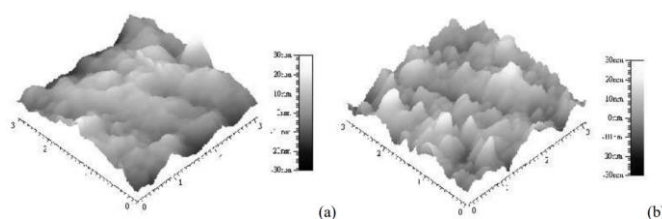


Figure 22 – AFM images of PA-6 films ($3\mu\text{m} \times 3\mu\text{m}$): (a) untreated, (b) 60s treated [69].

In case of the UV light, by breaking the weak chemical bonds and removing the small molecules and contaminants with low molecular weight, plasma treatment can ensure a clean surface of exposed materials, that are typically formed on the surface during the manufacturing and storage [65]. This cleaning effect generates changes in surface texture, wettability, improves surface quality, dyeability and adhesion, cross-linking, bendability etc., whereas radicals formed at the surface trigger secondary reactions, such as functionalization and intermolecular cross-linking [65].

There are also more techniques to change surface configuration on polymers, such as low-temperature plasma, which involves low-temperature plasma treatment of the polymer to incorporate fluorine as a labeling atom in the surface of the polymer [59].

Nonetheless, the modification induced only by the UV plasma and low-temperature plasma dominates at the surface and is considerably lower than that induced by DBD exposure which dominates processes in the bulk of the material [59,65].

The materials suggested for these treatments are: Polyethylene Terephthalate (PET), Nylon 6, Polymethyl Methacrylate (PMMA), and Polyethylene (PE) [59,66–69].

2.3.3 Ironing

Ironing is a superficial heat treatment available on some slicing software that enables the heated nozzle to travel over printed layers with reduced or even no extrusion, remelting the surface [3].

The heat added to the surface, illustrated on Figure 23, normally at low speeds, creates a uniform and smoother surface, reducing the surface roughness (Ra) [3]. This characteristic was added to the recent versions of the slicing software, only available on recent FFF printers and it is normally used for esthetic reasons [70].

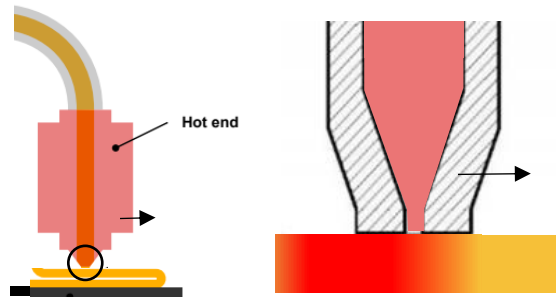


Figure 23 – Illustration of the ironing process.

For solid FFF polymers, it is essential that materials are correctly heat treated to remove internal stress which are located in the corners and the boundaries of each deposition web. Warping is a problem related with adhesion to the building plate so, applying a superficial heat treatment should not be considered, since slicer software like *Cura* only enables the ironing function on the last layer of the part [50,61].

However, Sardinha M. (2020) [3] developed a *Python* program capable of replicating ironing across different layers. This was a very experimental and preliminary study concerning the applicability and potential of the process. The authors propose the application of ironing during the first, second and third layers to reduce warping, reporting improvements in all tree setups (Figure 24) and a maximum average distortion reduction of 33%, when ironing was applied on the first layer.

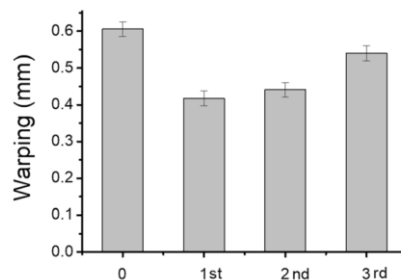


Figure 24 – Effect of ironing on the 1st, 2nd and 3rd layers on warping [3].

This paper also revealed a downside from ironing multiple layers, it seems that the nozzle over extrudes some material in the beginning of the printing, as it can be seen on the Figure 25.



Figure 25 – Unintended draining problem, adapted from [3]

From this paper [3] and relevant information from the 3D printer brand *Ultimaker* website, it was possible to depict the advantages and disadvantages for the ironing process on Table 5.

Table 5 – Advantages and Disadvantages of ironing process.

ADVANTAGES	DISADVANTAGES
The boundaries between individual print webs are less visible [70]	Over extrudes when applied multiple times on the same specimen (draining problem) [3]
Decreases surface roughness (Ra) [3]	Increases printing time [70]
Reduces warping when applied in the first layers [3]	Requires more energy [3]

Nozzle temperature is found to be a complex factor to the polymer crystallinity and mechanical properties because this temperature can not only influence the crystal melting process, but also the crystallization process, the interface between printing lines, and the deterioration phenomenon of polymer materials [71].

Apart from this study about the ironing process [3], no further studies were found, therefore conclusions concerning the effect of replicating ironing on various layers and more problems related with ironing are still to be studied.

3. METHODOLOGY

The objective of this work is to understand the effect of the ironing process on parts produced by FFF. Consequently, geometry and printing parameters were chosen, allowing the author to have consistent warped results, and multiple specimens were printed. Then the same printing conditions were used to print specimens, but this time adding *ironing* layers across the part.

The ironing process, as all thermal processes, changes the properties of the printed part however that analysis is not the focus of this thesis, so no mechanical tests were experimented, rather the dimensions and overall looks of the part were considered. Both the ironed and non-ironed specimens were measured to infer the impact the treatment has on FFF printed parts.

To ensure a correct analysis of the results afterwards, consistent prints must be performed therefore this chapter presents the methodology followed in 6 steps (Figure 26): the modeling of the part, the pre-processing of the file, the mid-processing of the file, the conditions for manufacturing, the procedure for measuring and finally the results.

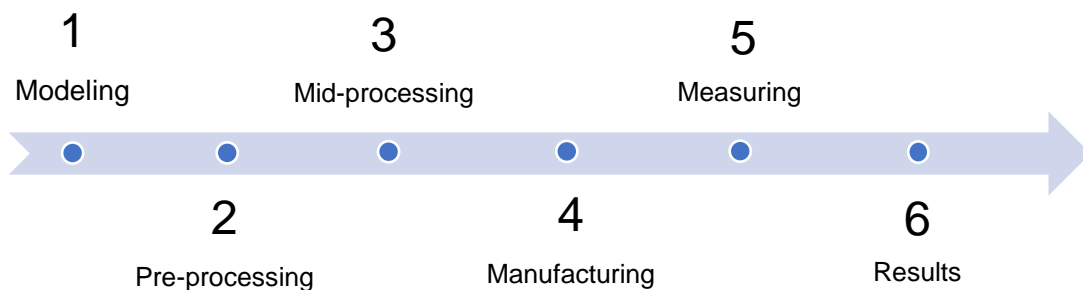


Figure 26 – 6 methodology steps.

3.1 Modeling

As stated before, the first step to any FFF project starts with the modeling of the part/specimen on a CAD software.

The design of the specimen is essential since the purpose of this work is to print the part with and without the ironing process and then compare the overall geometrical accuracy of both.

The main reason for choosing the specimen design was the repeatability of warped results so the first step of this work was finding a shape and dimensions that could enable it. Furthermore, the main criteria concerning the form choice were the following:

- It has enough surface area to remain stuck to the glass even when warped
- It has a maximum height of 50 layers. Wang (2007) [4] reveals that after the 50 layers mark, warping is residual compared with the height of the specimen
- It has a small volume to shorten printing time
- It has 90 degrees angles (corners) for the stresses to concentrate in those areas

Once chosen the specimen shape, it was designed in CAD software and exported as a .3MF file compatible with the next stage: the pre-processing.

3.1.1 CAD software and specimen's shape

The CAD software used to model the specimen was *Solidworks 2019 (student version)*.

A cuboid with 30x10x5 mm (Figure 27) was used for the vast majority of the preliminary tests and for all the main tests.

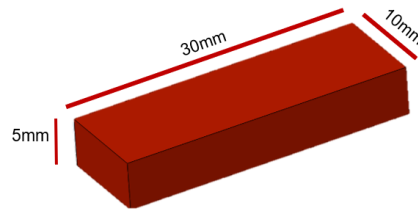


Figure 27 – Cuboid 30x10x5 mm illustration.

Additionally, similar shapes and dimensions to this specimen were used in the literature [3,49,72].

3.1.2 3D printer

This study was performed using the *Ultimaker S5* printer from Product Development Lab (LAB2ProD) at Instituto Superior Técnico visible on Figure 28.



Figure 28 – Ultimaker S5 from LAB2ProD.

Awarded internationally, it uses a cartesian coordinate system with a XY moving nozzle, a bowden extrusion type and it has a volume of 330 x 240 x 300 mm. In addition, it is capable of performing ironing and it has a user friendly self-calibrating system.

3.2 Pre-processing

Pre-processing is the stage where the printing parameters such as number of layers, nozzle temperature, printing speed and so on are considered using a slicing software.

3.2.1 Slicing software

The printer used in this work is considered to be one of the most versatile and robust professional printers [73] largely due to its optimized slicing software *Cura*. Visible on Figure 29, the slicer used in this project was *Ultimaker Cura 4.6*.

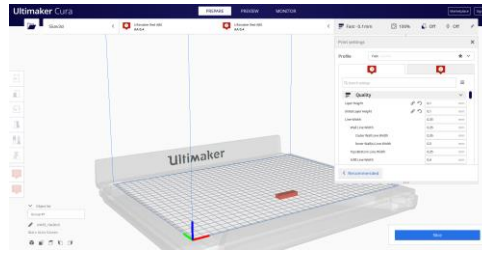


Figure 29– Ultimaker Cura 4.6.

Cura is an open-source slicing application for 3D printers. It was created by David Braam who was later employed by *Ultimaker* to maintain the software.

Ultimaker Cura is used by over one million users worldwide and handles 1.4 million print jobs per week (data from 2019) [74]. It is the preferred 3D printing software for *Ultimaker* 3D printers, but it can be used with other printers as well.

3.2.2 Slicer parameters

The printing parameters will be grouped into *warping* parameters and *ironing* parameters. Both are editable parameters existent in the slicer, the difference is that the *warping* parameters are referring to all the specifications chosen in order to achieve warping, whereas *ironing* parameters refer to the specifications regarding the heat treatment.

For the first, the objective was to simulate realistic printing parameters and conditions, altering as few parameters as possible while ensuring constant warped results. In order to decide which parameters better potentiate warping, a study was developed which was called “preliminary studies” (chapter 4.1). Once found, these parameters were kept constant throughout the main tests (chapter 4.2).

To access the *ironing* parameters, the ‘Enable Ironing’ function must be enabled on the slicing software. This function enables commands such as the flow or the inset and it is responsible for all the parameters regarding the ironing layers. As characteristic of the slicer software, only the highest layers of the part can be ironed, since this function has been thought for ‘finishing’ purposes, however a mid-processing software (chapter 3.3) was used to allow the application of this command to multiple layers.

The goal when choosing the *ironing* parameters values was trying to ensure that the final product had no visual defects resulting from this heat treatment. Moreover, since ironing requires a lower speed than the ‘normal layers’, the objective was to optimize its application. Once decided the printing parameter’s values, the information was saved as a *g-code* file that was then used as input to the mid-processing.

The slicing software *Cura* enables the user to edit the ironing parameters present on Figure 30.

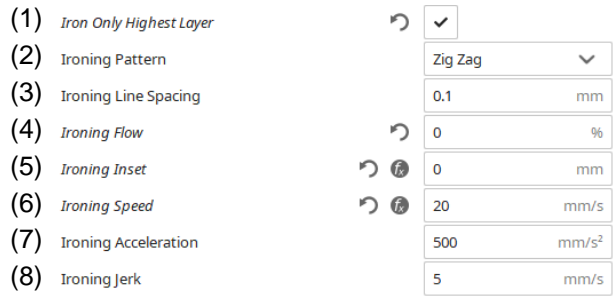


Figure 30 – Cura ironing parameters.

As it can be seen, *Cura*'s parameters do not include an editable temperature. This temperature remains the same as the 'printing temperature' explained in chapter 2.

(1) Iron only highest layer. The ironing function on *Cura* can only be applied to the highest layers of each part, but in case you have multiple top surfaces, this option allows you to only iron on the topmost surface layer as exemplified on Figure 31 [27].

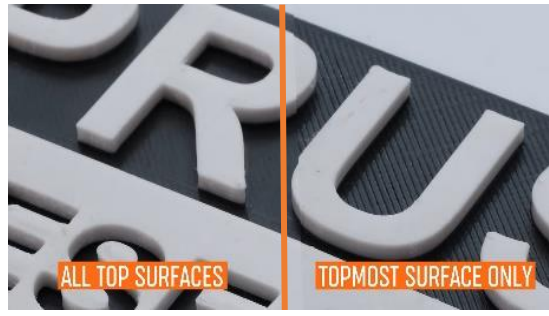


Figure 31 – Iron all top surfaces VS iron only highest layer, adapted from [75].

(2) Pattern. Ironing printing pattern can be chosen between Concentric and ZigZag patterns (Figure 32) regardless of the 'normal' layers printing pattern.

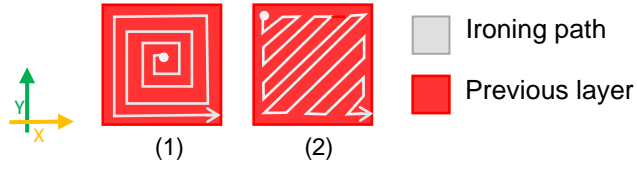


Figure 32 – Illustration of Ironing patterns (1) Concentric (2) ZigZag.

Both ZigZag and Concentric patterns swap direction on alternated ironing layers to better uniformize stressess [27].

On the one hand ZigZag patterns only seem to alternate between starting at the top or bottom of the same lateral. On the other hand, Concentric pattern changes from printing clockwise to anticlockwise (illustrated on Figure 33), remaining printing from the inside to the outside.

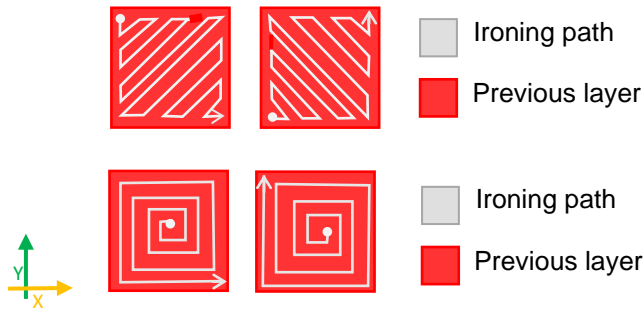


Figure 33 – Illustration of ZigZag and concentric patterns swapping direction.

(3) Line spacing. Line spacing is the distance between each parallel path of the nozzle [27]. By default, this value is the same as the layer thickness but it can be changed to a smaller value so that ironing printing path overlaps a previous ironed area, increasing the heat transfer and the printing time, or it can be changed into a higher value for faster printing despite not covering the whole layer area.

An illustration of line spacing can be found in Figure 34.

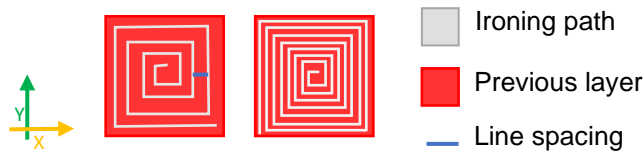


Figure 34 – Illustration of a high and low line distancing accordingly.

(4) Flow. Ironing flow is the amount of material measured in percentage (%), compared to a normal skin layer, to extrude during ironing [27]. In case this value is 100% it means that another normal layer is being built on top of the previous, whereas if the flow is equal to 0, the nozzle only supplies heat to the specimen.

(5) Inset. The inset parameter can be defined as the distance from the edges of the model to the outer layer of the ironing path, measured in millimeters (mm). Cura considers a positive inset measuring to the inside of the model and negative inset measuring to the outside as Figure 35 illustrates [27].

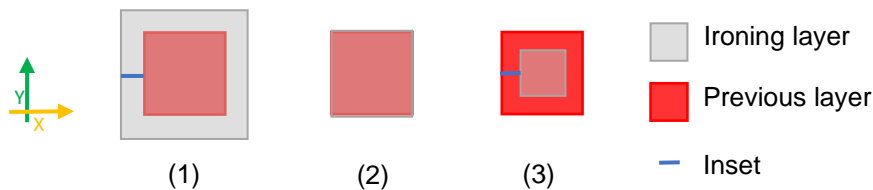


Figure 35 – Illustration of (1) Negative inset, (2) Zero inset, (3) Positive inset.

(6) Speed, (7) Acceleration. These parameters are very self-explanatory, the ironing speed [mm/s] and acceleration [mm/s²] are the speed and acceleration at which ironing is performed.

(8) Jerk. Jerk represents the maximum instantaneous velocity change while performing ironing measured in mm/s.

3.3 Mid-processing

Mid-processing was the name given to this extra step, whose input is the g-code from the slicer and the output is a modified g-code to send to the 3D printer. The goal of this stage was to replicate the ironing process, defined previously, across other layers.

To do so, a mid-processing software was used. This program was developed by Nuno Frutuoso for the BigFDM project [3], Nov2018, in Instituto Superior Técnico. Using the programming language Python, this software can find the ironing commands in the g-code and then replicate them to the layers chosen by the user. The front-office layout of the program can be seen in Figure 36.

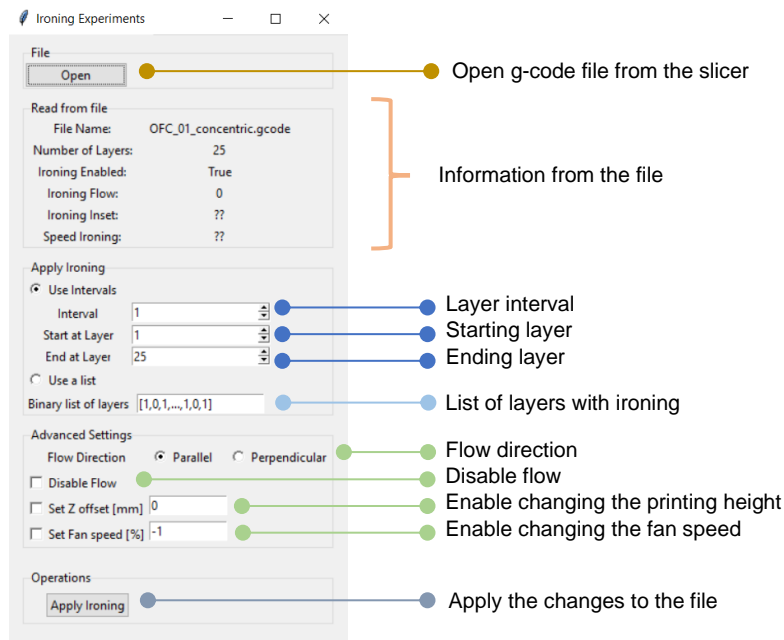


Figure 36 – Mid-processing program layout.

The program is responsible for identifying the specific information regarding *ironing* on the *g-code* and then copying that excerpt to the desired locations. Consequently, it can only be used for parts with a constant shape across all layers, otherwise the ironing layer would be different from the previous printed layer. For simplification purposes, this program will be referred throughout this work as “mpp” (mid-processing program).

The software allows to replicate ironing layers equally spaced across the part (illustrated as (1) in Figure 37) or replicating using a binary list (illustrated as (2) in Figure 37).

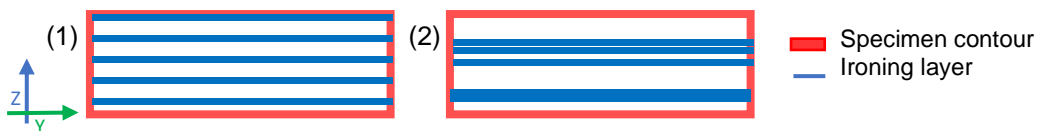


Figure 37 – Illustration of ironing applied (1) Equally spaced and using (2) Binary list.

Other than these 2 capabilities of the program no other ones, such as the advanced settings (visible in Figure 36), were used in this study. All the tests further explained were designed to understand the impact that different positioning of ironing layers across the specimen had on warping, letting the “Advanced settings’ as default. To understand the impact of those settings in warping, further studies should be done.

Since there is almost no information about the impact of the ironing process on FFF specimens, three approaches were planned:

- (3.3.1) Apply ironing on the first layers
- (3.3.2) Apply ironing evenly across the specimen
- (3.3.3) Apply ironing consecutively on the first layers

3.3.1 Ironing on the first layers

It was important to confirm whether ironing on the first layers had an impact on warping as proposed by M. Sardinha [3].

Therefore, ironing will be applied in the 1st, 2nd and 3rd layers to understand the importance of ironing in plate adhesion.

3.3.2 Ironing spaced equally

The impact of thermal stresses, already previously emphasized (chapter 2.2.4), has a significant relevance in warping, however, the advantages ironing could have on reducing them was still unknown. The possibility of distributing ironing layers evenly throughout the part aims at reducing the thermal stresses and that is what this chapter tried to tackle.

These series of tests consist in applying ironing in layers equally spaced across the part. The starting layer can also be editable, the logic is the same, simply the first ironed layer corresponds to the chosen 'starting layer'. Choosing the required interval parameters (*Start at Layer*, *End at Layer* and the *Interval*, visible on Figure 37) for these tests, required the following line of thinking:

- (1) The first layer to be ironed (*Start at layer*) was only decided after the realization of the first tests (explained in chapter 3.3.1). From those, the starting layer exhibiting the most warping should be the one chosen to be the starting layer for the equally spaced tests. For example, if ironing the 3rd layer presents the most warping compared with only ironing the 1st or the 2nd, then, all the equally spaced tests should start ironing on the 3rd layer. This way it is possible to better correlate the impact of spacing ironing across the part and the consequent warping reported.
- (2) Since there is no information about the impact of ironing in thermal stresses, it was chosen to apply the heat treatment very recurrently meaning intervals of 2, 4 and 6 layers.
- (3) The "*ending at layer*" command was always kept equal to the total number of layers to ensure no layers were forgotten.

3.3.3 Ironing consecutively on the first layers

Other than distributing ironing evenly across the part, concentrating all the ironing layers on the same zone could possibly reduce warping. The zone where ironing could have the most impact was agreed to be on the first layers so the ironing process was applied in consecutive layers in the beginning of the print.

In this case, two alternatives will be tested: ironing from the 1st to the 3rd layer and from the 3rd to the 8th.

3.4 Manufacturing

This section describes the methodology applied when working with the 3D printer. This sub-chapter will describe the precautions to be taken before the printing, as well as afterwards, in what concerns the hardware (e.g. the filament) or the tactical method (e.g. the number of parts per print).

3.4.1 Bed coating application

The choice of the best bed coating required the realization of some preliminary studies, furtherly explored (chapter 4.1), with the objective of finding the one with the most warped consistent results.

To ensure identical and replicable coating conditions, applying the coating required the following procedures:

(1st) Cleaning all the glass with glass cleaner with the glass at ambient temperature. Glass cleaner was applied over all the glass and, with the help of a blade, the existing traces of glue or filament were cleaned.

(2nd) Applying the bed coating uniformly. The solid glue was applied directly from the tube whereas the isopropyl alcohol required pouring the liquid to a cloth and then skim the glass in vertical non-overlapping columns.

(3rd) Letting the alcohol dry. After the application of each liquid, it was given 1 minute for it to dry before applying another one or start heating.

(4th) In case the first print had been successful, the bed coating application skips the first step (cleaning with glass cleaner), otherwise, all the four steps were repeated.

3.4.2 Parts per print

The number of printed parts per print may change the intensity of warping obtained since the time between layers would increase linearly with the number of parts. Given the almost inexistence information about the impact for the ironing process, it was decided that printing one part at a time would be the best way to ensure extrapolatable results.

3.4.3 Printing 'zero's

'Zero' was the name given to the printed part with no ironing process applied. When referring to the term 'zero' it implies that the file used was always the same and in case the outcome of the part is different from one print to another then, it is due to external conditions (e.g. bed coating conditions).

In the beginning of every series of prints, a zero was printed as a control specimen to ensure that the conditions were met. If the first zero presented visible warping (at least 10% of the specimen's height), then the series of tests with the ironing process could start, if not, the procedure referred in chapter 3.4.1 must be repeated before printing another *zero*.

In certain cases, *zeros* were printed interspersed with specimens with *ironing* for a better control of the results.

At the end, the measurements of the zero specimen(s) were compared with the results measured of specimens with ironing and conclusions were taken.

3.4.4 Number of prints per series

'Series' was the name given to a group of tests composed by one or more zeros and multiple prints with the same mid-processing parameters. These mid-processing parameters of that "ironed specimen" obviously vary from series to series.

Since the 3D printer was not allocated entirely for this project and the printing process for each part took an average of 1 hour and 15 min to complete, the number of non-zero specimens per series per day was limited. The existing limitation, combined with the need for constant bed conditions, led to choosing to produce 4 specimens per day. At the beginning of the next day, the bed coating and the printing zeros procedure was repeated.

3.4.5 Material

The material used for this work was *Ultimaker's* ABS (Acrylonitrile Butadiene Styrene) red 2.85mm. Its properties, provided by the brand [76], can be seen on Table 6:

Table 6 – Ultimaker's ABS characteristics.

Flexural strength	70.5 MPa
Impact strength	10.5 kJ/m ²
Hardness	76 Shore D
Melting Temperature	220°C
Glass Transition Temperature	95°C
Coef. Thermal Expansion	94x10 ⁻⁵ °C ⁻¹

ABS is particularly suitable for FFF since it is easily manageable in its pre-fusion state at low temperatures, steadily hardens as it cools down at glass transition temperature and reverts back to its initial properties [2].

The objective was to choose a material that was very relevant to the industry, and which had a significant problem with warping. Moreover, this study comes in sequence from M. Sardinha [3] paper which also studied ABS.

3.4.6 Various other conditions

To ensure the best and most consistent results, some other aspects were considered when printing.

- (1) The filament was always stored inside a dehumidifier cabinet overnight.
- (2) It was always used the same print core (Ultimaker AA 0.4).
- (3) The 3D printer door was always kept closed when printing.

3.5 Measuring

No mechanical tests will be performed, only the dimensions of the printed specimens will be compared.

After printing the specimens, the author proceeded to measure them. The specimens were measured at the laboratory of *Tecnologias Oficiais* in *Instituto Superior Técnico*.

The objective was to measure, as precisely as possible, the variations in the specimen's dimensions compared to the 3D CAD design.

When brainstorming the best way to measure the deformations on the specimen, it was concluded that:

1. The specimen's most accentuated deformation is on the Z axis so no variations on the other axis were measured.
2. The most relevant deformation (curling) occurs on the vertices of the part so it was given special attention to those spots.
3. 1D measurement of the part was enough given the negligible deformation on one of the XY surfaces, namely the top surface.

The most efficient and precise way considered to measure the parts dimensions was using an analog comparator. This last, would measure the distance between the top and the bottom layer (dz) on various points which could then be used to calculate warping (Figure 38). Since the top layer is flat, the specimen would be flipped, and comparator would skim the bottom surface.



Figure 38 – Illustration of the comparator's measurement on a warped specimen.

3.5.1 Measuring points (mp)

As explained on Chapter 2, the most warped regions are the vertices of the specimens [15], therefore 4 of the 6 measuring points chosen were located on those spots (mp 1, 2, 5 and 6) whereas only 2 were located on the center (Figure 39).

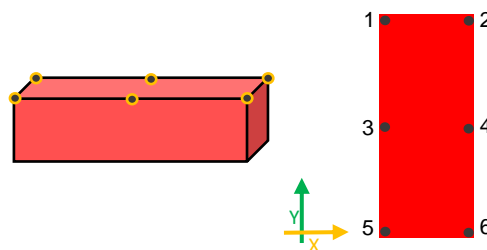


Figure 39 – Illustration of the measuring points.

3.5.2 Equipment

All the measuring setup and procedure required a flat surface, so a precision table was used. Additionally, ensuring consistent and repetitive measurements demanded building a 3D part to restrict the movement of the specimens when measuring. To this part was given the name "specimen holder" and magnets were used to keep it in position.

An analog precision comparator was used to measure the differences in height and a mobile set was used to assemble to the first. This last included a vernier height gauge, an adaptor for the comparator and a moving handle (Figure 40).

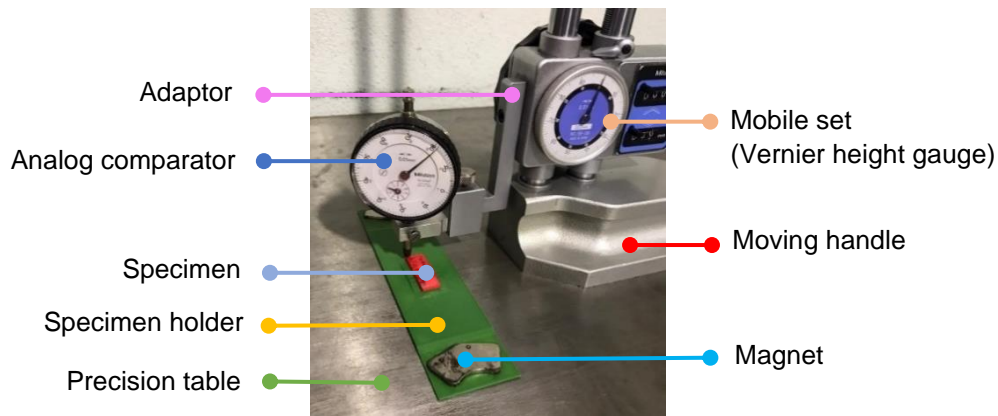


Figure 40 – Measurement equipment.

3.5.3 Procedure

1. The *specimen holder* was placed sensibly at the first third of the table, parallel to the laterals of the table.
2. Magnets were placed on each end of the *specimen holder* to keep it steady.
3. The *mobile set* was placed on the right side of the *specimen holder* allowing to measure on the center of the table (Figure 41).



Figure 41 – Initial measuring steps.

4. The specimen was placed in the *specimen holder* with the top layer faced down and the most warped side pointing to the worker.
5. The *comparator* was reset manually to the *precision table* (Figure 42).



Figure 42 – Comparator's reset to the precision table.

6. Only moving the *moving handle*, the measurements were done sequentially starting from point 1, moving inwards before moving to the next corner, as shown on Figure 43.

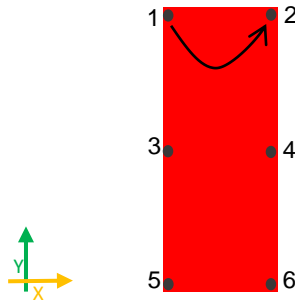


Figure 43 – Illustration of measurement sequence.

7. After measuring the 6 points, the *comparator* knob was pulled up and the *mobile set* was moved to the side.
8. The specimen was changed and the procedure was repeated.

3.5.4 Uncertainty

To calculate the uncertainty of the measuring process, two uncertainties were considered: from the equipment and from the method.

The first one is related with the uncertainty of the analog comparator which is half of the smallest scale: 0.005mm.

However, the second one, is related with the complexity of the measured shape, visible on Figure 44.

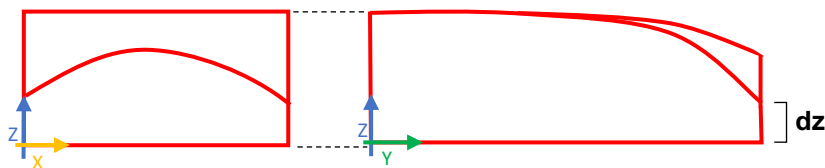


Figure 44 – Illustration a normal warped specimen (not at scale).

When moving the *mobile set*, it is very difficult to a naked eye to place the comparator exactly on the edge of the specimen. Besides the difficulty of perfectly aligning the comparator with the corner of the specimen, Figure 45 illustrates the under-measuring error resultant from the curvature of both the comparator and the specimen.

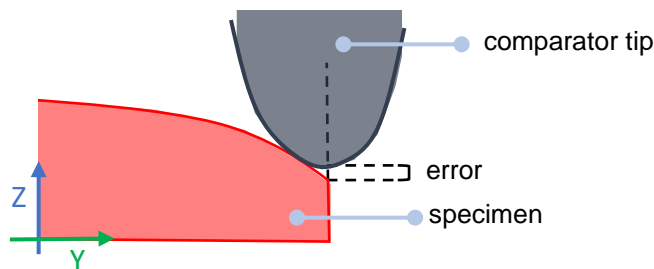


Figure 45 – Illustration of under-measuring error.

These errors became more relevant for extremely warped specimens, so it was decided to re-measure with a digital caliper the most warped corners and compare these with the results achieved by the comparator. Table 7 presents the difference between the most deviated value registered when measuring corners with both methods.

Table 7 – Measuring errors.

DIMENSION MEASURE BY THE COMPARATOR (dz)	ERROR
Between 4.5 and 5 mm	±0.01 mm
Between 4 and 4.5 mm	±0.01 mm
Between 3.5 and 4 mm	±0.02 mm
Between 3 and 3.5 mm	±0.05 mm
Between 2.5 and 3 mm	±0.07 mm
Between 2 and 2.5 mm	±0.10 mm
Between 1.5 and 2 mm	±0.15 mm

It is very clear that the most warped corners are the ones with the most unprecise results.

3.6 Results

The value h (Figure 46) is theoretically equal to the height of the specimen; yet, this value may decrease depending on the shrinkage of the part. The dimension marked as dz (Figure 46) refers to the value measured by the comparator (Figure 42).

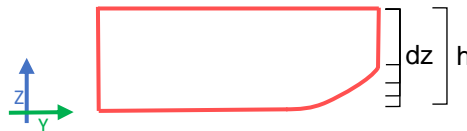


Figure 46 – Illustration of measured dimensions.

3.6.1 Formulas

Using these heights, the absolute and relative *warping* was calculated. The necessary formulas for this work can be found at Table 8.

Table 8 – Formulas to calculate warping.

Quantity	Symbol	Formula
Absolute warping	dw	$h - dz$ [mm]
Relative warping	w	$\frac{dw}{h} \times 100$ [%]
Average absolute warping	$\overline{dw_{5\&6}}$	$(dw_5 + dw_6)/2$ [mm]
Average relative warping	$\overline{w_{5\&6}}$	$(w_5 + w_6) \times 50$ [%]
Standard deviation	σ	$\sqrt{\frac{\sum(dw_i - \overline{dw_{5\&6}})^2}{n}}$ [mm]

3.6.2 Units

Throughout this thesis, several tables and graphics will be presented which for practical or esthetical reasons will not have the unit dimensions associated every time.

For cohesion purposes, all the results exhibited in this work follow the unit dimensions of Table 9.

Table 9 – Unit dimensions.

infill	%	T	°C	dw	mm
speed	mm/s	T_{bed}	°C	dz	mm
height	mm	spacing	mm	σ	mm
spacing	mm	accel	mm/s ²	$\overline{w_{5\&6}}$	%
flow	%	jerk	mm/s		

3.6.3 Tables

After measuring, the results will be presented in one table. This table layout can be seen in Table 10 which presents, on the left side, the absolute warping (dw) values from the zeros and the ironed specimens from that specific series of tests (e.g. C1 tests) and on the right side an analysis of some of the most important parameters regarding warping. Namely, the absolute and relative warping average, the standard deviation and the highest and lowest warping values.

It should be noted that only the measuring points 5 and 6 are relevant for this study since they are the most affected by warping so the parameters shown on the right only concern those.

Table 10 – Illustration of the results.

(C1)	1	2	3	4	5	6	C1.zero		C1	
C1.zero	dw						Average dw 5&6	$\overline{dw}_{5\&6}$	Average dw 5&6	$\overline{dw}_{5\&6}$
C1.1							Standard deviation	σ	Standard deviation	σ
C1.2							Average w 5&6	$\overline{w}_{5\&6}$	Average w 5&6	$\overline{w}_{5\&6}$
C1.3							Higher		Higher	
C1.4							Lower		Lower	

Apart from the warping relative average ($\overline{w}_{5\&6}$), all the other values are in millimeters (mm).

3.6.4 Graphics

For a better understanding and comparison, hexagonal radar charts will be used to show the results. At Chapter 5 two of these graphics will be presented, one showing (1) the value of dz at all measuring points and another one showing (2) warping (dw).

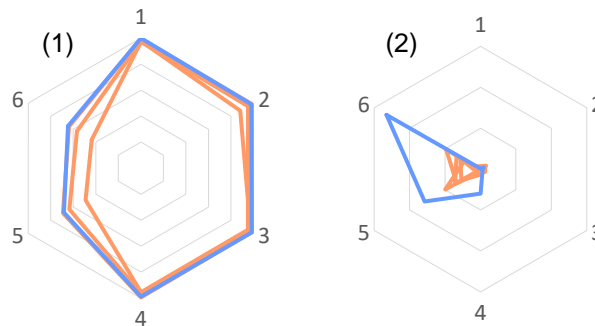


Figure 47 – Exemplification of the radar chart used in chapter 5.

An additional chart with the relative warping would have the same shape as the Figure 47 (2) since one is just the other divided by a constant, so it was not included. On the other hand, the value of the average distortions of the zero specimens is an extremely appropriate value to see. Therefore, it was included for a better analysis.

For a better distinction between the obtained results, it was decided to create a bar chart showing the relative warping (w) of point 5&6 ($\overline{w}_{5\&6}$) comparing the non-ironed and the ironed specimens.

For all the charts presented in Chapter 5, the scale was kept constant for a better visual comparison among them.

4. EXPERIMENTAL PROCEDURE

Determining how ironing influences warping required following a rigorous experimental procedure. This chapter intends to describe all the parameters considered on the experimental tests, from the printer and material used to the shape of the specimen. Additionally, this chapter already contains some preliminary studies and respective conclusions without which it would be very difficult to explain the fix parameters used on the main tests.

4.1 Preliminary studies

“Preliminary studies” was the name given to an initial group of prints performed to arrive at the most adequate parameters for the main tests. This analysis focused initially on the parameters that provided constant warping (chapter 4.1.1) and secondly on the parameters that better suited the ironing process (chapter 4.1.2).

In this part, will be presented not only the procedure and parameters used on the preliminary tests but also the results and its discussion.

4.1.1 Testing warping

Warping preliminary tests were the ones responsible for ensuring constant warped results. In order to decide which parameters better potentiated warping without compromising the overall look of the specimen, printing parameters were changed once at a time to arrive at the best combination.

4.1.1.1 Influence of bed temperature

From the very first tests performed, it was clear that the bed temperature had a great impact on warping. Therefore, a set of tests was conducted, to reach the temperature with the most consistent results.

The chosen shape was a 30x10x5mm specimen, the bed was always cleaned with isopropyl alcohol and the main printing parameters were kept constant. Only the bed temperature was changed. The layer height used is different from the one used further because at this time, the problems concerning $h=0.2\text{mm}$ had not surged yet. The bed temperatures tested were: No heat, 60°C, 65°C, 69°C, 74°C and 80°C.

The results obtained were divided between the specimens that were aborted due to lack of adhesion to the bed surface, the specimens which presented warping and the ones that did not present any sign of deformation (Figure 48).

Bed Temp.	Aborted	Warped	No Warp
No heat	3	0	0
60°C	4	0	0
65°C	3	1	0
69°C	2	4	0
74°C	1	6	1
80°C	1	3	2

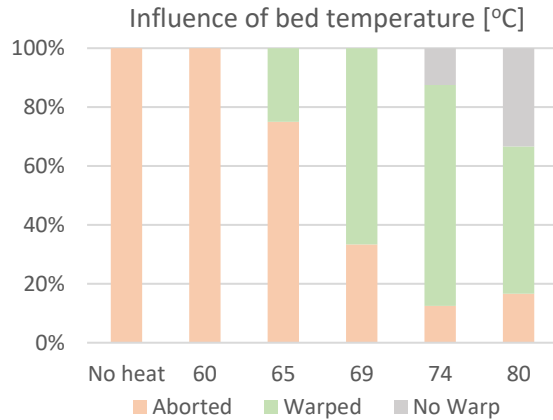


Figure 48 – Results of tests changing bed temperature.

The results from these tests were consistent with the literature: the bigger the bed temperature, the less likely it is for the part to warp.

4.1.1.2 Influence of bed coating

Other than the bed temperature, bed coating revealed to have a big impact on warping, therefore, three different surface coatings were tried: solid UHU glue, Isopropyl alcohol and glass cleaner.

The applying method was already explained in chapter 3.4.1. The chosen shape was a 30x10x5 mm specimen, the main printing parameters were kept constant, only the bed coating was changed (Table 11).

Table 11 – Printing parameters to test the best bed coating.

Printing parameters					
Infill (%)	Speed (mm/s)	Height (mm)	T (°C)	T _{bed} (°C)	Bed coating
100	40	0.2	220	74	UHU glue
100	40	0.2	220	74	Isopropyl alcohol
100	40	0.2	220	74	Glass cleaner

The results obtained from using different bed coatings are considerably different and were summarized on Figure 49.

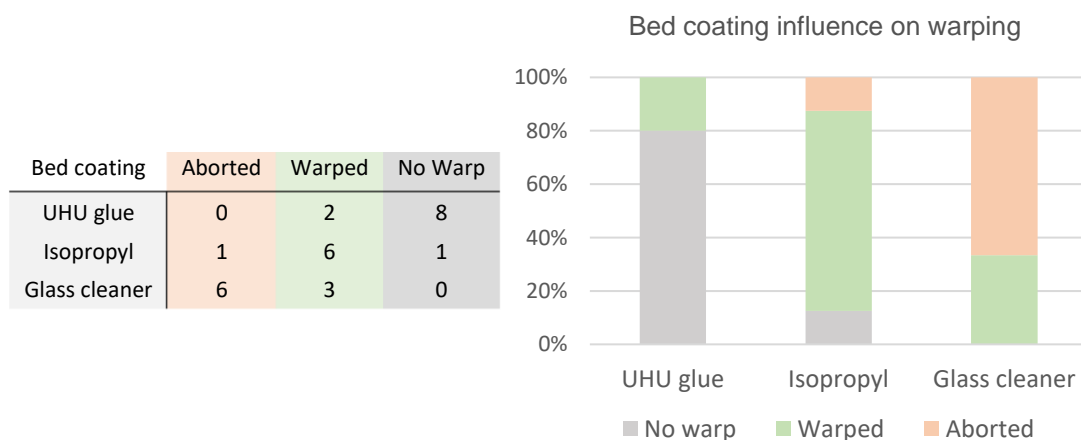


Figure 49 – Results of tests changing bed coating.

On the one hand, using glass cleaner led to disastrous results with the majority of the specimens not even completing the printing time. On the other hand, most results with UHU glue experienced no warping. Overall, isopropyl alcohol presented the most consistent warped results.

To illustrate the most common result for each bed coating, Figure 50 shows pictures of the obtained specimens.

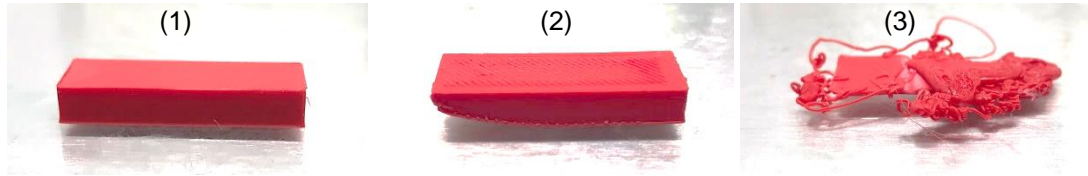


Figure 50 – Specimen results using (1) UHU glue (2) Isopropyl alcohol and (3) Glass cleaner.

4.1.1.3 Influence of plate adhesion type

As previously stated, there are 3 types of build plate adhesion on Cura: skirt, brim and raft. The difference between those has a big impact on warping given the increase in the contact area for brim and raft.

For these tests: the chosen shape was a 30x10x5 mm cuboid, the main printing parameters were kept constant and only 2 plate adhesion types were considered: skirt and brim. The printing parameters can be seen in Table 12.

Table 12 – Printing parameters for plate adhesion type tests.

Printing parameters						
Infill (%)	Speed (mm/s)	Height (mm)	T (°C)	T _{bed} (°C)	Bed coating	Plate adhesion type
100	40	0.2	220	74	Isopropyl alcohol	skirt
100	40	0.2	220	74	Isopropyl alcohol	brim

Skirt adhesion type only prints a halo with two perimeters (Figure 51 (1)), which does not directly interfere with the bed area in contact with the part; therefore, the printing of this adhesion type is irrelevant for warping. Brim, increases the surface area as the Figure 51 (2) shows, enabling the part to experience no warping.

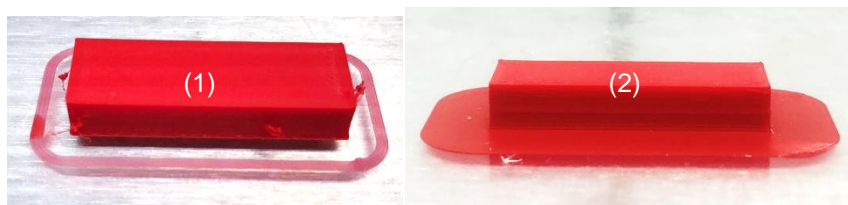


Figure 51 – Results from plate adhesion type tests with (1) skirt and (2) brim.

From the tests performed, only prints with skirt presented any sign of warping therefore the skirt adhesion type was used throughout this study.

4.1.1.4 Influence of positioning and bed cleaning

Once chosen the bed coating, the next questions was: Is it better to clean the glass every print or is better to only clean it once?

To understand the impact of positioning and bed cleaning, three setups were tried (Figure 52):

- (1) The bed was only cleaned once and the specimens were not printed on the same spot.
- (2) The bed was cleaned once and the specimens were printed on the same place.
- (3) The bed was cleaned every print and the specimens were printed on the same place

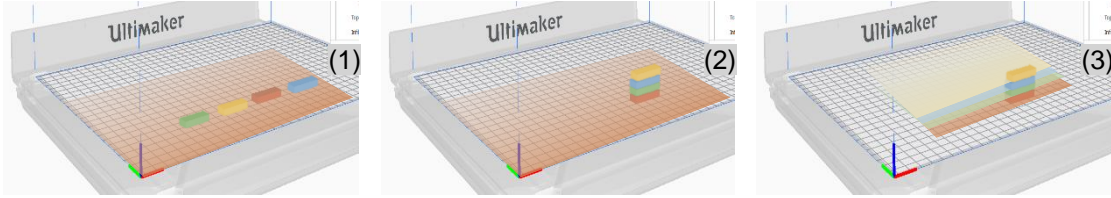


Figure 52 – Illustration of the 3 positioning setups.

Once again, a 30x10x5mm cuboid was printed, 4 specimens for each setup, following the cleaning procedure explored on chapter 3.4.1. The printing parameters can be seen on Table 13.

Table 13 – Printing parameters for positioning and bed cleaning tests.

Printing parameters						
Infill (%)	Speed (mm/s)	Height (mm)	T (°C)	T _{bed} (°C)	Bed coating	Plate adhesion type
100	40	0.1	220	74	Isopropyl alcohol	skirt

The overall results for (1), (2) and (3) can be seen on Table 14.

Table 14 – Warping average and standard deviation for case (1), (2) and (3).

	(1)	(2)	(3)
$\overline{dw_{5\&6}}$	0.554mm	1.102mm	0.736mm
$\sigma_{5\&6}$	0.436mm	0.292mm	0.272mm

(1) There were specimens presenting very little warping and specimens presenting significant warping, meaning that it is very difficult to clean evenly all the surface of the glass. The conditions of the bed were, thus, not the same for each specimen and a standard deviation of 0.436mm is the proof.

(2) The results obtained in the second case were the most warped ($\overline{dw_{5\&6}}=1.102\text{mm}$). However the standard deviation was 70% of the one verified on setup (1). Contrarily to (1), in this case, specimens experienced less warping as more parts were printed, potentially because each part removed a thin layer of bed coating each time.

(3) The third experiment presented consistent results with a standard variation of $\sigma_{5\&6}=0.272\text{mm}$. Additionally, the results obtained did not follow the tendency observed for setup (2). The full presentation of these results can be seen on chapter 5.

It seems obvious that the most relevant factor for the discrepancies in standard deviation from (1) to (2) and (3) is the initial bed cleaning. For the case (1) it is very hard to achieve a uniform coating when probably the density of glue stuck to the glass, from previous prints, is not the same all over the glass. So, for a more rigorous scientific study, all specimens should be printed in the same spot. Comparing (2) and (3) also emphasizes that it is possible to achieve very similar consistent results regarding the *absolute warping average* ($\overline{dw_{5\&6}}$).

From setup (3) it was possible to conclude that, using the alcohol isopropyl application procedure between every print can lead to reliable results.

For the main tests, the choice between cleaning once (2) and cleaning every print (3) fell to setup (3), since it exhibited a lower deviation and no systematic error.

4.1.1.5 Influence of deposition path

Similarly to the literature [3,4,55], the authors recognize the ZigZag pattern as one of the best printing patterns, especially when using an infill of 100%, therefore it is being used as the printing deposition pattern for the preliminary tests. As previously aborded on Chapter 2.2.4.3, adding contours improves the surface quality, without compromising warping [4], so these were included on the deposition pattern desired for these tests.

Except for very few specimens, 2 to be precise, all the other tests performed for chapter 4.1.1 exhibited major warping deformation on the left side of the specimen (viewed from above). This problem has already been reported on multiple online forums (e.g. [77]) without any clear answer to the problem.

The experiment performed to test the reason behind this systematic phenomenon consisted on changing the direction the ZigZag pattern was being applied and see if the specimen behaved differently.

After printing the skirt and the 3 perimeter contours, the first layer's infill pattern starts on the top left vertices of the specimen, marked on Figure 53 (1) by a black dot, whereas the second layer's infill pattern starts at the bottom left side, market on Figure 53 (2) by a blue dot.

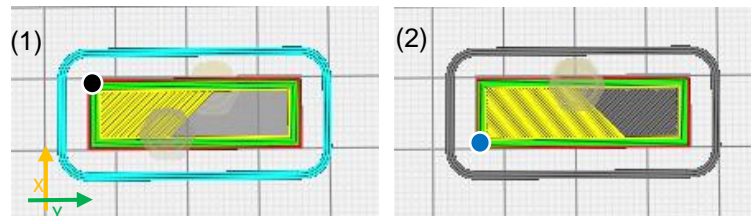


Figure 53 – Illustration of the ZigZag pattern applied on (1) the first and (2) second layers.

Given the coincidence of both warping and infill pattern starting on the left side, it was tried printing the same specimen, but this time, forcing the ZigZag pattern to start on the right side, as illustrated on Figure 54. This change in direction was named 'symmetrical ZigZag pattern'.

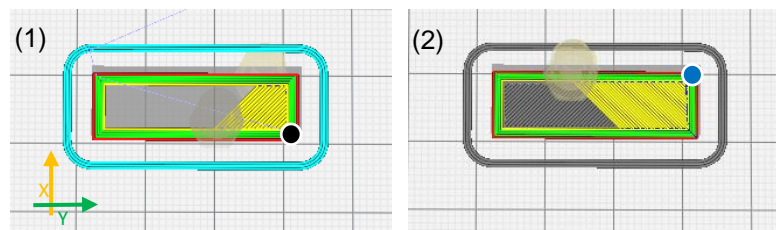


Figure 54 – Illustration of the ZigZag pattern modified applied on the (1) first and (2) second layers.

The printing parameters used can be seen on Table 15.

Table 15 – Printing parameters for deposition path influence tests.

Printing parameters						
Infill (%)	Speed (mm/s)	Height (mm)	T (°C)	T _{bed} (°C)	Bed coating	Plate adhesion type
100	40	0.1	220	74	Isopropyl alcohol	skirt

The results obtained from this experiment reveal a clear shift of the most warped side of the specimen. On Figure 55 (1) warping prevails on the left whereas on Figure 55 (2) warping is visible only on the right side of the part.

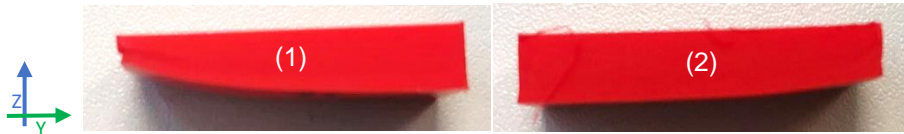


Figure 55 – Results from using (1) ZigZag pattern and (2) symmetrical ZigZag pattern.

Warping seems to be closely linked with the material deposition pattern meaning that: if the user chooses to use the ZigZag pattern, it is expected for the part to warp on the left side, whereas if the user chooses to use the symmetrical ZigZag pattern, it is expected for the part to warp on the opposite side.

Without further justification why this phenomenon is happening, the better explanation seems to be that the stresses concentrate more on the beginning of each deposition layer leading to higher deformation on that side.

It is very clear however that, this phenomenon has nothing to do with calibration or positioning of the part related to the glass.

4.1.1.6 Influence of bed calibration

Contrarily to other 3D printers (e.g. Prusa i3) Ultimaker S5 is equipped with sensors that enable “bed self-calibration” or “auto bed leveling”. With this function ‘on’, before each print, the printing bed calibrates itself in relation to the nozzle so that, when printing, the bed height is adjusted allowing printing into a horizontal surface.

The existence of extra-material on the nozzle or leftovers on the bed will influence the bed calibration. The result of a miscalibration is usually the nozzle starting printing at a bigger height than intended and consequently the filament not sticking to the surface, resulting in very warped specimens.

In line with what is being said, another factor that influences the bed calibration is the irregularities on the printing surface. In areas where the glass is not completely flat or even where there are parts of the glass missing, the first layers exhibit non-uniform printing thickness/height as Figure 56 illustrates.

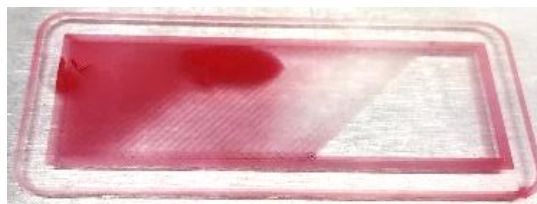


Figure 56 – Unfinished first layer on an irregular glass.

Both these problems interfere directly with warping, however, the author opted by not studying them in more depth since it is not the objective of this study.

4.1.2 Testing the ironing process

Since the information about ironing in the literature is scarce, this part will focus on the establishment of ironing process parameters influence. For that reason, the printing temperature, the printing height, the inset and the deposition path were studied.

4.1.2.1 Influence of printing temperature

As seen in chapter 2, the bigger the printing temperature, the less warping expected [49] however, when trying to print at a temperature of 240 °C and implementing ironing on various layers, the same problem reported by Sardinha M. occurred and it is visible on Figure 57.

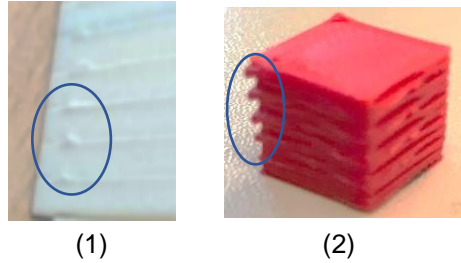


Figure 57 – Draining problem (1) from Sardinha M. paper [3] (2) from this thesis first tests.

Choosing the printing temperature became the most challenging parameter since Ultimaker Cura does not consider the ironing temperature as an editable parameter rather it remains the same as the printing temperature when performing ironing.

As seen above, for ABS, there is an ideal printing temperature from 215 to 240 °C yet, maintaining this temperature and asking for the nozzle to suddenly not extrude any material (flow=0) could potentiate an involuntary draining of material.

To test the influence of the printing temperature when applying multi-layer ironing, a small 10x10x10 cube was used. The ironing pattern chosen was ZigZag since it was the only pattern referenced by the literature [3]. Ironing was applied in intervals of 5 layers just so that the specimen had a considerable number of layers with the heat treatment. The printing/ironing temperatures tested were between 180°C and 260°C with 10°C intervals.

Comparing the results obtained required the creation of a qualitative method (Table 16). It was chosen grading from 1 to 5 according to the specimen's quality at a layer and overall level: a '5' meaning any specimen whose final and individual layer appearances did not show any signs of material draining and '1' meaning the specimen had been destroyed due to the excessive draining and temperature of ironing.

Table 16 – Draining, according to the ironing temperature, grading.

Grade	5	4	3	2	1
Layer level	No excess	Small excess	Medium excess	Medium excess	High excess
Overall level	No excess	No excess	Medium excess	Almost destroyed	Destroyed
Image					

Considering this grading table, the results can be seen in Figure 58.

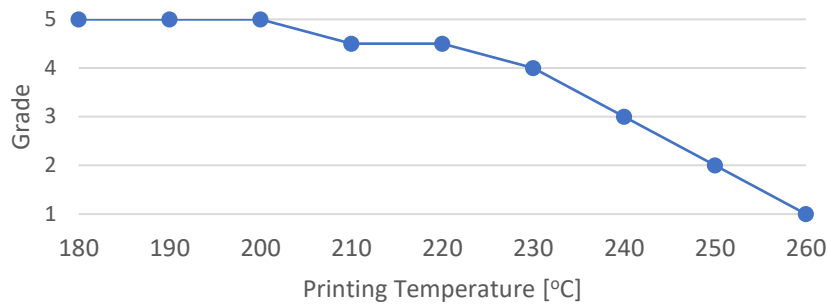


Figure 58 – Graded results for the influence of printing temperature on ironed layers.

For temperatures below 210°C, the nozzle temperature is not enough to melt/drain the leftover material on the tip; therefore, the finished part presents no visual deformations. However, such low printing temperatures lead to a not completely melting of the filament and the layer cohesion is compromised.

For temperatures higher than 230°C, unintended material extrudes for approximately 3 seconds, enough for the part to be compromised. The bigger the printing/ironing temperature, the bigger the ‘draining’ and the worse the final product.

Literature suggests increasing the printing temperature to reduce warping at the same time it refers that it should not be lower than 215°C for ABS [28,43]. For the specific case of *Ultimaker ABS*, the brand suggests 225-260°C [76].

4.1.2.2 Influence of inset

Inset is a very important parameter when ironing due to its impact on the printing time. To test the influence of inset on specimens, a 20x20x2 mm specimen was used. In this case, it was chosen not to replicate this test across multiple layers since the focus was just at a layer level.

As previously stated, printing at a higher temperature results in heavier draining, but it illustrates in detail the differences between printing with negative or positive inset. The printing temperature of 250°C [3] was tested for comparison reasons, whereas T=220 °C was kept in accordance with the remaining tests. Additionally, Table 17 better explores the printing parameters used.

Table 17 – Printing parameters to test the influence of inset in ironing.

Printing parameters					Ironing parameters						
infill	speed	height	T	T _{bed}	pattern	spacing	flow	inset	speed	accel	jerk
100	60	0.2	250	85	ZigZag	0.1	0	-7	20	500	5
100	60	0.2	250	85	ZigZag	0.1	0	-2	20	500	5
100	60	0.2	250	85	ZigZag	0.1	0	0	20	500	5
100	60	0.2	250	85	ZigZag	0.1	0	2	20	500	5
100	60	0.2	220	85	ZigZag	0.1	0	-7	20	500	5
100	60	0.2	220	85	ZigZag	0.1	0	-2	20	500	5
100	60	0.2	220	85	ZigZag	0.1	0	0	20	500	5
100	60	0.2	220	85	ZigZag	0.1	0	2	20	500	5

Such a negative value as inset= -7 mm was chosen so that the draining material dropped outside the part, but for this particular specimen, it almost doubled the ironing time. The other values for inset (i=-2;0;2) were chosen for an understanding of the parameter.

Figure 59 and Figure 60 show the results obtained using T=250°C and T=220°C.

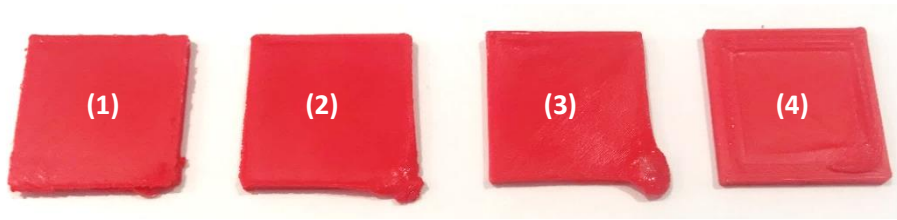


Figure 59 – inset of (1) -7 ; (2) -2; (3) 0; (4) 2 with $T=250^{\circ}\text{C}$.

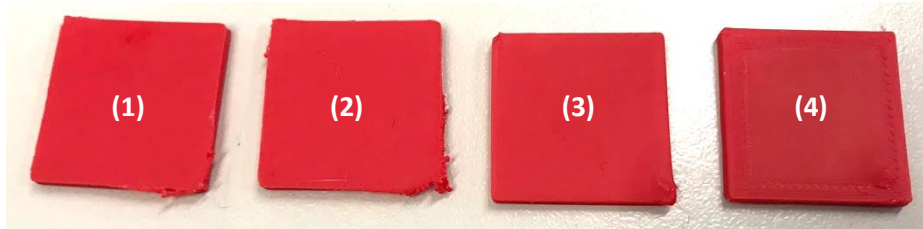


Figure 60 – inset of (1) -7 ; (2) -2; (3) 0; (4) 2 with $T=220^{\circ}\text{C}$.

From these pictures it is possible to conclude once more that the draining effect occurs much more drastically at higher temperatures. Furthermore, as an overall analysis on the advantages and disadvantages of using different insets, the following comparison was possible.

Negative	<ol style="list-style-type: none"> 1. For ZigZag pattern, in case some initial extra-material drains, the drained material does not affect the specimen. 2. The nozzle covers all printed area.
	<ol style="list-style-type: none"> 1. Ironing printing time increases. 2. The part experiences bigger gradients of temperature since there is more time between passages. 3. For ZigZag pattern, the nozzle keeps crossing the edges of the layer and some small scraps are formed. 4. For Concentric pattern, negative inset is the same as no inset since that pattern always starts at the center of the specimen.
Zero	<ol style="list-style-type: none"> 1. It covers the total area with the shortest printing time possible.
	<ol style="list-style-type: none"> 1. For ZigZag pattern and some initial material drains, the drained material spoils the corner of the specimen.
Positive	<ol style="list-style-type: none"> 1. It takes less time than Zero or Positive inset. 2. If there is drained material, it can be covered by the next layers. Both Concentric and ZigZag ironing patterns have no glaring draining visual effect on the overall specimen.
	<ol style="list-style-type: none"> 1. If the drained material is too much, it deforms the shape of the specimen as a whole. 2. Ironing does not cover the corners of the specimen which are where the maximum stresses are located.

4.1.2.3 Influence of specimen's shape

The shape of the specimen has a big influence on both the printing time [17] and even on warping [55]. However, the influence that changing the shape of the specimen had on the application of the ironing process was not clear.

A symmetrical T shape with the following dimensions in mm was tested:

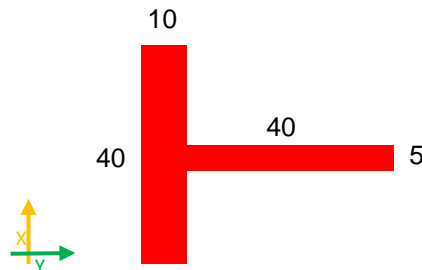


Figure 61 – T shape used to test the influence of printing shape on ironing.

The bed was cleaned with isopropyl alcohol and ironing was applied in intervals of 5 layers, starting at the first layer. ZigZag pattern was preferred as a printing and ironing pattern in this part, since it was used on the only literature information available [3]. Additionally, the complete list of parameters can be seen at Table 18.

Table 18 – Printing parameters to the test the effect of changing the printing shape on ironing.

Printing parameters					Ironing parameters							mpp	
infill	speed	height	T	T _{bed}	pattern	spacing	flow	inset	speed	accel	jerk	Int.	Start
100	40	0.1	220	74	ZigZag	0.1	0	0	20	500	5	5	1
100	40	0.2	220	74	ZigZag	0.1	0	0	20	500	5	5	1

As a consequence of the printing pattern chosen, namely the ZigZag pattern, the printing nozzle for a T-shape specimen follows a non-symmetrical path shown at Figure 62. It starts at point (1), which alternates with starting at point (2) every layer, then prints until touching point (3), continues filling until reaching point (4). It is only at this point that it continues where it left at point (3) till point (5).

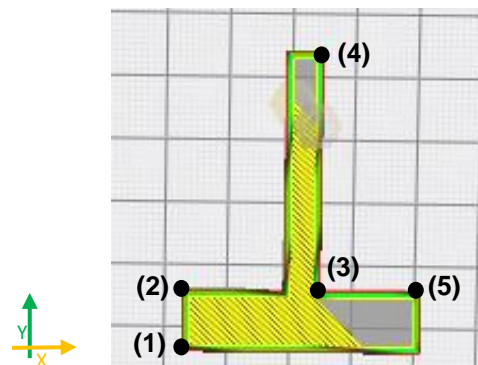


Figure 62 – Illustration of ZigZag printing/ironing pattern.

This non-uniform pattern is not just a characteristic of a t-shape specimen, but rather of any shape that does not let the nozzle cover all the layer area without sectioning the path.

This same nozzle path was verified for the ironing process zigzag pattern. Curiously, the results from this experiment reveal a tendency for the warping effect to start at point number (5) even on the first layer. Contrarily to a parallelepiped shaped specimen used before, this time, the most warped zone of the specimen was on the opposite side from where the zigzag pattern starts.

As a consequence of this early-stage warping, especially for the specimen with $h=0.1\text{mm}$, the nozzle melted the bottom right corner of the specimen when performing the ironing on the first layer.

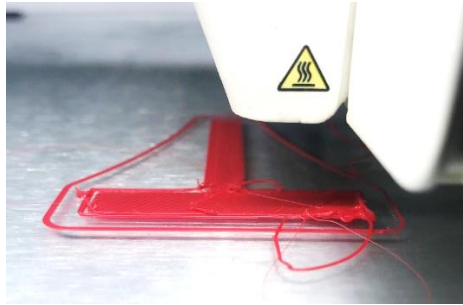


Figure 63 – Warping and consecutive corner melting when applying ironing on the first layer for $h=0.1\text{mm}$.

In certain cases, the corner anomaly caused by the ironing process got stuck to the nozzle and since the specimen was only one layer thin, it was easily destroyed (Figure 64).

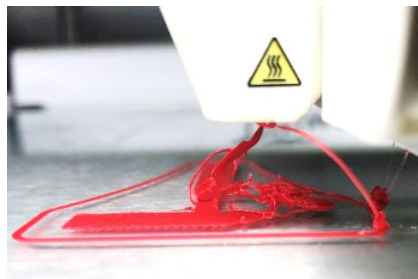


Figure 64 – Nozzle sticking to the warped zone for $h=0.1\text{mm}$.

For those specimens that did not get destroyed during the first ironing process, the results show a clear increase in warping on the previously specified zone of the part.



Figure 65 – Warped specimen with $h=0.1\text{mm}$.

This observation contrasts with the explanation explored on chapter 4.4.1.5 since, in this case, the most warped side does not align with the deposition starting side. However, it can be seen on Figure 65 that there is also warping on that area (left side), indicating that the phenomenon previously explored continues to happen.

Contrasting with these extremely warped specimens, for $h=0.2\text{mm}$, the results did not show relevant overall deformation, however, introduced a new problem which the author called “*stratified warping*”, visible on Figure 66.

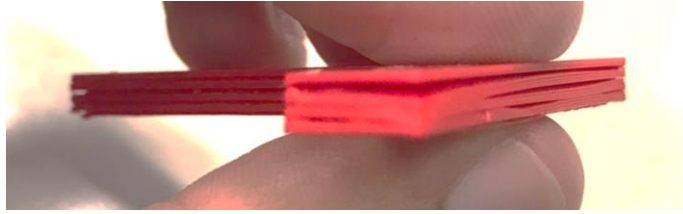


Figure 66 – Stratified warping for $h=0.2\text{mm}$.

This problem will be further explored in more detail on the sub-chapter 4.1.2.5.

4.1.2.4 Influence of deposition path

As previously explained, Cura allows the *ironing* pattern to be different from the printing pattern, so it would be interesting to notice the difference it makes between choosing ZigZag or Concentric *ironing* pattern. Additionally, the printing/*ironing* temperature was also changed from 220 to 250°C to take the draining problem into account.

To test the influence of the *ironing* path, a 20x20x2 mm specimen was used and the bed was cleaned with isopropyl alcohol. All the parameters used are visible at Table 19.

Table 19 – Printing parameters to test the influence of deposition path.

Printing parameters					Ironing parameters						
infill	speed	height	T	T _{bed}	pattern	spacing	flow	inset	speed	accel	jerk
100	60	0.2	250	85	ZigZag	0.1	0	0	20	500	5
100	60	0.2	250	85	Concentric	0.1	0	0	20	500	5
100	60	0.2	220	85	ZigZag	0.1	0	0	20	500	5
100	60	0.2	220	85	Concentric	0.1	0	0	20	500	5

The results obtained for 250°C showed an unintended draining on the right bottom corner for ZigZag pattern and on the center in the case of Concentric pattern, Figure 67.

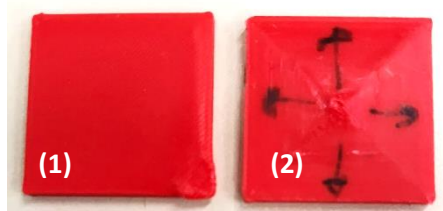


Figure 67 – Results from tests with (1) ZigZag (2) Concentric pattern at $T=250^\circ\text{C}$.

The results at a temperature of 220°C presented much less draining, still noticeable for ZigZag pattern but almost undetectable for the Concentric one.

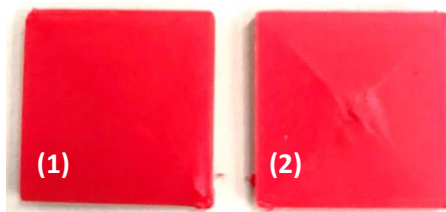


Figure 68 – Results from tests with (1) ZigZag (2) Concentric pattern at $T=220^\circ\text{C}$.

Once more, it is very clear that for $T=250^{\circ}\text{C}$ there is more drained material compared with $T=220^{\circ}\text{C}$. Furthermore, Concentric pattern seems a better choice since it does not compromise the corner of the specimen and presents almost no signs of a heat treatment application.

Beyond the draining problem, the ironing process deposition path can also have an impact on the esthetics of the final product, for instance, it may create undesired marks visible on Figure 69.



Figure 69 – Undesired ironing lines on a FFF print [78].

As previously explored on sub-chapter 4.1.2.3, for complex shapes, *Cura* is forced to divide the ironing area in sections, resulting in “double-ironing” over the border between them. This problem can be addressed by choosing the most adequate ironing pattern for the specific shape of the specimen, however, neither ZigZag nor Concentric pattern would solve the over-lapping problem on Figure 69 given the complexity of the design. Further solutions for this problem seem unclear on internet forums however suggestions like increasing the ironing speed or turning on the setting ‘avoid printed parts when travelling’ do not seem to work [78].

4.1.2.5 Influence of printing height

To test the influence of the printing height on specimens with multi-layer ironing, a 30x10x5 mm specimen was used. The bed was cleaned with isopropyl alcohol and ironing was applied in intervals of 5 layers, starting at the third layer.

Table 20 – Printing parameters to the test the effect of printing height on ironing.

Printing parameters					Ironing parameters							mpp	
infill	speed	height	T	T _{bed}	pattern	spacing	flow	inset	speed	accel	jerk	Int.	Start
100	40	0.2	220	74	Concentric	0.1	0	0	20	500	5	5	3
100	40	0.1	220	74	Concentric	0.1	0	0	20	500	5	5	3

Results for the layer height $h=0.2\text{mm}$ seemed to have experienced less overall warping but the deformation between layers was clearly visible, almost as if layers had their own segmented warping in groups of 5 layers.

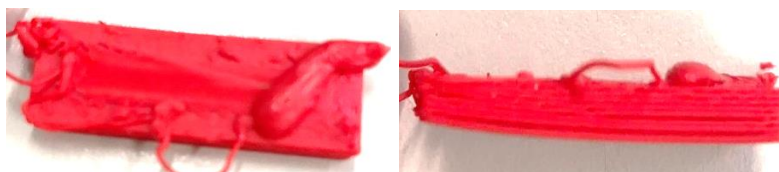


Figure 70 – Results for tests with ironing and $h=0.2\text{ mm}$.

As previously named in sub-chapter 4.1.2.3, *stratified warping* seems to be related with layer adhesion between ironed layers and non-ironed layers. In addition, using $h=0.2\text{mm}$ printing heights seemed to increase the ‘draining problem’, sometimes even leading to disastrous results as shown in Figure 70. A potential solution for the first problem, according to literature [49,53], would be to increase the printing/ironing temperature, however that would aggravate the draining problem, already addressed on sub-chapter 4.1.2.1.

Results for layer height $h=0.1\text{mm}$ were more consistent ‘warping wise’ and even showed almost no visible signs of a heat treatment application, as it can be seen in Figure 71.



Figure 71 - Results for tests with ironing and $h=0.1\text{ mm}$.

It was very clear from these tests that the most adequate printing height, for the chosen printing and ironing parameters, to use is $h=0.1\text{mm}$.

4.2 Main tests

After the preliminary tests, the author gathered enough information to achieve consistent warped results with optimized parameters. The following tests target the impact that different positioning of *ironing* layers has on FFF parts.

4.2.1 Fix parameters

The main goal when choosing the parameters was to replicate the normal 3D printing values for ABS, only changing some necessary ones to achieve consistent warping. Even those parameters emphasized to achieve warping were chosen considering reasonable intervals.

For an easier understanding, *Cura* parameters were divided in ‘Non-ironing layers’ and ‘Ironing layers’; however, it is important to stress that some ‘Non-ironing layers’ parameters remain active for ‘Ironing layers’ (e.g. Printing temperature).

Table 21 – Fix parameters list.

Non-ironing layers	Ironing layers
(1) Pattern	(a) Iron only highest layer
(2) Speed	(b) Pattern
(3) Infill density	(c) Line spacing
(4) Printing temperature	(d) Flow
(5) Bed temperature	(e) Inset
(6) Layer height	(f) Speed
(7) Adhesion plate type	(g) Acceleration
(8) Bed coating	(h) Jerk

4.2.1.1 Non-ironing layers

(1) Pattern. All the non-ironing layers were printed using ZigZag pattern with 3 perimeter contours as recommended by *Cura* [27] and the literature [4]. This configuration not only provides great

mechanical strength prevented from the raster pattern, but it also yields good surface quality from the contours [4].

(2) Speed. The printing speed used was 40mm/s which is perfectly acceptable, as the normal speed for 3D printing ABS is between 30 and 60mm/s [3,4,17,28,38].

(3) Infill density. The infill density chosen was 100%. Warping has the major manifestation for 100% infill density parts [43] and the available literature using ironing to reduce warping also used 100% [3].

(4) Printing temperature. Bearing in mind the attempt to conciliate a grading of 4.5 or 5 (Chapter 4.1) and getting the best out of interlayer cohesion, the printing temperature used for the tests was 220 °C. Similar choices are found in the literature [28,43,49].

(5) Bed temperature. Since the first objective of this thesis is to arrive at constant and replicable parameters that potentiate warping, the bed temperature of 74°C was chosen. A similar study used this same bed temperature [3].

(6) Layer height. The usual layer thickness/height for ABS is 0.2mm. Higher layer heights such as h=0.3mm or h=0.4mm are usually used for faster and rougher prints or for first layers only in case the part requires extra grip to the glass. Lower layer heights are usually used for more thorough parts, despite increasing the printing layer [34]. Given the particularity of applying ironing to the specimen, previous tests indicated that the most suitable layer height was h=0.1mm.

(7) Adhesion plate type. The results from chapter 4.1 indicate that brim and raft reduce warping drastically, so the adhesion plate type used was skirt.

(8) Bed coating. From the previous tests (chapter 4.1), isopropyl alcohol achieved the most warped consistent results, so isopropyl alcohol was chosen as a bed coating.

As a summary, the chosen printing parameters are visible on Table 22:

Table 22 – Summary of the printing parameters of non-ironing layers.

Pattern	Printing parameters				T	T _{bed}	Adhesion plate
	Infill	Speed	Height				
ZigZag with 3 perimeters	100 %	40 mm/s	0.1 mm		220 °C	74 °C	skirt

Only the bed temperature and the infill parameters were deliberately chosen to potentiate warping, all the other printing parameters were kept neutral or intently reducing warping. Table 23 shows the theoretical warping outcome of these choices.

Table 23 – Theoretical warping outcome according to the chosen printing parameters.

	If	Warping	Source	Value	Warping outcome ²
Layer thickness	↑	↑	[17][53][54]	Low	↓
Road width	↑	↑↓	[17]	Low	↑↓
Time of cooling cycles	↑	↓	[17]	Low	↑ ³
Chamber temperature	↑	↓	[4]	Not high	↑↓
Printing temperature	↑	↓	[49][53]	Not high	↑↓
Bed temperature	↑	↓	[35][38]	Low	↑
Stacking section length	↑	↑	[4][17][53]	Not high	↑↓
Number of layers	↑	↓	[4][53]	Not high	↑↓
Path alongside the boarder	↑	↑	[17]	Low	↓
Infill density	↑	↑	[43][3][50]	High	↑
Printing speed	↑	↑	[4][17]	Low	↓
90°/0° or 0°/0° or 90°/90°	-	↑	[4][3][55]	ZigZag	↓
Brim or Raft	-	↓	[27]	Skirt	=

4.2.1.2 Ironing layers

(a) Ironing only last layer. For a cuboid like the shape used, enabling the option: “iron only highest layer” would have no effect since there is only one highest layer; however, it could not be enabled since the mid-processing program would not accept it.

(b) Pattern. According to the previous study (chapter 4.1), the concentric pattern presented the best overall visual quality; therefore, the deposition path chosen was concentric.

(c) Line spacing. Line spacing should be the same value as the layer height which is $h=0.1\text{mm}$. A higher value would mean that not all the layer area would be covered, and a smaller value would mean certain areas would have 2 passages of ironing and an increase in printing time. The line spacing chosen was 0.1mm , because no tests were performed regarding this parameter in this thesis. Furthermore, this is the default value on *Cura* [27] and the value used on a similar study [3].

(d) Flow. Flow was always kept equal to 0% to ensure that the nozzle only applies heat to the ironing surface. A similar choice was taken by Sardinha M. (2020) [3].

(e) Inset. Considering the results of the previous tests (chapter 4.1), the value chosen for inset was 0 mm. This value was contemplated in the referred tests, performing with almost no overall visual deformation due to ironing and covering the entire area of the layer. A similar value was also used by M. Sardinha in his study [3].

(f) Speed. For the top layers to run or fuse together, the ironing speed should be kept as low as possible [3,70] thus the speed used was 20mm/s .

(g) Acceleration. Acceleration was kept as default (500mm/s^2).

(h) Jerk. Jerk was kept as default (5mm/s).

As a summary, the chosen ironing parameters are visible on Table 24.

² ↑↓ - means that this value is in correspondence with the adequate value for the parameter so it does not accentuate or reduce warping

³ The time of cooling cycles is a consequence of the chosen shape. It was considered as increasing warping since the chosen specimen dimensions are small.

Table 24 – Summary of ironing parameters.

Ironing only highest layer	Ironing parameters						
	Pattern	Line spacing	Flow	Inset	Speed	Acceleration	Jerk
No	Concentric	0.1 mm	0%	0 mm	20 mm/s	500 mm/s ²	5 mm/s

4.2.2 List of tests

The following list of prints/tests was conceived in accordance with the methodology explored in chapter 3, to analyze the impact of replicating ironing across other layers. The tests were divided in: non-ironed tests, ironing on the first layers, equally spaced ironing, concentrated ironing and best ironing setup applied to a different shape.

An overall summary of the characteristics of each setup can be found on Appendix I.

4.2.2.1 Non-ironed tests

For future comparisons, it was crucial to identify the distortions present in specimens without any *ironing* process application, previously named as ‘zeros’. The illustration of the printed specimen can be seen at Figure 72.



Figure 72 – Illustration of section view of the specimen without any ironing process applied (zero).

These tests were divided in 2 similar groups of prints: (A1) and (A2). The glass was cleaned before every print with the procedure previously addressed and the specimens were printed always on the same location of the build plate, the only difference between them was the printing day.

4.2.2.2 Ironing on the first layers

It was important to understand whether ironing on the first layers had an impact on warping. And if so, how was the performance compared with ironing applied with equal spacing across the part.

As previously stated, a study regarding this analysis has been conducted [3] for another shape. The following tests, illustrated on Figure 73, try to replicate the same line of thinking although applying it to this 30x10x5mm specimen:



Figure 73 – Representation of ironing on the (B1) first, (B2) second and (B3) third layers, accordingly.

All the setups performed had an initial zero being printed and then there were print 4 of each. The only difference between the B setups was the layer where the ironing process was applied which was either on the first, second or third layer of the specimen.

4.2.2.3 Ironing spaced equally

On chapter 3.3.2, the author explained that the ironing 'starting layer' for these tests was related with the results from the 'ironing on the first layers' tests. The 'starting layer' was then chosen to be the 3rd meaning that all the tests with the ironing process applied spaced equally across the specimen begin the ironing application just after the third layer.

Given the part height of 5mm and the printing layer height of 0.1mm, the total number of layers is equal to 50. The intervals chosen for these tests were: 2, 4 and 6, resulting in 24, 11 and 7 ironed layers correspondingly.

4.2.2.3.1 Interval of 4 layers

For the following tests the ironing process was applied each 4 layers, starting at layer 3, and to this setup was called 'C' specimens (Figure 74).



Figure 74 – Illustration (not at scale) of the ironing process with 4 layers in between (C specimens).

Since this specific configuration was considered to be of high importance for the conclusions of this thesis, 3 series of tests were performed. The first two series of tests, (C1) and (C2), have exactly the same setup and parameters, only differing on the days they were performed. On the last series, it was tried printing zeros and C specimens alternately totaling 6 specimens.

4.2.2.3.2 Interval of 2 layers

For the following tests it was applied the ironing process each 2 layers, starting at layer 3. This setup was called 'D' specimens (Figure 75).

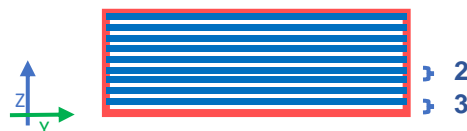


Figure 75 – Illustration (not at scale) of the ironing process with 2 layers in between (D specimens).

Again, one zero was performed and then 4 D specimens were printed.

4.2.2.3.3 Interval of 6 layers

For the following tests it was applied the ironing process each 6 layers, starting at layer 3. This setup was called 'E' specimens (Figure 76).

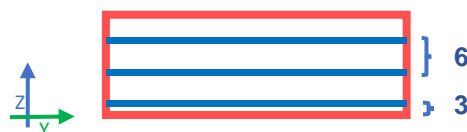


Figure 76 – Illustration (not at scale) of the ironing process with 6 layers in between (E specimens).

For this specimen were printed 4 ironed and 1 non-ironed specimen.

4.2.2.4 Ironing consecutively on the first layers

If warping is caused by the initial deformations and if ironing could eventually reduce warping, then using the ironing process at a concentrated area in the bottom of the specimen would be a promising matter to test.

There were tested two different setups, both ironing the initial layers of the specimen, to infer the impact that ironing the first layers has on warping. In both, the setup of 1 zero and 4 ironed specimens was kept.

4.2.2.4.1 From the 3rd to the 8th layer

For the following tests, it was applied the ironing process in 6 consecutive layers, starting at the third layer. This setup was called 'F' specimens (Figure 77).



Figure 77 – Ironing illustration (not at scale) of 'F' specimens.

4.2.2.4.2 From the 1st to the 3rd layer

For the following tests, it was applied the ironing process in 3 consecutive layers, starting on the first layer. This setup was called 'G' specimens (Figure 78).



Figure 78 – Ironing illustration (not at scale) of 'G' specimens.

4.2.2.5 Best ironing setup applied on a different sized specimen

These series of tests intended to apply the most effective ironing setup learned from the previous tests to a scaled-up version of our specimen. It was decided to maintain the number of layers so the height of the specimen was kept at 5mm whereas the length and width were doubled (Figure 79).

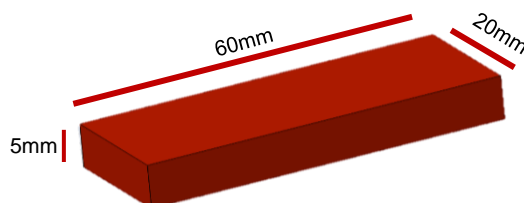


Figure 79 – 60x20x5 mm specimen illustration.

To this new shape, it was applied the ironing process only on the first layer since it was the one presenting the most effective warping reduction. This setup was called 'H' specimens and it is illustrated on Figure 80.



Figure 80 – Ironing illustration (not at scale) of 'H' specimens.

5. RESULTS

This chapter presents the results from the tests explored in chapter 4.5. No mechanical tests were performed so the results will be purely evaluated on the geometric accuracy and looks of the prints.

5.1 Non-ironed tests

The goal of these tests was to ensure that the fix parameters, defined in chapter 4, were in fact capable of producing consistent warped results.

This sub-chapter presents the results from the tests whose setup did not include any ironing process application.

(A1) None ironed layers

Table 25 reveals a much severe impact of the absolute warping (dw) on measuring points (mp) 5 and 6 than on other ones.

Table 25 – Warping (dw) results from A1 tests.

(A1)	1	2	3	4	5	6	$\overline{dw_{5\&6}}$	0.736
zero1	0.100	0.195	0.135	0.120	0.430	0.900	$\sigma_{5\&6}$	0.272
zero2	0.081	0.150	0.105	0.242	0.218	0.927	$\overline{w_{5\&6}}$	14.73%
zero3	0.125	0.115	0.045	0.144	0.730	1.040	Higher	1.040
zero4	0.000	0.140	0.090	0.190	0.651	0.995	Lower	0.000

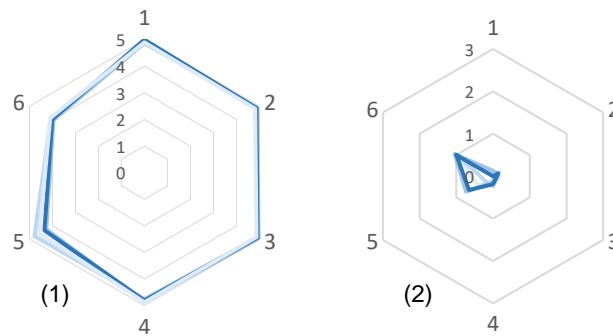


Figure 81 – Graphic results of (1) dz and (2) dw of A1 tests.

Results from A1 tests indicated a distortion on the height of the specimen (shrinkage on the z axis) on points 1 to 4 of about 2.5%. Nevertheless, that value averages 14.73% for 5 and 6 ($\overline{w_{5\&6}}$).

From Figure 81 analysis, the results seem very consistent, almost always overlapping each other, proved by a standard variation of only $\sigma_{5\&6}=0.272\text{mm}$.

The lowest registered value was 0.000mm which means that at least for that specific point, the printed specimen was in accordance with the CAD 3D part. The biggest offset registered more than 1mm (20%) difference from the expected, luckily meaning that there is a lot of room for improvements.

The non-ironed specimens look very similar to each other, indicating once again that the setup used by the other is consistent. Figure 82 shows the A1 specimens.

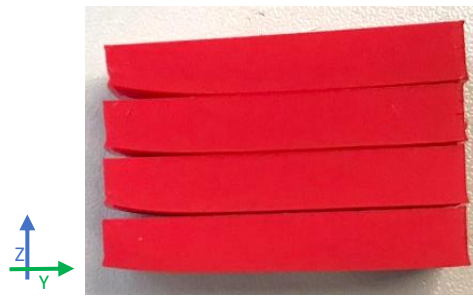


Figure 82 – A1 specimens.

(A2) None ironed layers

The results of the A2 setup can be seen on Table 26 and on Figure 83.

Table 26 – Warping (dw) results from A2 tests.

(A2)	1	2	3	4	5	6	$\overline{dw}_{5\&6}$	0.866
zero1	0.320	0.191	0.120	0.040	1.041	0.540	$\sigma_{5\&6}$	0.225
zero2	0.085	0.186	0.053	0.075	1.200	1.099	$\overline{w}_{5\&6}$	17.33%
zero3	0.300	0.255	0.210	0.021	0.678	0.640	Higher	1.200
zero4	0.187	0.200	0.144	0.144	0.970	0.785	Lower	0.021

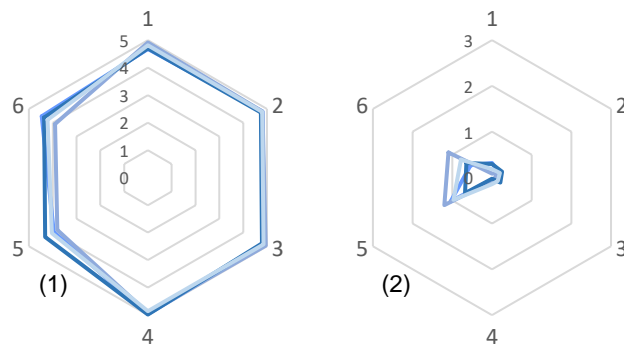


Figure 83 – Graphic results of (1) dz and (2) dw of A2 tests.

By observing the color differences on Table 26 it is possible to identify 2 areas with the most warping, mp 1&2 with around 5% relative warping and on mp 5&6 with 17.33%. Both areas are located on the bottom tips of the specimen, indicating that this phenomenon is in fact warping.

Yet again, Figure 83 (1) shows overlapping results which with a standard deviation of 0.225mm gives the author the confidence that these non-ironed tests will be a good reference for further results comparison.

A2 specimens can be seen on Figure 82.

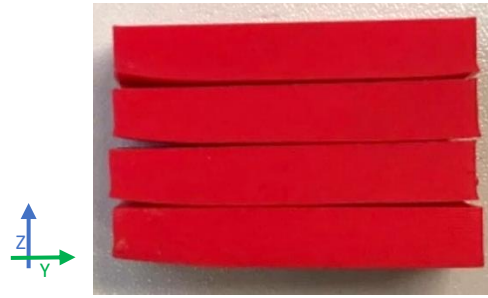


Figure 84 – A2 specimens.

5.2 Ironing on the first layers

This sub-chapter presents the results from the tests whose setup only included one ironed layer on each specimen, either on the first, second or third layer.

(B1) Ironed on the 1st layer

Applying ironing on the first layer of the specimen exposed the author to a new phenomenon, characterized by having some areas of the layer very strongly stuck to the glass almost not enabling it to be released. This phenomenon was named ‘bed over-sticking’ and can be seen on Figure 85.



Figure 85 – Specimen with ‘bed over-sticking’.

Even after waiting for the bed to completely cool down, the author had to apply a lot of force, risking, or/and damaging the specimen. As a result, certain areas of the specimen’s first layer were removed, increasing the difficulty to measure the height in each measuring point. The places where the comparator touched the second layer were given an extra 0.1mm increment on their height and are marked on Table 27 with an asterisk (“*”).

Table 27 – Warping (dw) results from B1 tests.

(B1)	1	2	3	4	5	6	zero	B1
zero	0.049	0.018	0.023	0.095	1.630	2.146	$\overline{dw_{5\&6}}$ 1.888	$\overline{dw_{5\&6}}$ 0.229
B1.1	-0.015*	-0.036*	-0.010*	0.015*	0.037	0.102	$\sigma_{5\&6}$ 0.258	$\sigma_{5\&6}$ 0.175
B1.2	0.033*	0.076*	0.045*	0.055*	0.495	0.475	$\overline{w_{5\&6}}$ 37.76%	$\overline{w_{5\&6}}$ 4.59%
B1.3	0.110*	0.037	0.076*	0.015*	0.145*	0.065*	Higher 2.146	Higher 0.495
B1.4	-0.035	0.200	0.064	0.005	0.145	0.370	Lower 0.018	Lower -0.036

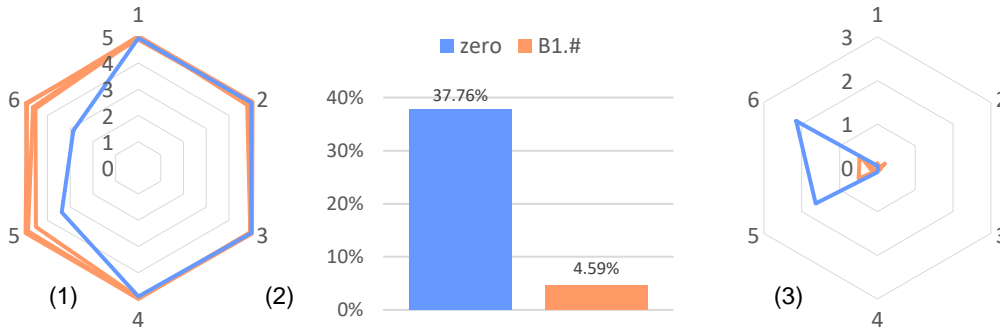


Figure 86 – Graphic results of (1) dz, (2) $\overline{w_{5\&6}}$ and (3) dw of B1 tests.

The effect on warping of ironing the first layer, comparing to the zero specimen, is considerable, decreasing from a relative warping average of 37.76% to 4.59%. Although largely due to the over-sticking effect, this ironing setup seems to be extremely effective in what reducing warping is concerned.

B1 specimens reported very consistent results too, being $\sigma_{5\&6} = 0.175\text{mm}$ one of the best standard deviations achieved in this project.

It can be noticed from the B1 specimen's results on Table 27 that there is negative warping on some specimens, which means that in those spots it had more than 5mm of height. This phenomenon is characteristic of specimens with very low to no warping where the printed dimensions of the part get very close to those designed on the CAD software therefore the slightest deformation results in heights over, or under, 5mm.

(B2) Ironed on the 2nd layer

In these tests, ironing only the second layer of the specimen, the results presented, in general, lower warping, as Table 28 and Figure 87 show.

Table 28 – Warping (dw) results from B2 tests.

(B2)	1	2	3	4	5	6	zero	B2
zero	0.052	0.020	0.045	0.012	0.430	0.385	$\overline{dw_{5\&6}}$ 0.408	$\overline{dw_{5\&6}}$ 0.121
B2.1	0.019	0.040	0.124	-0.090	0.293	0.015	$\sigma_{5\&6}$ 0.022	$\sigma_{5\&6}$ 0.106
B2.2	0.070	0.026	0.050*	0.048	0.211*	0.250	$\overline{w_{5\&6}}$ 8.15%	$\overline{w_{5\&6}}$ 2.43%
B2.3	0.008	0.001	0.005	0.034	0.102	0.060	Higher 0.430	Higher 0.293
B2.4	-0.053*	0.026	-0.032	-0.007	0.000	0.040	Lower 0.012	Lower -0.090

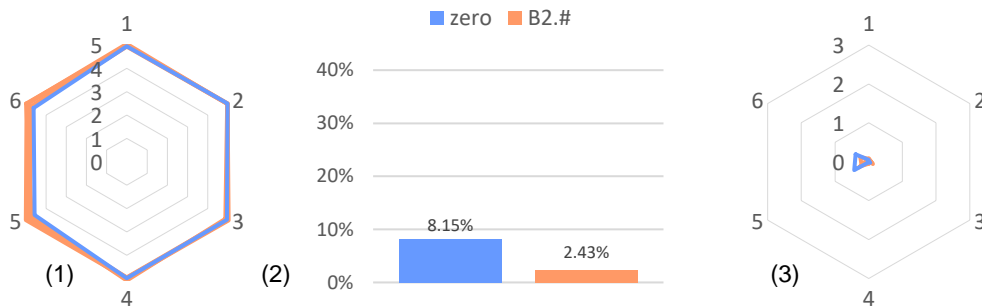


Figure 87 – Graphic results of (1) dz, (2) $\overline{w_{5\&6}}$ and (3) dw of B2 tests.

Similarly to B1 results, B2 specimens presented very promising and consistent results, all the ironed specimens presented lower warping values than the non-ironed specimen strongly indicating that this setup is effective. Figure 87 (2) reveals the decrease on warping, from 8.15% without the ironing process to 2.43% whit ironing process.

The over-sticking effect reported in this case is much lower than in B1, therefore the effort needed to remove the part was almost inexistent and the final appearance of the part was greater.

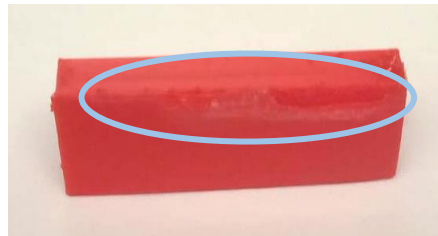


Figure 88 – Over-sticking effect on B2 specimens.

(B3) Ironed on the 3rd layer

B3 setup is characterized by the application of the ironing process just after the third layer. Observation of the specimens revealed a slight presence of extra-material (scraps) on the sides of the part but did not encounter any over-sticking effect, as Figure 89 shows.



Figure 89 – Side view from one B3 specimen.

The complete look at the results from the B3 setup can be seen on Table 29 and on Figure 90.

Table 29 – Warping (dw) results from B3 tests.

(B3)	1	2	3	4	5	6	zero	B3
zero	0.040	0.000	0.028	0.037	0.384	0.744	$\overline{dw_{5\&6}}$	0.564
B3.1	0.057	0.056	0.055	0.100	0.720	1.165	$\sigma_{5\&6}$	0.180
B3.2	0.010	0.010	0.015	0.039	0.097	0.135	$\overline{w_{5\&6}}$	11.28%
B3.3	0.005	0.034	0.013	0.092	0.231	0.410	Higher	0.744
B3.4	0.000	0.036	-0.040	-0.046	0.008	0.040	Lower	0.000
								$\overline{dw_{5\&6}}$
								0.351
								$\sigma_{5\&6}$
								0.378
								$\overline{w_{5\&6}}$
								7.01%
								Higher
								1.165
								Lower
								-0.046

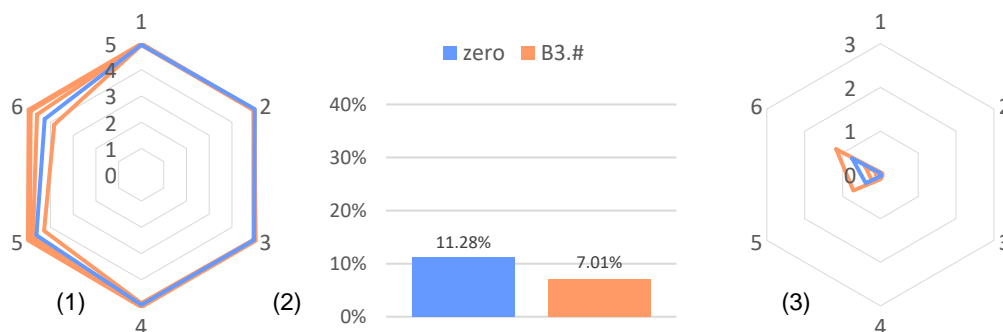


Figure 90 – Graphic results of (1) dz , (2) $\overline{w_{5\&6}}$ and (3) dw of B3 tests.

Figure 90 (1) shows that not all the ironed specimens performed better than the non-ironed one, even though the relative warping average as decreased from 11% to 7%. Contrarily to the 2 prior setups, this one presented one ironed specimen (B3.1) with greater warping than the non-ironed one (zero), indicating a reduction in efficiency in warping reduction probably linked to the non-existence of the over-sticking effect.

The standard deviation of the B3 specimens was 0.378mm, more than double the value registered from B1 and B2.

5.3 Ironing spaced equally

This chapter presents the results of applying the ironing process every 2, 4 and 6 layers.⁴

(C1) Interval of 4 layers

C specimens was the name given to the tests with the ironing process applied every 4 layers, starting at layer 3.

The first thing that is easily noticeable from the C1 specimens is the existence of little scraps resultant from the application of the ironing process very intensively across the specimen, as Figure 91 shows.



Figure 91 – Scraps on C1 specimens: (1) General and (2) Detailed view.

The results of the C1 tests are visible on Table 30 and Figure 92.

Table 30 – Warping (dw) results from C1 tests.

(C1)	1	2	3	4	5	6	zero	C1
zero	0.008	0.045	0.030	0.300	0.290	0.326	$\overline{dw_{5\&6}}$ 0.308	$\overline{dw_{5\&6}}$ 0.349
C1.1	-0.020	-0.013	-0.071	0.010	0.498	0.218	$\sigma_{5\&6}$ 0.018	$\sigma_{5\&6}$ 0.093
C1.2	-0.041	0.080	-0.070	0.069	0.270	0.285	$\overline{w_{5\&6}}$ 6.16%	$\overline{w_{5\&6}}$ 6.97%
C1.3	-0.053	0.066	0.066	0.041	0.360	0.336	Higher 0.326	Higher 0.498
C1.4	-0.022	-0.026	0.019	0.000	0.337	0.485	Lower 0.008	Lower -0.073

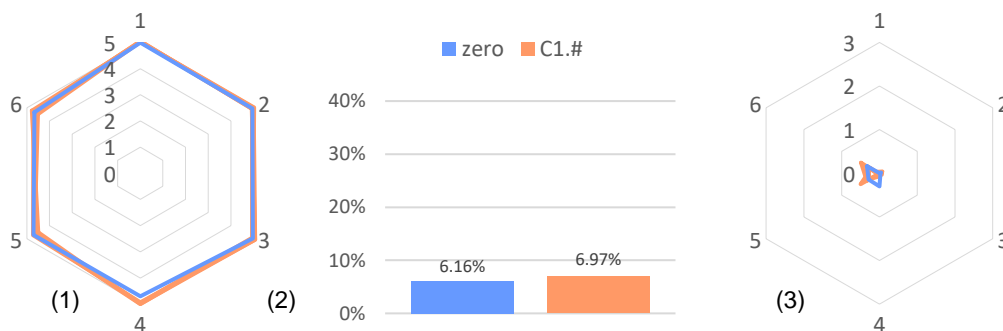


Figure 92 – Graphic results of (1) dz , (2) $\overline{w_{5\&6}}$ and (3) dw of C1 tests.

⁴ The order at which they are named and presented was the order at which they were printed

C1 data revealed a slight increase in the warping average when applying the C specimen setup; however, the author decided not to consider these results since they defer a lot from all the other tests.

A systematic error seemed to have been influencing the results given so many negative warping results, combined with a standard average of 0.093mm, indicating something was wrong, probably the bed coating application.

To better understand the influence of applying ironing every 4 layers, a new set of tests, this time with a bigger non-ironed warpage, was conducted.

(C2) Interval of 4 layers

C2 tests were the tests performed to better understand the results obtained in C1 and the results can be seen in Table 31.

Table 31 – Warping (dw) results from C2 tests.

(C2)	1	2	3	4	5	6	zero	C2
zero	0.000	0.095	0.075	0.060	1.585	1.760	$\overline{dw}_{5\&6}$ 1.673	$\overline{dw}_{5\&6}$ 2.161
C2.1	0.115	0.590	0.122	0.190	1.825	2.162	$\sigma_{5\&6}$ 0.088	$\sigma_{5\&6}$ 0.402
C2.2	0.021	0.080	0.079	0.029	1.541	1.805	$\overline{w}_{5\&6}$ 33.45%	$\overline{w}_{5\&6}$ 43.21%
C2.3	0.142	0.240	0.250	0.230	2.545	2.821	Higher 1.760	Higher 2.821
C2.4	0.095	0.220	0.210	0.230	2.130	2.455	Lower 0.000	Lower 0.021

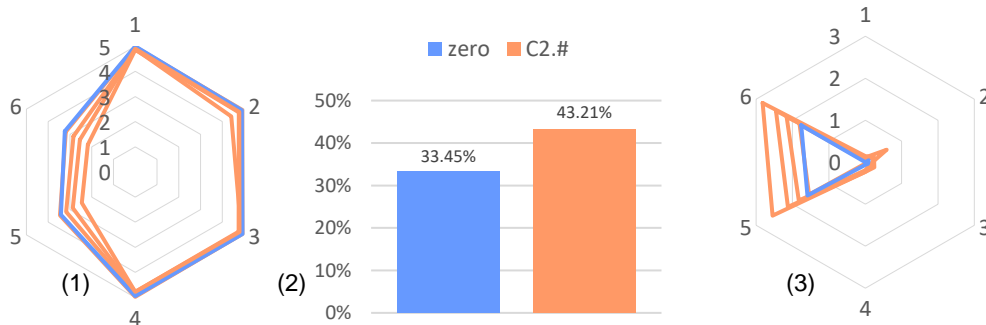


Figure 93 – Graphic results of (1) dz, (2) $\overline{w}_{5\&6}$ and (3) dw of C2 tests.

All the reported data from mp 5&6 show relative warping results of above 30% of the specimen height, strongly indicating that the author applied too many glass cleaner during the bed cleaning procedure. Again, the error seems to be influencing both the ironed and the non-ironed specimens so conclusions can be taken.

Figure 93 (1) and (3) illustrate a clear pattern of results with almost no warping at points 1-4 and proportional warping results on points 5 and 6.

The ironed specimens consistently performed worst then the non-ironed one, increasing from an average of 33.45% to 43.21%. Applying the ironing process each 4 layers, starting at layer 3, seems not only not to decrease warping but even to amplify it.

(C3) Interval of 4 layers

Contrarily to the last tests, C3 tests alternated from non-ironed to ironed specimens, the obtained results can be seen in Table 32 and Figure 94.

Table 32 – Warping (dw) results from C3 tests.

(C3)	1	2	3	4	5	6	zero	C3		
zero1	0.081	0.150	0.105	0.242	0.218	0.927	$\overline{dw}_{5\&6}$	0.760	$\overline{dw}_{5\&6}$	1.505
C3.1	0.040	0.115	0.086	0.285	1.155	1.330	$\sigma_{5\&6}$	0.279	$\sigma_{5\&6}$	0.454
zero2	0.125	0.115	0.045	0.144	0.730	1.040	$\overline{w}_{5\&6}$	15.20%	$\overline{w}_{5\&6}$	30.11%
C3.2	0.288	0.590	0.088	0.210	1.959	2.270	Higher	1.040	Higher	2.270
zero3	0.000	0.140	0.090	0.190	0.651	0.995	Lower	0.000	Lower	0.040
C3.3	0.062	0.170	0.108	0.241	0.998	1.320				

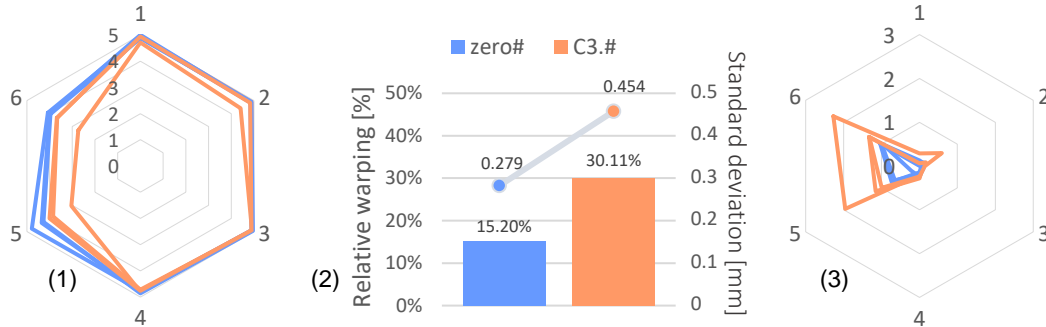


Figure 94 – Graphic results of (1) dz, (2) $\overline{w}_{5\&6} + \sigma_{5\&6}$ and (3) dw of C3 tests

The average warping of the ironed specimens ($\overline{dw}_{5\&6}=1.505\text{mm}$) almost doubled the average of the non-ironed specimens ($\overline{dw}_{5\&6}=0.760\text{mm}$), yet only one test presented very different results from the others (C3.2). Furthermore, and similarly to C2 tests, all the non-ironed specimens presented less warping on the mp 5&6 than the ironed ones.

Non-ironed results were more consistent too, reporting a standard deviation of 0.279mm, whereas on the ironed ones it was 0.454mm. Visually, the C3 ironed tests exhibited little scraps on the side of each specimen, similarly to the B3 specimens, but this time across all the part, as shown by Figure 95.

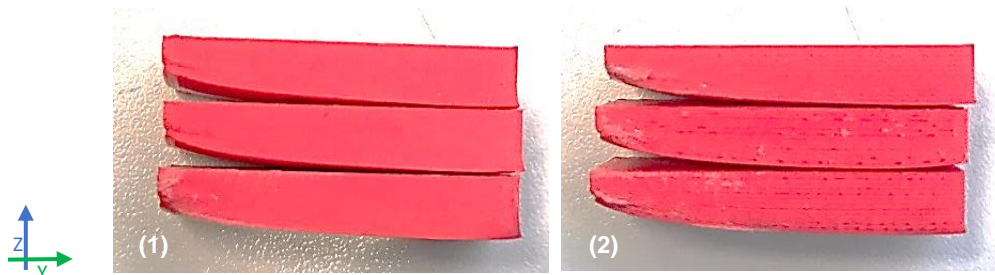


Figure 95 – C3 (1) non-ironed and (2) ironed specimens.

(D1) Interval of 2 layers

In these tests the ironing process was applied to every two layers, starting at layer 3. As experienced at chapter 4.4.2, applying the ironing process very frequently results in 'stratified warping' and D specimens were not an exception (Figure 96).



Figure 96 – Stratified warping on D specimens.

On Figure 96 it is also possible to see the ‘scraps’ characteristic from the C specimens. Both these phenomena destroyed the appearance and the internal cohesion of the part.

The overall warping experienced can be seen in Table 33.

Table 33 – Warping (dw) results from D1 tests.

(D1)	1	2	3	4	5	6	zero	D1		
zero	0.140	0.127	0.262	0.223	1.033	0.897	$\overline{dw}_{5\&6}$	0.965	$\overline{dw}_{5\&6}$	2.111
D1.1	0.140	0.025	0.420	0.388	1.910	2.270	$\sigma_{5\&6}$	0.068	$\sigma_{5\&6}$	0.313
D1.2	0.370	0.710	0.105	0.200	2.410	2.500	$\overline{w}_{5\&6}$	19.30%	$\overline{w}_{5\&6}$	42.22%
D1.2	0.125	0.055	-0.110	-0.055	2.236	2.274	Higher	1.033	Higher	2.500
D1.4	0.185	0.639	0.078	0.160	1.667	1.622	Lower	0.127	Lower	-0.110

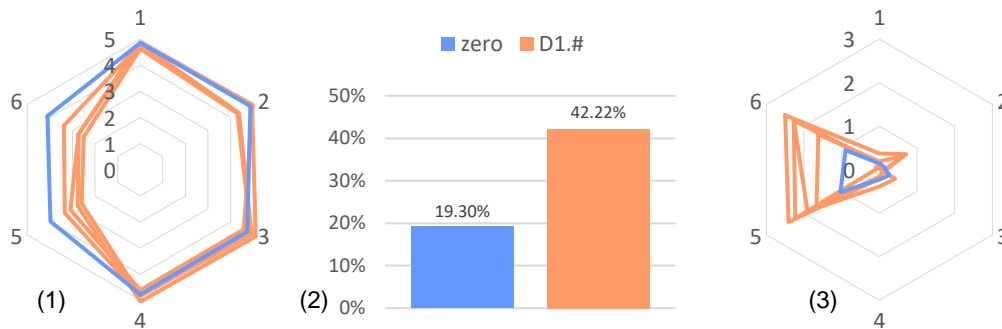


Figure 97 – Graphic results of (1) dz, (2) $\overline{w}_{5\&6}$ and (3) dw of D1 tests.

The results concerning D specimens were in line with what has been presented for C specimens, the application of spaced ironing does not contribute for the warping reduction. In this case, the average relative warping increased from 19.30% to 42.22%, reporting one of the most warped specimens in this work.

Consistency also prevailed, considering the level of absolute warpage of more than 2mm, the results were more less similar throughout the D specimens, experiencing 0.313mm standard deviation.

(E1) Interval of 6 layers

E specimens are defined by applying the ironing process every 6 layers, starting at the third.

Table 34 – Warping (dw) results from E1 tests.

(E1)	1	2	3	4	5	6	zero	E1		
zero	0.016	0.110	0.030	0.088	0.970	0.894	$\overline{dw}_{5\&6}$	0.932	$\overline{dw}_{5\&6}$	1.704
E1.1	0.145	0.098	0.210	0.222	2.650	2.750	$\sigma_{5\&6}$	0.038	$\sigma_{5\&6}$	0.620
E1.2	0.000	0.038	0.022	0.040	1.773	1.711	$\overline{w}_{5\&6}$	18.64%	$\overline{w}_{5\&6}$	34.08%
E1.3	0.028	0.027	0.485	0.389	1.200	1.110	Higher	0.970	Higher	2.750
E1.4	0.000	0.030	0.046	0.180	1.203	1.235	Lower	0.016	Lower	0.000

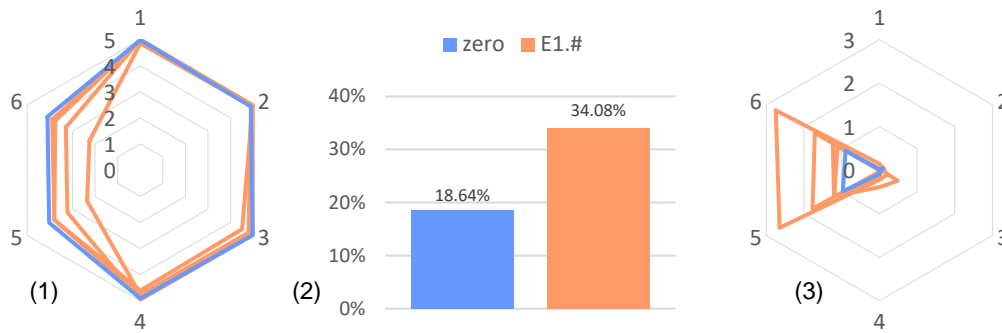


Figure 98 – Graphic results of (1) dz , (2) $\overline{w_{5\&6}}$ and (3) dw of E1 tests.

The average relative warping registered by the E specimens was 34%, 15 percentual points more than the correspondent zero. The results also presented a considerable standard deviation of 0.620mm, yet always with higher warping values than the non-ironed reference specimen.

E specimens also presented superficial ironing traces, presented on Figure 99.



Figure 99 – Ironing traces on E specimens (E1.3).

5.4 Ironing concentrated

The next two setups tried to understand the impact of applying the ironing process on consecutive layers. Both setups focused on the first layers of the specimens, namely on the first 3 layers and on the 6 consecutive ones.

(F1) 6 concentrated layers

F1 setup included applying the ironing process between the third and the eighth layers of the specimen.

After the printing and the measurements, the final results were summarized on Table 35 and on Figure 100.

Table 35 – Warping (dw) results from F1 tests.

(F1)	1	2	3	4	5	6	zero	F1
zero	0.065	0.550	0.090	0.115	1.130	1.902	$\overline{dw_{5\&6}}$ 1.516	$\overline{dw_{5\&6}}$ 2.266
F1.1	0.109	1.380	0.139	0.155	1.120	2.440	$\sigma_{5\&6}$ 0.386	$\sigma_{5\&6}$ 0.858
F1.2	0.220	0.678	0.270	0.335	3.200	3.380	$\overline{w_{5\&6}}$ 30.32%	$\overline{w_{5\&6}}$ 45.32%
F1.3	0.158	0.467	0.153	0.088	1.728	3.210	Higher 1.902	Higher 3.380
F1.4	0.145	0.482	0.152	0.080	1.250	1.800	Lower 0.065	Lower 0.080

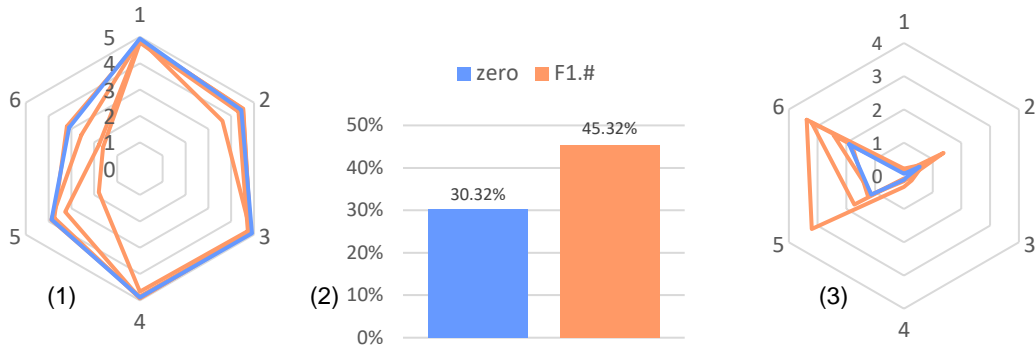


Figure 100 – Graphic results of (1) dz , (2) $\overline{w_{5\&6}}$ and (3) dw of F1 tests.

In this case, the zero specimen contrasts with the results obtained earlier, as this time the non-ironed part experienced a 30.32% deformation due to warping, much higher than the 16% average of the A tests.

F specimens presented the most warping of all the tests performed in this thesis with an average of 45.32% relative warping. It is very clear that this method did not help reduce warping as all the ironed F specimens performed worse than the zero.

The consistency of the results did not help either, as $\sigma_{5\&6} = 0.858\text{mm}$ means that the expected warping for a F specimen is very difficult to predict.

As a consequence of applying the ironing process on consecutive layers, Figure 101 reveals a completely melted zone from the third to the eighth layers of the specimen.



Figure 101 – Melted layers on F1 specimens.

Not only it did not help decrease warping, but it also destroyed the bottom part of specimen both visual and mechanically. This factor is probably the responsible for such a high standard deviation of results.

(G1) 3 concentrated layers

G1 setup included the ironing process application on the 3 first layers of the specimen. The results of this tests is summarized on Table 36.

Table 36 – Warping (dw) results from G1 tests.

(G1)	1	2	3	4	5	6	zero	G1
zero	0.038	0.018	0.023	0.055	0.630	1.056	$\overline{dw_{5\&6}}$ 0.843	$\overline{dw_{5\&6}}$ 0.180
G1.1	0.000*	0.000*	-0.010*	0.002*	0.033*	0.109*	$\sigma_{5\&6}$ 0.213	$\sigma_{5\&6}$ 0.125
G1.2	0.013*	0.026*	0.044*	0.045*	0.395*	0.334*	$\overline{w_{5\&6}}$ 16.86%	$\overline{w_{5\&6}}$ 3.60%
G1.3	0.076*	0.037*	0.056*	0.018*	0.125*	0.075*	Higher 1.056	Higher 0.395
G1.4	-0.002	0.100	0.064	0.009	0.100	0.270	Lower 0.018	Lower -0.010

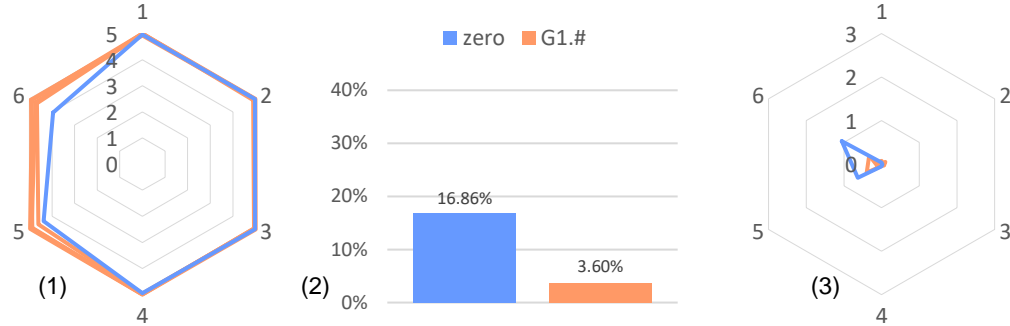


Figure 102 – Graphic results of (1) dz, (2) $\overline{w_{5\&6}}$ and (3) dw of G1 tests.

As a result of the application of the ironing process in such a way, the ironed specimen presented a decrease in the relative warping from 16.86% to 3.60%, a reduction of almost 80%. Although largely due to the over-sticking effect, this ironing setup seems to be extremely effective in what reducing warping is concerned.

The results concerning the ironed specimens reported very consistent results too, being $\sigma_{5\&6} = 0.125\text{mm}$ among the best standard deviations registered in this study.

3 of the 4 specimens exhibited ‘bed over-sticking’, a term introduced in this study on chapter 5.2 when studying the application of the ironing process on the first layer of the specimen.



Figure 103 – Bed over-sticking effect on G1 specimens: (1) General and (2) Detailed view.

Figure 103 shows the result of the bottom part of the G1.3 specimen whose first layer was separated from the specimen due to the bed over-sticking effect.

5.5 Ironing on a different sized specimen

These series of tests intended to apply the most effective ironing setup learned from the previous tests to a scaled-up version of our specimen. It was decided to maintain the number of layers so the height of the specimen was kept at 5mm, whereas the length and width were doubled.

(H1) Print 1 ‘zero’ and then print a series of 4 specimens applying ironing only on the first layer

On the last series of tests (H1) it was applied the best performing ironing setup (in reducing warping) from the previous tests into a specimen with 4x times the contact area. The best performing setup was the B1 setup therefore H1 setup had ironing applied to the first layer of a 60x20x5mm specimen.

The same effect experienced in the B specimens was also evident in these specimens. The bed over-sticking made it very hard to remove the part from the glass, only possible with the application of a lot of force and thus damaging the part.



Figure 104 – Bed over-sticking on a H1 specimen.

In this case, 100% of the H1 ironed specimens presented the phenomenon already explained, contributing, in large scale, for the low warping registered and present on Table 37.

Table 37 – Warping (dw) results from H1 tests.

(H1)	1	2	3	4	5	6	zero	H1
zero	0.060	0.090	0.040	0.090	0.288	0.310	$\overline{dw}_{5\&6}$ 0.299	$\overline{dw}_{5\&6}$ 0.235
H1.1	0.027*	0.052	0.046	0.090	0.065	0.100	$\sigma_{5\&6}$ 0.011	$\sigma_{5\&6}$ 0.153
H1.2	0.122*	0.090*	0.043	0.098	0.280*	0.166	$\overline{w}_{5\&6}$ 5.98%	$\overline{w}_{5\&6}$ 4.70%
H1.3	0.157	0.017	0.345	0.182*	0.421	0.488	Higher 0.310	Higher 0.488
H1.4	0.110	0.095*	0.083	0.085	0.058	0.300	Lower 0.040	Lower 0.017

A particularity of this setup results is the similarity between the non-ironed and ironed results. On Figure 105 (1) the results overlay each other, indicating that even the non-ironed specimen presented very low warping.

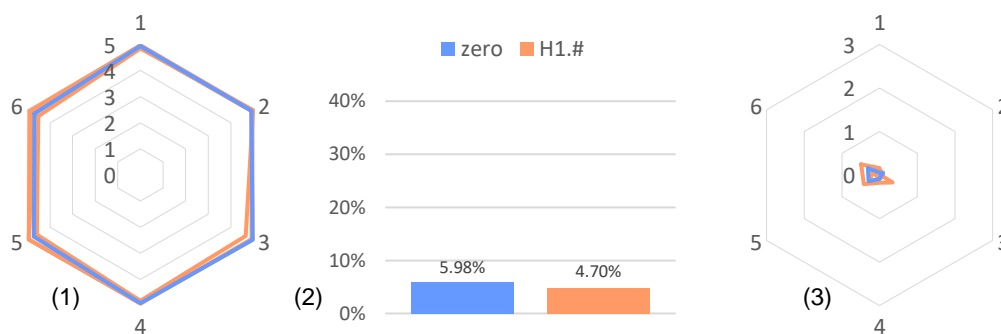


Figure 105 – Graphic results of (1) dz, (2) $\overline{w}_{5\&6}$ and (3) dw of H1 tests.

The calibration of the bed coating application to achieve warping on the first specimen (the ‘zero’), as better explored on chapter 3.4.1, required the author to repeat the procedure 6 times before having any signs of warping. This difficulty in achieving warping in a non-ironed specimen was only experienced with this setup, nevertheless, the application of the ironing process reduced the warping from 5.98% to 4.70%.

One possible explanation for this finding is that larger contact areas reduce the changes of experiencing warping, as already backed by the tests using the plate adhesion type brim. However, all the parameters used in this setup were optimized for a specimen 4 times smaller so, in that sense, indirect factors such as time between passages or gradients of temperature across the layers may play a role on the cause. Therefore, and even though it indicates in that direction, it would be unwise for the author to conclude that the only reason why the H1 specimens reported less warping was because of its larger contact area.

6. RESULTS ANALYSIS

This chapter intends to discuss the results obtained in Chapter 4 and 5.

6.1 Warping on non-ironed tests

Before discussing the results of the ironed specimens, it was essential to verify the validity and consistency of the non-ironed ones.

It was expected that the warping absolute average ($\overline{dw_{5\&6}}$) might change across the different series since there are variables that escape the authors control, yet it is crucial to assure that the standard deviation was consistently low so that comparisons with non-ironed layers could be made.

Series A1, A2 and C3 included multiple non-ironed specimens in their tests so they were the ones considered. The standard deviation in these testes varied from 0.225mm to 0.279mm which is a good indication of the validity of these results.

Coincidentally, the absolute warping ($\overline{dw_{5\&6}}$) registered by these 3 series, as Table 38 shows, varied from 0.736 to 0.866mm, a variation of only 2.6% of the total height of the specimen, which is impressive given the time gap between the 3 different setups.

Table 38 – Comparison of the warping results of the non-ironed tests.

Tests	Number of zeros	Warping $\overline{dw_{5\&6}}$ [mm]	Standard deviation $\sigma_{5\&6}$ [mm]
A1	4	0.736	0.272
A2	4	0.866	0.225
zeros from C3	3	0.760	0.279
Average	11	0.787	0.259

These results prove the adequacy of the setup chosen for the tests, from the bed coating to the positioning on the glass bed, giving the author confidence of his methodology accuracy. If, for example, the recurrent cleaning of the glass had a considerable impact on warping, then the specimens from A1, A2 and C3 would have presented more warping as more specimens were printed but that outcome is not, by any means, confirmed by the results obtained.

From the results presented in Table 38 and the experience gathered from these tests, the author was confident that including only one non-ironed specimen for calibration in the ironed series of tests would be enough for accurate conclusions. Additionally, the value of the average standard deviation $\sigma_{5\&6} = 0.259mm$ is going to be used as the reference value for future comparisons.

6.2 Warping when only applying ironing on the first layers

Understanding the impact of ironing the first layers was consider from the beginning one of the most relevant factors when choosing the setup for the other ironed tests since its relevance was already mentioned by Sardinha M. (2020) [3] in a previous analysis.

The comparison between the B series, present in Table 39, revealed that, on average, the absolute warping reduced 75%, from 0.953 to 0.234mm, when applying ironing on the first layers.

Table 39 – B specimens overall results.

Tests	NON-IRONED			IRONED		
	amount	$\overline{dw}_{5\&6}$ [mm]	$\sigma_{5\&6}$ [mm]	amount	$\overline{dw}_{5\&6}$ [mm]	$\sigma_{5\&6}$ [mm]
B1	1	1.888	0.258	4	0.229	0.175
B2	1	0.408	0.022	4	0.121	0.106
B3	1	0.564	0.180	4	0.351	0.378
Average	1	0.953	0.153	4	0.234	0.220

The results obtained for the relative warping, presented in Figure 106, show that the lowest result was obtained by the B2 setup (e.g. ironing the second layer).

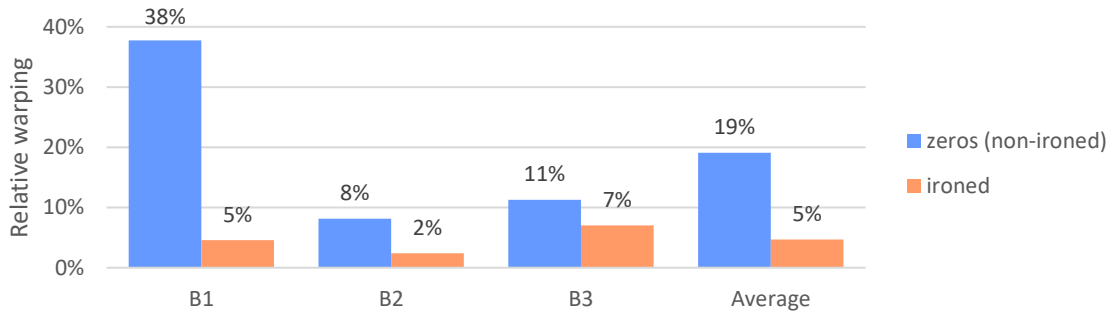


Figure 106 – Relative warping comparison of ironed B specimens.

On the other hand, if the warping reduction from the non-ironed specimen is considered, the conclusions change. The highest warping reduction was achieved by ironing the first layer (B1 setup), followed by the second and the third (Figure 107).

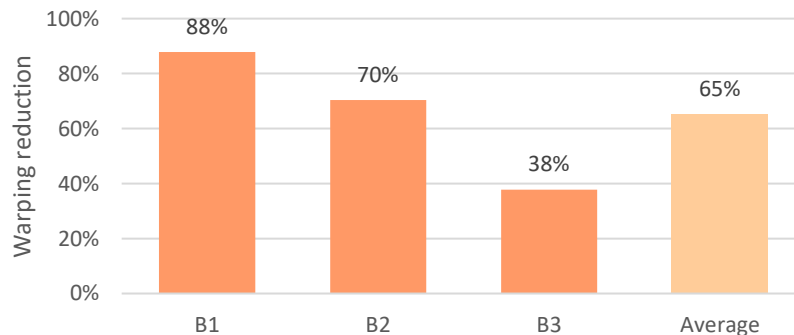


Figure 107 – Warping reduction on B specimens.

To compare the consistency of the B specimen results the standard deviation should be taken into account, yet the average standard deviation of $\sigma_{5\&6}=0.180\text{mm}$ seen by the non-ironed specimens in the B series has no real meaning since only one specimen was considered in each test.

The comparison however can be made if it is considered the result obtained by the A tests. In this case the average standard deviation of $\sigma_{5\&6}=0.220\text{mm}$ for the ironed B tests is higher than the $\sigma_{5\&6}=0.259\text{mm}$ of the non-ironed tests from A series, adding to the conviction that ironing the first layers of the specimen not only decreases warping but also reports more trustworthy results.

These conclusions match with Sardinha M. (2020) [3] study which also stated that applying ironing on the first layers decreases warping.

The authors [3] achieved a maximum average distortion reduction, by ironing the first layer of the specimen, of 33%, contrasting with the 88% reduction reported by this study. Even though the conclusions point on the same direction, these discrepancies can probably be explained by the different experimental conditions, namely the use of bed coating and specimen dimensions.

Additionally, a characteristic present throughout the B series is the presence of ‘bed over-sticking’ which led to the partial destruction of many specimens. This characteristic was considered in the presentation of the results on Table 27 and Table 28 by a ‘*’, marked by a red rectangle on Figure 108.

(B1)	1	2	3	4	5	6	(B2)	1	2	3	4	5	6
B1_zero	0.049	0.018	0.023	0.095	1.630	2.146	B2_zero	0.052	0.020	0.045	0.012	0.430	0.385
B1.1	-0.015*	-0.036*	-0.010*	0.015*	0.037	0.102	B2.1	0.019	0.040	0.124	-0.090	0.293	0.015
B1.2	0.033*	0.076*	0.045*	0.055*	0.495	0.475	B2.2	0.070	0.026	0.050*	0.048*	0.211*	0.250*
B1.3	0.110*	0.037	0.076*	0.015*	0.145*	0.065*	B2.3	0.008	0.001	0.005	0.034	0.102	0.060
B1.4	-0.035	0.200	0.064	0.005	0.145	0.370	B2.4	-0.053*	0.026	-0.032	-0.007	0.000	0.040

Figure 108 – Comparison of the ‘bed over-sticking’ effect on B series.

The reported phenomenon was very predominant when ironing the first layer and decreased its importance when ironing the second and third one, as Figure 109 illustrates.

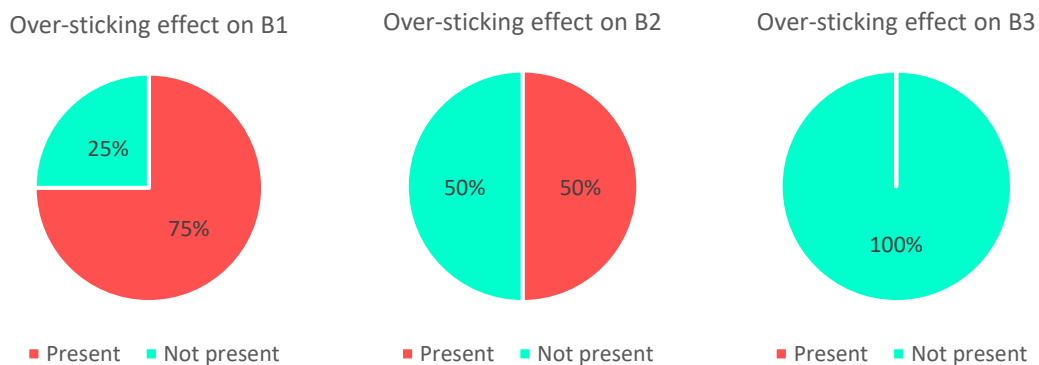


Figure 109 – ‘Over-sticking’ effect predominance on B series.

Figure 109 illustrates the percentage of ironed specimens where over-sticking effect damaged the overall looks of the specimen. Given the esthetic consequences of the effect, the adoption of these setups must be pondered considering the importance of reducing warping over the looks.

For this reason, for the other setups, the author chose to only start applying the ironing process after the third layer, except from two specific setups (G1 and H1).

6.3 Warping when applying ironing spaced evenly across the specimen

Understanding the impact of the ironing process inevitably required for the author to understand the effect of applying it across multiple layers of the specimen. The approach used included the application every two, four and six layers, corresponding to D, C and E setups respectively.

The detailed results were displayed on chapter 5.3 and a general comparison of the data obtained can be seen on Table 40.

Table 40 – C, D and E specimens overall results.

Tests	(ZEROS) NON-IRONED		IRONED	
	$\bar{d}w_{5\&6}$ [mm]	$\sigma_{5\&6}$ [mm]	$\bar{d}w_{5\&6}$ [mm]	$\sigma_{5\&6}$ [mm]
C1	0.308	0.018	0.349	0.093
C2	1.673	0.088	2.161	0.402
C3	0.760	0.279	1.505	0.454
C2+C3 Average	1.222	0.279	1.834	0.428
D1	0.965	0.068	2.111	0.313
E1	0.932	0.038	1.704	0.620
Average	0.928	-	1.566	0.376

From analyzing the data, the author decided not to consider the results from the C1 tests for further calculations and conclusions because, even though the results point in the same direction of the rest, this series indicates a systematic error given the so little warping effect compared with the others.

Applying the ironing treatment across the specimen not only increased the time of printing but notably increased warping. All the performed tests exhibited on average more warping with than without the process, as illustrated on Figure 110.

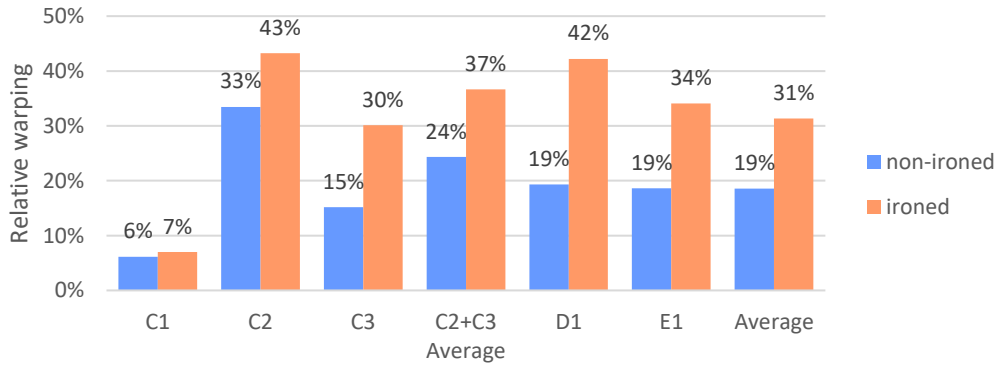


Figure 110 – Relative warping average of C, D and E specimens.

Similarly to the previous analysis on sub-chapter 6.2, the non-ironed specimens ('zeros') exhibited very distinct results from setup to setup so it is important to consider the warping variation instead of the direct relative value (Figure 111).

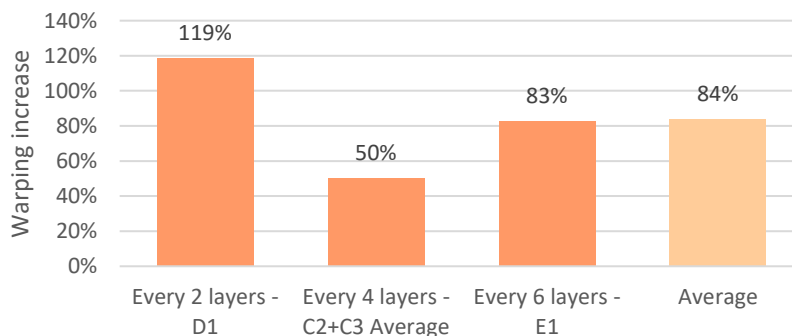


Figure 111 – Warping increase on C, D and E specimens.⁵

⁵ Note that Y axis is referring to the “warping increase” to avoid presenting all the results negative.

Ironing every 2 layers proved to be the worst solution so far, increasing the distortions on the specimen by 119%, followed by the application every 6 and 4 layers, reporting increases of 83 and 50% overall.

As a result of these results, it seems that there is no advantage on ironing layers across the specimen. Applying this process so intensively increases the number of thermic cycles resulting in non-uniform thermal gradients causing internal stresses and leading to distortions/warping.

From Figure 112 it is possible to see that the standard deviation of the tests increased as the spacing between ironing layers increased. Additionally, all the ironing tests presented higher standard deviation than the 'zero tests' average explored in chapter 6.1.

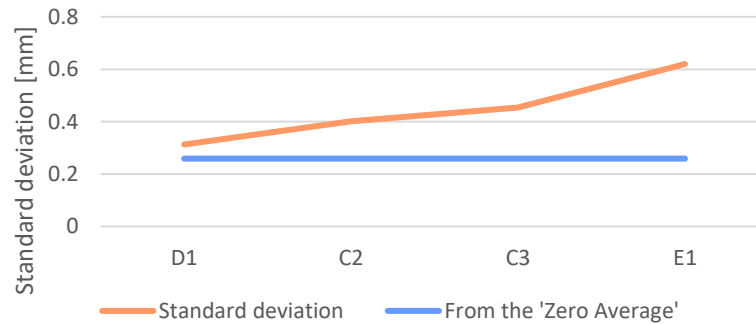


Figure 112 – Standard deviation from D, C and E specimens.

The perception that spacing the ironing process across the specimen does not come as a viable solution for warping not only comes from the dimension results but also from the final looks of the specimen. Applying many layers of ironing, principally the ones with 2 and 4 layer interval, led to an excessive deposition of material, responsible for a partial destruction of the specimen, certainly disabling the use of the part.

6.4 Warping when applying concentrated ironing

The fourth type of setup studied in this work involved applying the ironing process in consecutive layers. F1 tests applied the ironing process from the 4th to the 9th layer whereas G1 specimens from the 1st to the 3rd. Table 41 summarizes the absolute warping and standard deviation registered by both.

Table 41 – F and G overall results.

Tests	NON-IRONED			IRONED			
	amount	$\overline{dw}_{5\&6}$ [mm]	$\sigma_{5\&6}$ [mm]	amount	length	$\overline{dw}_{5\&6}$ [mm]	$\sigma_{5\&6}$ [mm]
F1	1	1.516	0.386	4	6 layers	2.266	0.858
G1	1	0.843	0.213	4	3 layers	0.180	0.125

An explicit visualization of the warping increase/reduction resultant of these the setups can be seen at Figure 113.

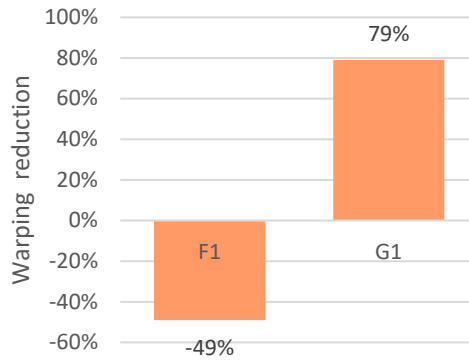


Figure 113 – Warping reduction on F and G specimens.

The results show a clear difference on warping between the application of the ironing process until the 3rd layer (G1 specimens) and after the 3rd layer (F1 specimens). F1 specimens registered an increase of warping of 49% whereas G1 specimens registered a decrease of 79%, proving that there is no advantage on ironing the zone just after the 3rd layer of the specimen.

Given the inefficacy of results registered by F1, the most adequate comparison to make would be to compare the B setups with G1, seen at Figure 114.

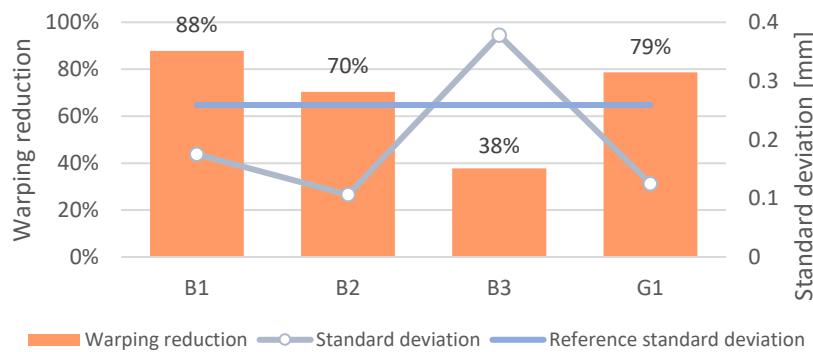


Figure 114 – Warping reduction and standard deviation on B and G specimens.

In this case, G1 and B1 were the only tests analyzed so far that included the ironing process application on the first layer of the specimen and interestingly they both share bed over-sticking effect on 75% of its specimens and more than 75% warping reduction.

G1 standard deviation is very similar to the ones registered by B1 and B2, corroborating the thesis that applying the ironing process on the first layers presents consistent low-warped results; however, the standard deviation seems to increase as the ironing process is applied in higher layers (e.g. 3rd layer).

As mentioned on Chapter 4.1, all the measurements performed have an error associated with the difficulty of measuring warped specimens, however, given the discrepancies between ironed and non-ironed specimens in all setups tried, none of the conclusions would have changed, in fact, including the uncertainties would only favor the non-ironed specimens which globally performed better than the ironed ones.

6.5 Warping when applying ironing on a different shaped specimen

As mentioned on Chapter 2, as the size of the specimen change, the likelihood of achieving warping change too.

In order to understand the impact of changing the dimensions of the specimen in warping, H1 specimens presented double the width and double the length of the 30x10x5mm standard specimen used in all the other tests.

Before applying the ironing process, the author repeated the printing procedure 6 times before achieving a warped specimen. Contrasting with the 30x10x5mm specimens which only required on average 1.53 specimens before achieving a warped non-ironed result.

Even after achieving warping, the results were the lowest registered in this work, even when comparing with the lowest among the other tests (as shown on Figure 115).

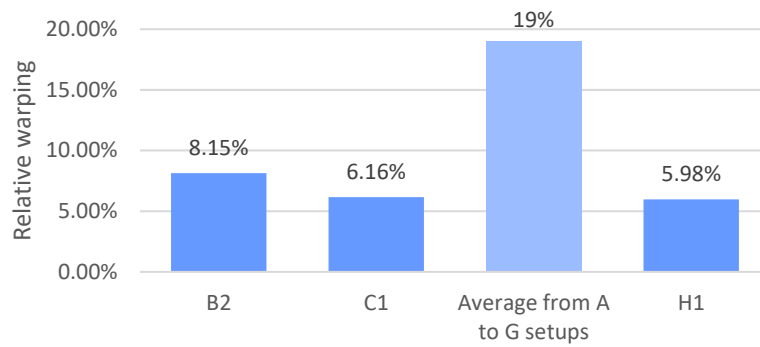


Figure 115 – Lowest non-ironing relative warping results.

When comparing to the relative warping average from the A-G setups, the H1 specimens presented less than 1/3 of the warping so it is very clear that increasing the contact area was responsible for these discrepancies.

Looking at the ironed specimens, the results for ironing only the first layer of the specimen on a 60x20x5mm specimen revealed the same phenomenon as the B1, B2 and G1 specimens, where the first layer got stuck to the glass (over-sticking effect).

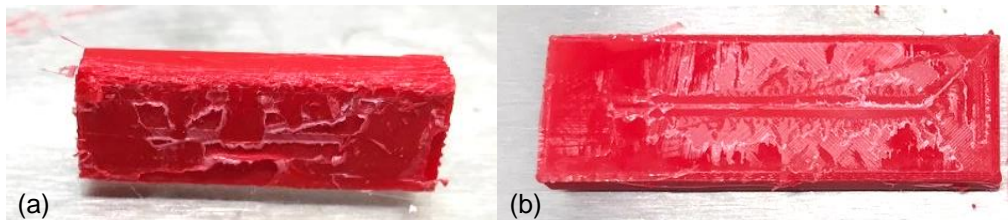


Figure 116 – Over-sticking effect on (a) 30x10x5mm (b) 60x20x5mm specimens.

6.6 Warping on different sides

When comparing the warpage on the left (mp 5) and on the right (mp 6) side of the specimen, the difference between both became evident. Figure 117 shows that in the vast majority of the setups tried, the mp 6 exhibits more distortions than the mp 5.

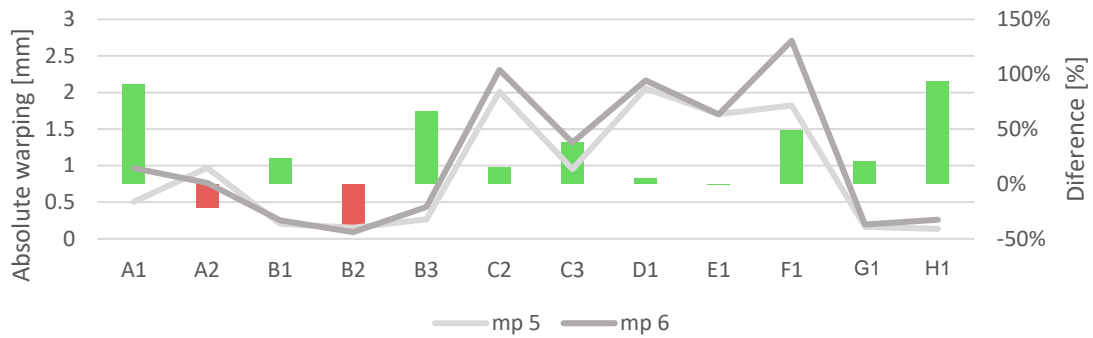


Figure 117 – Difference between mp 5 and 6 on all setups.

The overall average difference indicates that point 6 is 28% more affected by warping than the point 5.

Coincidentally, the same happens between point 1 and 2, where the second measuring point performs, on average, two times worse (Figure 118).

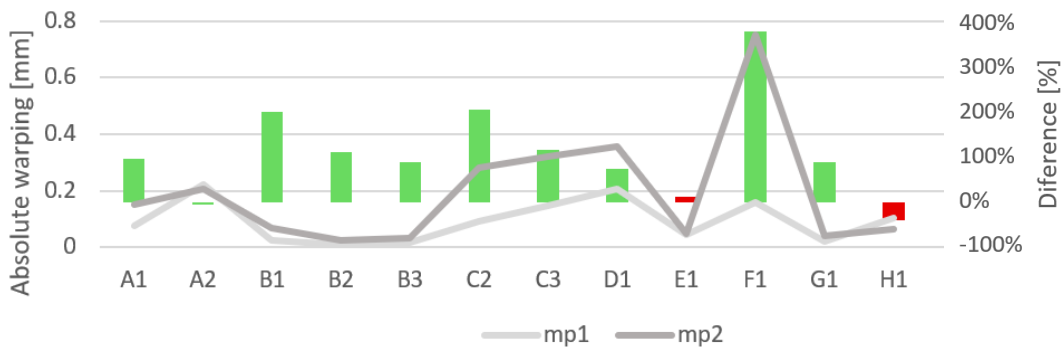


Figure 118 – Difference between mp 1 and 2 on all setups.

The experimental procedure carried out in this dissertation does not allow for further conclusions on the reasons why this phenomenon has happened, further studies must be performed to determine the cause of this consistent discrepancy.

6.7 Printing times

For the specimen size 30x10x5mm, each ironing layer takes 2min and 42 seconds to complete so the differences in printing time between setups is noticeable, as Figure 119 shows.

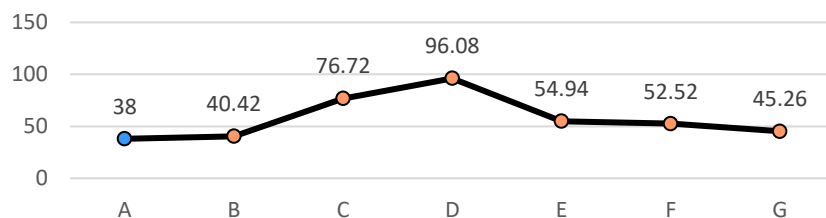


Figure 119 – Printing time by setup (in minutes).


6.8 Performance

To perform a final comparison between the setups tested, the author decided to use a decision table.

The 4 main criteria used were: warping intensity, the lateral appearance, the bottom appearance, and the printing time. It was then assigned, to each setup and criteria, a score from 1 (very unsatisfactory) to 6 (optimized), based on each individual performance already elaborated in this chapter (Table 42).

Table 42 – Final score comparison table.

	Warping	Lateral appearance	Bottom appearance	Printing time
A	3	6	6	6
B1	6	5	1	5
B2	5	5	2	5
B3	5	5	6	5
C	2	4	6	2
D	1	2	6	1
E	1	4	6	3
F	2	1	6	3
G	6	4	1	4



The impact that each criterion has on deciding which setup is the best differs, therefore different weights were attributed to each criterion. The range of values chosen was again from 1 (less important) to 6 (extremely important).

In order to account for different environments, 3 scenarios were created:

- (1) The printed part is part of a small batch of a non-visible component of a machine which requires both the upper and the lower surfaces to be geometrically precise.
- (2) The printed part will be sold to consumers, in large scale, however it may have some deformations.
- (3) The printed part is only required to have the least warping possible.

Considering the previous scenarios, the weights chosen by the author are visible on Table 43.

Table 43 – Weights of each scenario.

	Warping intensity	Lateral appearance	Bottom appearance	Printing time
(1)	6	2	5	1
(2)	3	6	5	6
(3)	6	1	1	1

By multiplying the weights of each criterion (Table 43) by its correspondent score (Table 42), the performance was achieved.

Figure 120 presents the results for the environment (1).

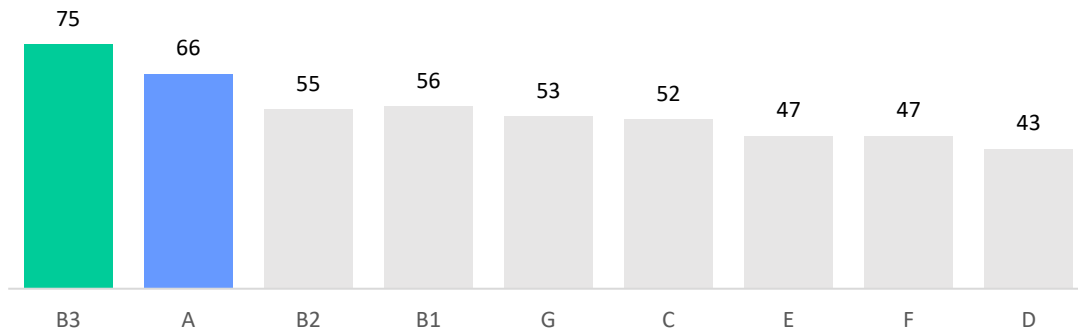


Figure 120 – Performance score of specimens A-G on scenario (1).

In this case, the best solution would be applying setup B3 which means only applying the ironing process on the third layer of the specimen. It is possible to see that only this option performs better than A (non-ironed specimens) given that all the other setups tested have lower performance scores.

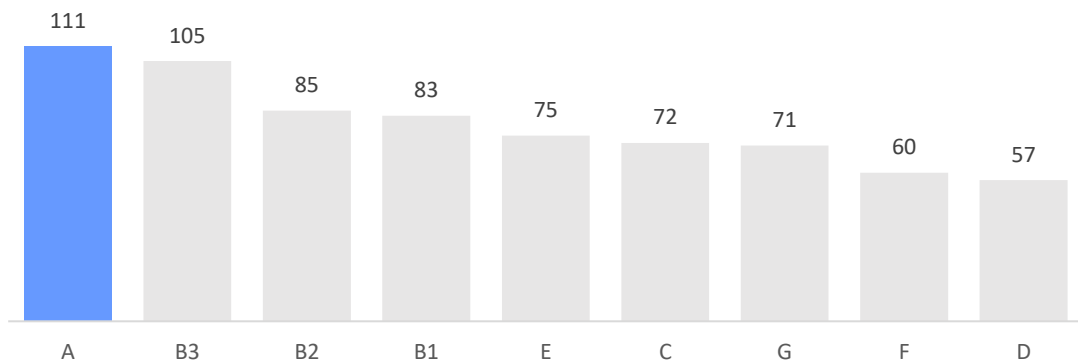


Figure 121 – Performance score of specimens A-G on scenario (2).

For the scenario (2), presented on Figure 121, the outcome is different. In this case the better performance would be achieved by simply not applying any ironing process to the specimen.

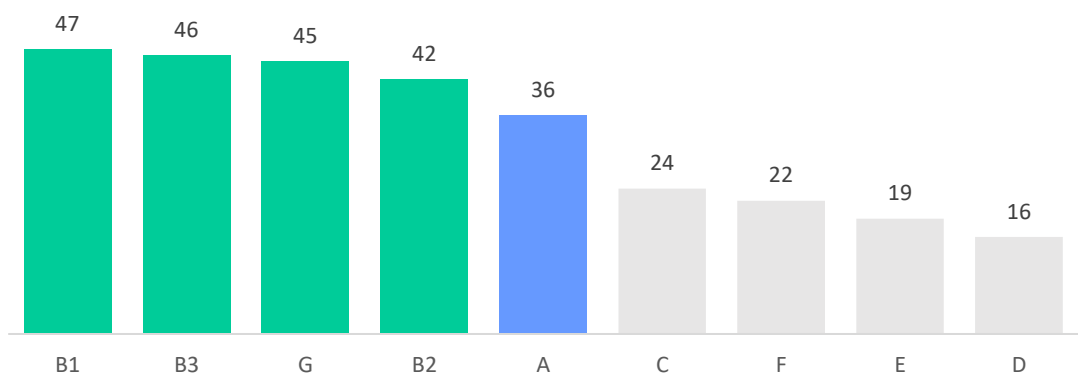


Figure 122 – Performance score of specimens A-G on scenario (3).

For the third scenario conceptualized, the performance scores on Figure 122 indicate that 4 setups would improve the original specimen. The most successful one would be only ironing the first layer of the specimen (B1), potentiating the bed-sticking effect and eliminating warping.

7. CONCLUSION

This chapter summarizes the research conclusions while discussing further work.

Initially, the author tried to potentiate warping so that he could understand the impact of ironing. During that process it became very clear that there are already various parameters that could reduce warping, namely using the plate adhesion type “brim”, using higher bed temperatures or applying glue to the printing bed.

From the tests performed, principally when trying to understand the warping effect, the author concluded that, above all, the bed coating is the most determining factor on warping reduction. Another curious finding is that applying glue to the bed, as normally practiced on the 3D printing community, is not the most effective solution for its reduction, principally when using high bed temperatures, rather applying hand sanitizer on the printing glass presented substantially better results.

As proposed in the beginning, the first big objective of this work was the author to arrive at a set of parameters, conditions and specimen shape that successfully replicated warping. This objective was achieved for very particular condition however indicating that this deformation can be tackled and controlled.

As another of its objectives, the second conclusion of this work is that ironing can, in fact, reduce warping. For some setups tested, the ironing process consistently proved to reduce the distortions on the part. Nevertheless, its application encountered some drawbacks.

It requires the user to know beforehand the most appropriate settings for an effective usage which may include using undesired printing settings on the rest of print just so that the ironing layer is performed correctly. Since the ironing process uses the same layer height and nozzle temperature as the other layers, it may force the user to choose a lower layer height and a lower printing temperature during all printing to make sure that the ironed layer performed as intended. These changes could increase the printing time and fragilize the internal cohesion of the part. Even so, the improvement and widening of ironing process capabilities in the future, can be used to tackle the issue.

Another disadvantage of applying ironing to combat warping is the extra processing step, named ‘mid-processing’ in this work. Here, the g-code has to be modified to replicate the ironing layer across the part, adding at least 3 min of work to the user to be completed.

The author may conclude that the ironing process, as a solution for warping, at this time, is most adequate on parts that have a constant shape across the part, that would already use a layer height of 0.1mm or less and that would not be subjected to mechanical forces. Nevertheless, for these particular cases, this solution should only be considered if all the others failed to solve the problem. All these conditions may change if either the slicer or the mid-processing software update to newer version that included more detailed ironing parameters.

In case it is used, the best performing solution, in the author’s opinion, is only applying the ironing process on the third layer of the specimen. Even though it may depend on the objective (further exploited on chapter 6.8), applying this ironing setup proved to reduce warping while it did not damage the first layer of the specimen, it did not show considerable signs of its application and it increased the printing time very residually.

7.1 Original contributions

For the conditions tested, the conclusions considered noteworthy are the following:

- Warping will occur with higher intensity on the opposite side from where the nozzle starts printing each layer.
- The best performing printing temperature when applying the ironing process is 220°C.
- The ironing process performs better for a layer height of $h=0.1\text{mm}$ than for $h=0.2\text{mm}$.
- The ironing process reduces warping only if applied on the first layers.
- Applying the ironing process spaced equally around the part creates scraps and does not reduce warping.
- Applying the ironing process, on consecutive layers, noticeably damages the part.
- Applying ironing on the first and/or second layers potentiates the part to over-stick to the glass.

7.2 Future work

Rather than being a finished project, this thesis can serve as a baseline for future work, namely:

- Continue studying and understanding the characteristics of warping.
- Understand why does warping affect more one side than the other.
- Test these conclusions on other specimens.
- Optimized the parameters of ironing so that it takes less time.
- Update the mid-processing software so that it can include more degrees of freedom to the user.

The author visions that the actual panorama will evolve in the direction of the slicing software including a 'Warping reduction' option, as one of its parameters on the 'Advanced settings', with probably 2 levels of intensity (1) Soft and (2) High:

- (1) The softest option would automatically iron the 3rd layer of the specimen.
- (2) The more drastic option would automatically iron the 1st layer of the specimen.

Contrary to what the current software versions can do, both these options would require the software to correctly apply the ironing process on a specific layer of the specimen regardless of its shape. The software should at the same time try to avoid the draining problem. The author suggests for the program to automatically start lower the nozzle temperature to 230°C before the ironing layer or to effectively retract the filament just before ironing. Other solutions may appear as knowledge and technology improve being therefore essential further studies on the subject.

If the authors vision is implemented, this solution would potentiate the use of ABS to vaster applications since the fear of it warping would reduce substantially, and it would decrease the printing setup time, before and after the print, since it would reduce the need to apply and clean the bed coating (e.g. glue).

Bibliography

- [1] Forbes. Significant 3D Printing Forecast Surges To \$35.6 Billion n.d. <https://www.forbes.com/sites/tjmccue/2019/03/27/wohlers-report-2019-forecasts-35-6-billion-in-3d-printing-industry-growth-by-2024/> (accessed January 10, 2021).
- [2] Gibson I, Rosen D, Stucker B. Additive manufacturing technologies: 3D printing, rapid prototyping, and direct digital manufacturing, second edition. 2015. <https://doi.org/10.1007/978-1-4939-2113-3>.
- [3] Sardinha M, Vicente CMS, Frutuoso N, Leite M, Ribeiro R, Reis L. Effect of the ironing process on ABS parts produced by FDM. *Mater Des Process Commun* 2020. <https://doi.org/10.1002/mdp2.151>.
- [4] Wang TM, Xi JT, Jin Y. A model research for prototype warp deformation in the FDM process. *Int J Adv Manuf Technol* 2007;33. <https://doi.org/10.1007/s00170-006-0556-9>.
- [5] Yuan S, Strobbe D, Li X, Kruth JP, Van Puyvelde P, Van der Bruggen B. 3D printed chemically and mechanically robust membrane by selective laser sintering for separation of oil/water and immiscible organic mixtures. *Chem Eng J* 2020;385. <https://doi.org/10.1016/j.cej.2019.123816>.
- [6] Zhao R, Gao J, Liao H, Fenineche N, Coddet C. Selective laser melting of elemental powder blends for fabrication of homogeneous bulk material of near-eutectic Ni–Sn composition. *Addit Manuf* 2020;34. <https://doi.org/10.1016/j.addma.2020.101261>.
- [7] Eleftheriadis GK, Monou PK, Bouropoulos N, Boetker J, Rantanen J, Jacobsen J, et al. Fabrication of Mucoadhesive Buccal Films for Local Administration of Ketoprofen and Lidocaine Hydrochloride by Combining Fused Deposition Modeling and Inkjet Printing. *J Pharm Sci* 2020;109. <https://doi.org/10.1016/j.xphs.2020.05.022>.
- [8] Tofail SAM, Koumoulos EP, Bandyopadhyay A, Bose S, O'Donoghue L, Charitidis C. Additive manufacturing: scientific and technological challenges, market uptake and opportunities. *Mater Today* 2018;21. <https://doi.org/10.1016/j.mattod.2017.07.001>.
- [9] Prof P, Rui P, Fernandes A. Influência dos parâmetros de fabrico nas propriedades mecânicas de peças obtidas por impressão 3D com um único material Tomás Sousa Martins Engenharia Mecânica Novembro 2017 Agradecimentos. 2017.
- [10] Rauch E, Unterhofer M, Dallasega P. Industry sector analysis for the application of additive manufacturing in smart and distributed manufacturing systems. *Manuf Lett* 2018;15. <https://doi.org/10.1016/j.mfglet.2017.12.011>.
- [11] Jörg Bromberger and Kelly Richard. Additive manufacturing: A long-term game changer for manufacturers 2017. <https://www.mckinsey.com/business-functions/operations/our-insights/additive-manufacturing-a-long-term-game-changer-for-manufacturers#> (accessed January 10, 2021).
- [12] Liaw CY, Guvendiren M. Current and emerging applications of 3D printing in medicine. *Biofabrication* 2017;9. <https://doi.org/10.1088/1758-5090/aa7279>.
- [13] Murr LE. Frontiers of 3D Printing/Additive Manufacturing: from Human Organs to Aircraft Fabrication. *J Mater Sci Technol* 2016;32. <https://doi.org/10.1016/j.jmst.2016.08.011>.
- [14] Pereira D, Libano DB. Development of a cylindrical coordinate based fused deposition modeling machine with multiple print heads 2018.
- [15] Zhang Y, Kevin Chou Y. 3D fea simulations of fused deposition modeling process. *Proc. Int. Conf. Manuf. Sci. Eng.*, vol. 2006, 2006.
- [16] Sun Q, Rizvi GM, Giuliani V, Bellehumeur CT, Gu P. Experimental study and modeling of bond formation between ABS filaments in the FDM process. *Annu. Tech. Conf. - ANTEC, Conf. Proc.*, vol. 1, 2004.

- [17] Zhang Y, Chou K. A parametric study of part distortions in fused deposition modelling using three-dimensional finite element analysis. *Proc Inst Mech Eng Part B J Eng Manuf* 2008;222. <https://doi.org/10.1243/09544054JEM990>.
- [18] Mohamed OA, Masood SH, Bhowmik JL. Mathematical modeling and FDM process parameters optimization using response surface methodology based on Q-optimal design. *Appl Math Model* 2016;40. <https://doi.org/10.1016/j.apm.2016.06.055>.
- [19] Galantucci LM, Lavecchia F, Percoco G. Experimental study aiming to enhance the surface finish of fused deposition modeled parts. *CIRP Ann - Manuf Technol* 2009;58. <https://doi.org/10.1016/j.cirp.2009.03.071>.
- [20] Huang SH, Liu P, Mokasdar A, Hou L. Additive manufacturing and its societal impact: A literature review. *Int J Adv Manuf Technol* 2013;67. <https://doi.org/10.1007/s00170-012-4558-5>.
- [21] Patrikalakis NM, Maekawa T. Shape interrogation for computer aided design and manufacturing. 2010. <https://doi.org/10.1007/978-3-642-04074-0>.
- [22] Couldwell WT, MacDonald JD, Thomas CL, Hansen BC, Lapalika A, Thakkar B, et al. Computer-aided design/computer-aided manufacturing skull base drill. *Neurosurg Focus* 2017;42. <https://doi.org/10.3171/2017.2.FOCUS16561>.
- [23] Carlota V. Top 10 Best CAD Software For All Levels 2019. <https://www.3dnatives.com/en/top10-cad-software-180320194/#/> (accessed January 15, 2021).
- [24] 9 TYPES OF CAD SOFTWARE COMPANIES USE (2021) 2021. <https://www.apollotechnical.com/cad-software-companies-use/> (accessed January 15, 2021).
- [25] Evans B. *Practical 3D Printers: The Science and Art of 3D Printing*. 2012.
- [26] Wallack Kloski L, Kloski N. *Make: Getting Started with 3D Printing*. vol. 53. 2019.
- [27] Cura 4.6 process parameters definition 2020.
- [28] Alsoufi MS, Elsayed AE. Surface Roughness Quality and Dimensional Accuracy—A Comprehensive Analysis of 100% Infill Printed Parts Fabricated by a Personal/Desktop Cost-Effective FDM 3D Printer. *Mater Sci Appl* 2018;09. <https://doi.org/10.4236/msa.2018.91002>.
- [29] Lubombo C, Huneault MA. Effect of infill patterns on the mechanical performance of lightweight 3D-printed cellular PLA parts. *Mater Today Commun* 2018;17. <https://doi.org/10.1016/j.mtcomm.2018.09.017>.
- [30] Hay Z. Best 3D Printing Temperatures for PLA, PETG, Nylon, TPU. *Mater Sci Eng A* 2020. <https://all3dp.com/2/the-best-printing-temperature-for-different-filaments/> (accessed November 20, 2020).
- [31] Rohringer S. 2020 3D Printer Filament Buyer's Guide. *Ultim Filam Guid* 2020; <https://all3dp.com/1/3d-printer-filament-types-3d-> <https://all3dp.com/1/3d-printer-filament-types-3d-printing-3d-filament/> (accessed October 31, 2020).
- [32] Arnold C, Monsees D, Hey J, Schweyen R. Surface quality of 3D-printed models as a function of various printing parameters. *Materials (Basel)* 2019;12. <https://doi.org/10.3390/ma12121970>.
- [33] Schmitt BM, Zirbes CF, Bonin C, Lohmann D, Lencina DC, Da Costa Sabino Netto A. A comparative study of cartesian and delta 3d printers on producing PLA parts. *Mater. Res.*, vol. 20, 2017. <https://doi.org/10.1590/1980-5373-mr-2016-1039>.
- [34] Fernandes JFM. Estudo da Influência de Parâmetros de Impressão 3D nas Propriedades Mecânicas do PLA. 2016.
- [35] Choi Y-H, Kim C-M, Jeong H-S, Youn J-H. Influence of Bed Temperature on Heat

- Shrinkage Shape Error in FDM Additive Manufacturing of the ABS-Engineering Plastic. *World J Eng Technol* 2016;04. <https://doi.org/10.4236/wjet.2016.43d022>.
- [36] Dul S, Fambri L, Pegoretti A. Fused deposition modelling with ABS-graphene nanocomposites. *Compos Part A Appl Sci Manuf* 2016;85. <https://doi.org/10.1016/j.compositesa.2016.03.013>.
- [37] Weng Z, Wang J, Senthil T, Wu L. Mechanical and thermal properties of ABS/montmorillonite nanocomposites for fused deposition modeling 3D printing. *Mater Des* 2016;102. <https://doi.org/10.1016/j.matdes.2016.04.045>.
- [38] Nazan MA, Ramli FR, Alkahari MR, Abdullah MA, Sudin MN. An exploration of polymer adhesion on 3D printer bed. *IOP Conf. Ser. Mater. Sci. Eng.*, vol. 210, 2017. <https://doi.org/10.1088/1757-899X/210/1/012062>.
- [39] Olivieri G. ABS+/Plus Filament: What Is It & Is It Worth It? 2020. <https://all3dp.com/2/abs-plus-filament-what-is-it/> (accessed October 31, 2020).
- [40] Reddy AB, Reddy GSM, Jayaramudu J, Sudhakar K, Manjula B, Ray SS, et al. Polyethylene Terephthalate-Based Blends: Natural Rubber and Synthetic Rubber. *Poly(Ethylene Terephthalate) Based Blends, Compos. Nanocomposites*, 2015. <https://doi.org/10.1016/B978-0-323-31306-3.00005-1>.
- [41] Ultimaker. Ultimaker ABS Material: Specifications 2020. <https://support.ultimaker.com/hc/en-us/articles/360011953520> (accessed November 1, 2020).
- [42] Ken Giang. PLA vs. ABS: What's the difference? n.d. <https://www.3dhubs.com/knowledge-base/pla-vs-abs-whats-difference/> (accessed November 1, 2020).
- [43] Tootooni MS, Dsouza A, Donovan R, Rao PK, Kong Z, Borgesen P. Assessing the geometric integrity of additive manufactured parts from point cloud data using spectral graph theoretic sparse representation-based classification. *ASME 2017 12th Int. Manuf. Sci. Eng. Conf. MSEC 2017 collocated with JSME/ASME 2017 6th Int. Conf. Mater. Process.*, vol. 2, 2017. <https://doi.org/10.1115/MSEC2017-2794>.
- [44] Jacobs P. The effects of random noise shrinkage on rapid tooling accuracy. *Mater Des* 2000;21. [https://doi.org/10.1016/s0261-3069\(99\)00060-6](https://doi.org/10.1016/s0261-3069(99)00060-6).
- [45] Schmutzler C, Zimmermann A, Zaeh MF. Compensating Warpage of 3D Printed Parts Using Free-form Deformation. *Procedia CIRP*, vol. 41, 2016. <https://doi.org/10.1016/j.procir.2015.12.078>.
- [46] Yang HJ, Hwang PJ, Lee SH. A study on shrinkage compensation of the SLS process by using the Taguchi method. *Int J Mach Tools Manuf* 2002;42. [https://doi.org/10.1016/S0890-6955\(02\)00070-6](https://doi.org/10.1016/S0890-6955(02)00070-6).
- [47] Jin M, Giesa R, Neuber C, Schmidt HW. Filament Materials Screening for FDM 3D Printing by Means of Injection-Molded Short Rods. *Macromol Mater Eng* 2018;303. <https://doi.org/10.1002/mame.201800507>.
- [48] Held M, Pfligersdorffer C. Correcting warpage of laser-sintered parts by means of a surface-based inverse deformation algorithm. *Eng Comput* 2009;25. <https://doi.org/10.1007/s00366-009-0136-3>.
- [49] Alsoufi MS, Elsayed AE. Warping deformation of desktop 3D printed parts manufactured by open source fused deposition modeling (FDM) system. *Int J Mech Mechatronics Eng* 2017;17.
- [50] Zhang W, Wu AS, Sun J, Quan Z, Gu B, Sun B, et al. Characterization of residual stress and deformation in additively manufactured ABS polymer and composite specimens. *Compos Sci Technol* 2017;150. <https://doi.org/10.1016/j.compscitech.2017.07.017>.
- [51] Zhang Y, Pursell C, Mao K, Leigh S. A physical investigation of wear and thermal

- characteristics of 3D printed nylon spur gears. *Tribol Int* 2020;141. <https://doi.org/10.1016/j.triboint.2019.105953>.
- [52] Shih WK. Shrinkage modeling of polyester shrink film. *Polym Eng Sci* 1994;34. <https://doi.org/10.1002/pen.760341405>.
- [53] Peng A. Research on the interlayer stress and warpage deformation in FDM. *Adv. Mater. Res.*, vol. 538–541, 2012. <https://doi.org/10.4028/www.scientific.net/AMR.538-541.1564>.
- [54] Kantaros A, Karalekas D. Fiber Bragg grating based investigation of residual strains in ABS parts fabricated by fused deposition modeling process. *Mater Des* 2013;50. <https://doi.org/10.1016/j.matdes.2013.02.067>.
- [55] Nickel AH, Barnett DM, Prinz FB. Thermal stresses and deposition patterns in layered manufacturing. *Mater Sci Eng A* 2001;317. [https://doi.org/10.1016/S0921-5093\(01\)01179-0](https://doi.org/10.1016/S0921-5093(01)01179-0).
- [56] Haimbaugh RE. *Practical Induction Heat Treating*. 2015.
- [57] Specialty steel treating. The benefits of steel heat treatment 2016. <https://www.sst.net/benefits-of-heat-treatment/> (accessed December 20, 2020).
- [58] Dosset JL, Boyer HE. *Practical Heat Treating: Second Edition*. 2019. <https://doi.org/10.31399/asm.tb.pht2.9781627082624>.
- [59] Yasuda H, Charlson EJ, Charlson EM, Yasuda T, Miyama M, Okuno T. Dynamics of Surface Property Change in Response to Changes in Environmental Conditions. *Langmuir* 1991;7. <https://doi.org/10.1021/la00058a070>.
- [60] Shin JS, Lee DY, Ho CC, Kim JH. Effect of annealing on the surface properties of poly(*n*-butyl methacrylate) latex films containing poly(styrene/ α -methylstyrene/acrylic acid). *Langmuir* 2000;16. <https://doi.org/10.1021/la9906370>.
- [61] Carville. Heat Treatment of Plastics 2020. <https://www.carvilleplastics.com/services/heat-treatment-plastics/> (accessed December 5, 2020).
- [62] Ishikawa M, Narisawa I. The effect of heat treatment on plane strain fracture of glassy polymers. *J Mater Sci* 1983;18. <https://doi.org/10.1007/BF00547600>.
- [63] Peruzzo PJ, Anbinder PS, Pardini OR, Costa CA, Leite CA, Galembeck F, et al. Polyurethane/acrylate hybrids: Effects of the acrylic content and thermal treatment on the polymer properties. *J Appl Polym Sci* 2010;116. <https://doi.org/10.1002/app.31795>.
- [64] Wang C, Chu F, Graillat C, Guyot A, Gauthier C. Hybrid polymer latexes - Acrylics-polyurethane: II. Mechanical properties. *Polym Adv Technol* 2005;16. <https://doi.org/10.1002/pat.557>.
- [65] Borcia C, Borcia G, Dumitrascu N. Surface treatment of polymers by plasma and UV radiation. *Rom Reports Phys* 2011;56.
- [66] Steiner C, Fichtner J, Fahlteich J. Nanostructuring of polymer surfaces by magnetron plasma treatment. *Surf Coatings Technol* 2018;336. <https://doi.org/10.1016/j.surfcoat.2017.09.023>.
- [67] Mittal KL. *Polymer surface modification: Relevance to adhesion, Volume 3*. 2004. <https://doi.org/10.1201/b12183>.
- [68] Borcia G, Anderson CA, Brown NMD. The surface oxidation of selected polymers using an atmospheric pressure air dielectric barrier discharge. Part II. *Appl Surf Sci* 2004;225. <https://doi.org/10.1016/j.apsusc.2003.10.002>.
- [69] Borcia G, Dumitrascu N, Popa G. Influence of dielectric barrier discharge treatments on the surface properties of polyamide-6 films. *J. Optoelectron. Adv. Mater.*, vol. 7, 2005.
- [70] C. Martin. *Cura Ironing – How It Works, What to Expect & Examples* 2019. <https://the3dprinterbee.com/cura-ironing/> (accessed November 5, 2020).

- [71] Yang C, Tian X, Li D, Cao Y, Zhao F, Shi C. Influence of thermal processing conditions in 3D printing on the crystallinity and mechanical properties of PEEK material. *J Mater Process Technol* 2017;248. <https://doi.org/10.1016/j.jmatprotec.2017.04.027>.
- [72] Energy C for AR on. *Proceedings of Mechanical Engineering Research Day 2017 (Ch 8). Proc MERD 2017 UTeM 2017*.
- [73] Ultimaker. Ultimaker S5 n.d. <https://ultimaker.com/3d-printers/ultimaker-s5> (accessed January 3, 2021).
- [74] MANUFACTUR3D. Ultimaker Moves to New Headquarters as Company Expands on Global Scale 2019:1. <https://manufactur3dmag.com/ultimaker-moves-to-new-headquarters-as-company-expands-on-global-scale/> (accessed November 11, 2020).
- [75] Mikolas Zuza. Guide to Ironing: How to make top surfaces super smooth with PrusaSlicer 2.3 2020. https://blog.prusaprinters.org/make-top-surfaces-super-smooth-ironing-prusaslicer-2-3-beta_41506/ (accessed January 1, 2021).
- [76] Ultimaker. Ultimaker ABS specifications n.d. <https://ultimaker.com/materials/abs> (accessed January 3, 2021).
- [77] Shajahan SI. Why FDM parts made in Makerbot always tend to warp on the bottom left corner of the object (when seen from the top view) ? 2016. <https://www.researchgate.net/post/Why-FDM-parts-made-in-Makerbot-always-tend-to-warp-on-the-bottom-left-corner-of-the-object-when-seen-from-the-top-view> (accessed January 22, 2021).
- [78] Trish. Lines appearing during ironing 2020. <https://3dprinting.stackexchange.com/questions/11659/lines-appearing-during-ironing> (accessed December 2, 2020).

Appendix I

Appendix 1- Summary of the tests performed on chapter 4.2

Tests	Ironing			General information						
	N	interval	start	number of layers	coating	parts per print	spot	cleaning	#Zeros	#Ironed
(A1)	0	0	0	0	isopropyl	1	same	every print	4	0
(A2)	0	0	0	0	isopropyl	1	same	every print	4	0
(B1)	0	1	1	1	isopropyl	1	same	every print	1	4
(B2)	0	2	2	2	isopropyl	1	same	every print	1	4
(B3)	0	3	3	3	isopropyl	1	same	every print	1	4
(C1)	4	3	3	11	isopropyl	1	same	every print	1	4
(C2)	4	3	3	11	isopropyl	1	same	every print	1	4
(C3)	4	3	3	11	isopropyl	1	same	every print	3	3
(D1)	2	3	3	23	isopropyl	1	same	every print	1	4
(E1)	6	3	3	7	isopropyl	1	same	every print	1	4
(F1)	3 rd to the 8 th		3	6	isopropyl	1	same	every print	1	4
(G1)	1 st to the 3 rd		1	3	isopropyl	1	same	every print	1	4
(H1)	0	1	1	1	isopropyl	1	same	every print	1	4